NSF/CEE-82027
College of Engineering Report No. 59
PB83-100404

Analytical Study of Irregular R/C Structures Subjected to In-Plane Earthquake Loads

by
Mehdi Saiidi
and
Kenneth E. Hodson, Jr.

A Report to the
NATIONAL SCIENCE FOUNDATION
Research Grant PFR-80-06423

COLLEGE OF ENGINEERING
University of Nevada Reno
Reno, Nevada 89557-0030

May 1982

ANALYTICAL STUDY OF IRREGULAR R/C STRUCTURES SUBJECTED TO IN-PLANE EARTHQUAKE LOADS

by

Mehdi Saiidi

and

Kenneth E. Hodson, Jr.

A Report to the

NATIONAL SCIENCE FOUNDATION

Research Grant PFR-80-06423

College of Engineering Report No. 59
University of Nevada
Reno, Nevada
May 1982

ABSTRACT

A new version of a simple "single-degree" model (called the Q-Model) is used for approximate displacement response history calculation of irregular planar reinforced concrete frames subjected to earthquakes. Nonlinearity of the response is accounted for at an idealized base spring with a set of simple hysteresis rules. The model is evaluated for four small-scale physical model structures and a full-scale hypothetical frame. Irregularity of stiffness in small-scale structures was provided by "soft" story and discontinued shear walls. In the full-scale frame, irregularity was due to 67 percent setbacks. It is shown that the new version of the Q-Model led to an acceptable displacement estimate for these structures.

The model is used to study the effect of a few parameters on the seismic response. Effect of different earthquakes with the same spectral intensities (SI) on two structures are described. It is shown that neither SI nor peak ground acceleration are adequate to signifiy the expected structural response. Study of effect of different wall cutoff points is discussed. Walls of only a few stories high are found to provide sufficient resistance against excessive story drifts. Influence of wall stiffness on the displacement response is also demonstrated. The results of the study indicate that it is possible to obtain an optimal wall stiffness such that displacements and story drifts are minimal.

DISCLAIMER

Any opinions, findings, and conclusions or recommendations expressed in this publication are those of the authors and do not necessarily reflect the views of the National Science Foundation.

TABLE OF CONTENTS

LIST OF TABLES

LIST OF FIGURES

CHAPTER ONE

INTRODUCTION

1.1 Object and Scope

Researchers and design engineers in the field of earthquake engineering generally agree that reinforced concrete structures are nonlinear systems. While behavior during pre-yielding stages may be realistically simulated by the use of equivalent linear systems, a realistic representation of post-yielding behavior requires an explicit consideration of nonlinearity. Such consideration usually leads to substantial increase in computation effort, making the computer and engineer cost of nonlinear analysis prohibitive. This is particularly true for response history analyses involving several iterations.

Attempts have been made to develop simple models for the nonlinear analysis. One of these models is the Q-Model which has been found to estimate the displacement response history of uniform planar structures reasonably well [25, 28, 29]. The development of this model was considered the first step toward simplification of the nonlinear analysis.

In addition to substantial computation necessary for the nonlinear analysis and design, lack of adequate information about effect of different design parameters on the nonlinear seismic response has discouraged many designers from using the nonlinear methods.

The primary objective of the research reported herein was to simplify the Q-Model further, expand its application to irregular planar reinforced concrete structures, and carry out a sensitivity study to identify the important design parameters in the nonlinear analysis. Four small-scale test structures and ten artifical small-scale and

full-scale irregular structures were studied throughout the course of this investigation. All of these structures were planar systems subjected to one component of in-plane horizontal motion.

1.2 Review of Previous Research

The nonlinear seismic analysis of multistory reinforced concrete structures involves consideration of several parameters and is complex. This is true even if only the in-plane response is calculated. Simpler alternatives have been sought. The main goal in developing simple models has been to include principal features of the nonlinear response with relatively small effort to determine only the necessary dynamic response which provides information about the structural behavior. Complex analytical models usually compute displacement, velocity, and acceleration at different structural nodes. Among these, lateral deflection appears to give more insight about the behavior of the structure. Hence, simple models have been developed to calculate lateral displacement response histories. Generally, two types of simplified methods have been introduced: shear beam idealization and single-degree-of-freedom (SDOF) modeling.

In the shear beam method, the multistory structure is represented by a cantilever column element with lateral stiffness equal to that of the multistory structure. This method leads to simple expressions for dynamic properties of elastic structures [18]. On the other hand, the formulation is more involved for inelastic systems in that a hysteresis model should be incorporated in the analysis. Elasto-plastic and simple bilinear hysteresis models were used in the earlier works [20, 32], as well as in more recent investigations [37], despite the fact that elasto-plastic and bilinear models do not show good correlations with

experimental data obtained for reinforced concete [27, 30, 31]. More realistic hysteresis models were used by Aoyama [3] and Aziz [4]. The basis for evaluation of the shear beam model in the research by Aziz was correlation between the results from the shear beam model anlaysis and those from multi-degree-of-freedom (MDOF) analysis.

While shear beam models reduce the computations to a great extent, they still require solution of simultaneous equations. A more attractive approach is perhaps the "equivalent" SDOF modeling. In the equivalent SDOF method, the multistory structure is represented by a generalized mass, stiffness, and damping. In order to have a successful formulation for elastic systems, a single shape function should be found which represents the lateral deflection of the structure with reasonable accuracy. Because seismic response of elastic multistory structures is usually dominated by the fundamental mode, the fundamental mode shape or a shape function close to that does provide an acceptable approximate deflected shape. The properties of the equivalent SDOF system is found based on the shape function and energy principles [7, 9].

For inelastic structures, formulation of an equivalent SDOF system is more complicated because: (1) inelastic structures have variable mode shapes, and (2) a hysteresis model to represent the behavior of reinforced concrete structures is necessary. Takizawa used a degrading tri-linear hysteresis model in a shear beam model of a weak girder three-story building [36]. Results were compared with those of a rigorous model, but unacceptable correlation was found.

Pique developed an equivalent SDOF model using the first mode shape of the structure during elastic stage as the shape function [22]. The analysis was primarily concerned with the maximum response. The

model was evaluated based on the correlation between the SDOF model results and those from a MDOF model.

Saiidi and Sozen used a deflected shape obtained from nonlinear static analysis of the multistory structure as the displaced shape [25]. A simple hysteresis model was developed and incorporated in the model which was called the "Q-Model". Unlike the previous works which were concerned with only the maximum response, the Q-Model was used to determine response history of the structure. The model was evaluated by comparing the calculated results with experimental data obtained in dynamic testing of eight small-scale uniform structures.

Moehle and Sozen modified the Q-Model slightly to include cracking and analyzed four small-scale structures and found that both the Q-Model and their version led to a reasonable estimate of the response [16].

Several parameters are involved in the nonlinear analysis of reinforced concrete structures. One of the major analytical investigations on the effect of these parameters was carried out by Powell and Row [24]. In this study, earthquakes, column overdesign factor, and hysteresis models were varied. The first two were found to influence the maximum response significantly, while hinge rotations were insensitive to the type of the assumed hysteretic behavior. Saiidi studied the effect of the hysteresis model on the displacement response history and found that the response waveform and the number of large-amplitude cycles were affected by the hysteresis model [27,30]. Derecho, et.al., investigated the effect of different earthquakes and wall stiffness and yield level on several isolated shear walls [10]. It was concluded that, depending on the shape of response spectra and the initial period of the shear wall, the response may or may not be sensitive to the

input earthquake. It was also established that the maximum rotations are substantially affected by the yield moment of the wall section.

1.3 Acknowledgments

The research described in this report was part of an investigation aiming at the development of simple analytical models for nonlinear seismic response evaluation for planar reinforced concrete structures. The study was sponsored by the National Science Foundation under Grant PFR-80-06423.

The writers are grateful to the program manager, Dr. Michael Gaus of the National Science Foundation, for his support and advice.

Special gratitude is due to Professor Mete Sozen of the Civil Engineering Department at the University of Illinois for his encouragement and criticism. Jack Moehle of the University of California is thanked for providing the experimental data.

Mrs. Ruthe Berryman is specially thanked for typing this report.

The CDC 6400 and CYBER 171 computers at the University of Nevada, Reno, were used throughout the course of this study. Ellen Jacobson of the Computer Center provided valuable consulting service.

Parts of this report are based on a masters thesis by K.E. Hodson directed by M. Saiidi.

1.4 Notation

The following notations are used in the main body of this report:

A_1 = area in between calculated and measured responses

A_2 = area in between measured response and time axis

C = damping factor

D_e = displacement at equivalent height

D_i = displacement at floor i

f'_c = compressive strength of concrete

h_i = height from floor i to the base

h_n = height of structure

I = Occupancy importance factor

k = factor related to ductility of the structure

K_e = stiffness calculated from the hysteresis model

K1 = pre-yielding stiffness

K2 = post-yielding stiffness

L_e = equivalent height

M_e = equivalent mass

M_i = mass at floor i

M_t = total mass

N = number of floors

S = soil-structure interaction coefficient

S'_1 = modulus of elasticity of steel

S'_2 = strain-hardening slope in stress-strain curve for steel

W = gravity load

x_g = base acceleration

X_{max} = maximum displacement

$\ddot{x},\dot{x},x$ = acceleration, velocity, and displacement at height L_e, relative to base

X_y = displacement at break point of the primary curve

z = descending slope in stress-strain curve for concrete

Z = seismicity zoning factor

ϕ_e = normalized displaced shape at equivalent height

ϕ_i = normalized displaced shape at floor i

CHAPTER TWO

ANALYTICAL MODELS

2.1 Introductory Remarks

Although the main thrust of the research described in this report was the development and evaluation of a simple analytical model, other models for MDOF analysis of structures subjected to static and dynamic loads were used in the course of this study in many instances. These models were developed previously and detailed information about them may be found in Ref. 25. This Chapter presents a brief description of these models in Sections 2.2 and 2.3.

The simple model introduced in this report is a refined version of another model, called the Q-Model, which was previously found successful in simulating the seismic response of uniform plane structures [28]. The new version is called the Q-Model(L), and is described in Section 2.5 following a section on the old version.

2.2 Multi-Degree-of-Freedom Model for Static Analysis

This is an analytical model for nonlinear static analysis of planar reinforced concrete frames and frame-wall structures subjected to lateral loading. The model is for the analysis of only structures with orthogonal elements. Structural elements are idealized as line members. For beams and columns, element end portions in joint cores are considered infinitely rigid. In between the rigid end portions, a prismatic elastic member is assumed which is connected to each rigid end by a hinged connection and a nonlinear rotational spring (Fig. 2.1). This would limit yielding to the vicinity of beam ends, and is a reasonable assumption for structures subjected to large lateral loads. Variations in spring stiffness follow the rules of the Takeda

hysteresis model [35]. To determine the nonlinear rotations, each half of the member is treated as a cantilever beam, and rotations are found based on a trilinear skeleton curve representing moment curvature relationship for uncracked, cracked, and yielded stages for individual elements. The skeleton curve used in the model may or may not include bond slip rotations. Detailed information about the element idealization is provided in Ref. 19 and 25. Structural walls may be treated as regular elements. However, because walls are likely to yield only at and near the base, the model includes special wall element with one rotational spring at the base. Nonlinear rotations are found using the maximum moment at the base and an estimated cantilever length specified by the analyst.

Axial deformations are neglected in the model, but shear deformations are included. Masses are assumed to be lumped at floor levels. Gravity effects may be included. External loads act only at floor levels, and may be applied in several increments. Stiffness properties of the structure are assumed to remain unchanged during each loading. The model determines lateral displacements, joint rotations, and member end moments for each loading. The model is implemented in a computer program called LARZ2 [26]. An updated user's manual is presented in Appendix A.

2.3 Multi-Degree-of-Freedom Model for Seismic Analysis

This model is similar to the MDOF model described in Section 2.2 with the exception that it is for the analysis of structures subjected to horizontal base accelerations. Dynamic formulation and other basic assumptions are explained in detail in Ref. 25.

In its current form, the model is coupled to six hysteresis

models, five of which were incorporated in the original version and one, the Clough model [8], was added recently. The Takeda model is considered the most reliable model in this group, and it was the only model used in the "multi-degree" analyses discussed in this report. The model is used to calculate displacement and acceleration histories at different floors, base moment and base shear histories, and the maximum end moments and rotational ductilities (defined as the ratio of maximum rotation and the yield rotation).

The computer program implementing the model is called LARZ [26]. Appendix B presents an updated user's manual for this program.

2.4 Q-Model

The Q-Model is a simple SDOF model for nonlinear displacement history calculations for plane reinforced concrete structures subjected to base acceleration. The model has been found to estimate the response in reasonably close agreement with experimental data [16,28,29]. Two basic assumptions have been incorporated in the model about: (1) SDOF idealization and (2) hysteretic behavior.

(a) SDOF Idealization - Representation of a MDOF system by an equivalent SDOF oscillator has been introduced and used [7,9]. This simplification is possible because it has been known that seismic response of ordinary building structures is dominated by their fundamental mode of vibration. Such an idealization reduces computational effort especially if used for response history analysis. This reduction is due to the considerably smaller size of the SDOF system and due to the substantially smaller number of solution steps. While the reduction in size is obvious when a MDOF model is substituted by a SDOF system, the reduction in the number of time steps for a SDOF analysis needs

some explanations as follows.

To determine the response, the dynamic equilibrium equation is usually integrated numerically. The time step required to insure stability and convergence of the solution has to be well below the period of the highest mode of vibration of the structure, even though this mode may not contribute significantly to the response [9]. For ordinary multistory structures, the period of highest mode is very short, and a very small time step must be used for a MDOF analysis. Even unconditionally stable methods of numerical integration require small time steps to yield convergence.

The equivalent SDOF model has a period close to the fundamental period of the MDOF system. Therefore, contrary to a MDOF analysis, a SDOF analysis requires a time step which depends on the fundamental period of the structure rather than the shortest period. As a result, the necessary time step for numerical integration is considerably longer than that needed for a MDOF analysis, and fewer solution cycles are necessary. It is, therefore, apparent that idealization of a MDOF system by an equivalent SDOF model results in substantial saving in computations.

(b) Hysteretic Behavior - Experimental studies of the cyclic behavior of reinforced concrete structures have shown that force-deformation relationships are associated with progressive stiffness degradation and "pinching" action [15,23]. An equivalent SDOF system would have to take these characteristics into account in order to yield satisfactory results. Several hysteresis models have been developed which include pinching or stiffness degradation, or both [15,25,35]. Most of these models are relatively complex and their use in a simplified SDOF system is unjustified. However, one of the models

introduced in Ref. 25 (called Q-hyst) is simple while it includes the basic features observed in experimental results. In this model, the value of the incremental stiffness at any stage of loading or unloading is defined by a set of rules operating on a bilinear primary curve. The primary curve is symmetrical with respect to the origin (Fig. 2.2). The model is described using four rules [25].

The last largest excursion point (U_m) in both directions is treated as the largest excursion point in either direction. This assumption was made to include pinching effect without addition of a new rule, and to keep the model simple. Unloading stiffness on either side of the deformation axis is defined by

$$K = K1 * (X_y/X_{max})^{0.4}$$

In which

K1 = pre-yielding stiffness

X_y = displacement at "knee" point

X_{max} = maximum dsiplacement

Loading stiffness on either side of the deformation axis is

(1) K1 if $X_{max} \leq X_y$

(2) K2 if the point is on the portion of the primary curve with the slope K2 (with K2 = post-yield stiffness)

(3) Equal to the steeper of (a) the slope obtained joining the most recent deformation axis intercept with the point on the primary curve corresponding to X_{max} on the same side of the deformation axis and (b) the most recent return slope.

(c) The Q-Model - Properties of the Q-Model are related to those of the MDOF model of a building following the procedure used by Biggs [7]. Minor modifications are made in Biggs' derivation [25], and

different parameters are found. The Q-Model is shown in Fig. 2.3.

Hysteretic response of the "spring" in the Q-Model is based on a nonlinear force-displacement primary curve relationship obtained using a nonlinear static analysis and the properties of the structure, with the assumption that it is subjected to a set of monotonically increasing external lateral forces. The basic bilinear curve, assumed to be symmetrical with respect to the origin defined by zero load and zero displacement, is calculated for a force distribution assuming that the lateral force at a given level is proportional to the height and the mass at that level. This force distribution was chosen because it is simple, and because it is compatible with the distribution recommended by the Uniform Building Code [14]. Base moment is plotted in terms of roof displacement and the resulting curve is idealized by a bilinear curve (primary curve). Lateral floor displacements corresponding to the break point of the bilinear curve are normalized with respect to the roof displacement, and form the deflected shape. This shape is insensitive to the exact location of the break point as long as the break point is taken at a reasonable location on the primary curve.

Using the Q-Model, lateral displacement histories at different floors and the base moment history can be found.

2.5 Q-Model(L)

The Q-Model reduces the complex and lengthy nonlinear analysis of multistory structures to the analysis of a SDOF system, once the Q-Model properties are determined. However, in the process of calculating the properties, a computer program for nonlinear static analysis of reinforced concrete structures subjected to lateral loads is needed to obtain the primary curve. This may not be convenient for the analysts

who do not have access to such programs or the necessary computer facilities. In the new version of the model, attempts were made to determine the bilinear moment-displacement relationship without a nonlinear static analysis. The alternative method used in the new verson is a limit analysis method. This approach has been also used in Ref. 16. The new version is called Q-Model(L), with (L) standing for "limit analysis."

The main characteristics of the new and old versions are the same. In the new version, the elastic stiffness of the spring is calculated based on a static analysis of the multistory structure for lateral loads applied at floor levels. These loads are proportional to floor masses and heights from base. Because beams in reinforced concrete structures are cracked under service load conditions, cracked moment of inertia is used for beams in the static analysis. The break point of the primary curve (the apparent "yield" point) represents the base moment for the collapse loads. Structural elements are assumed to behave elasto-plastic at this stage, and strain-hardening effects are taken into account at a later stage. The "yield" base moment is found from a limit analysis of the multistory structure with different hinging locations (Fig. 2.4). Current guidelines for seismic design recommend an overdesign of columns to limit yielding to beams [1]. For buildings so designed, hinging takes place primarily in beams, and number of collapse mechanisms to be considered is minimal.

Strain-hardening effects are accounted for by assigning a slope to the post-yielding part of the primary curve. This slope is related to increase in moment for individual sections: (1) due to increase in the moment arm as steel strain is raised and (2) due to strain hardening of reinforcement. An explicit consideration of the first factor

would be involved. Therefore, the following simple relationship is used to determine the post-yielding slope of the primary curve:

$$K2 = 2(S_2'/S_1') \times K1 \tag{2.1}$$

where $K1$ = elastic slope of the primary curve

$K2$ = post-yielding slope of the primary curve

S_1' = modulus of elasticity of reinforcement steel

S_2' = strain-hardening slope in stress-strain curve for reinforcement steel

The Q-hyst model explained in Sec. 2.4 is used to determine stiffness variation of the base spring. This model accounts for stiffness degradation characteristics of reinforced concrete structures subjected to cycling loads.

The floor displacements obtained from the static analysis are normalized with respect to the top-floor displacement. The normalized values are assumed to represent the displaced shape of the structure throughout the response. The equivalent mass and height (Fig. 2.3) are found from the following relationships:

$$M_e = \left(\sum_{i=1}^{N} m_i \phi_i^2 / \sum_{i=1}^{N} m_i \phi_i \right)(M_t) \tag{2.2}$$

and

$$L_e = \sum_{i=1}^{N} m_i \phi_i h_i / \sum_{i=1}^{N} m_i \phi_i \tag{2.3}$$

where L_e = equivalent height

M_e = equivalent mass

M_t = total mass

N = number of floors

h_i = height from the base at floor i

m_i = mass at floor i

ϕ_i = normalized displacement at floor i

The equation of motion is formulated as:

$$M_e \ddot{x} + C \dot{x} + K_e x = -M_t \ddot{x}_g \qquad (2.4)$$

where C = damping coefficient

K_e = stiffness calculated using the hysteresis model

x_g = base acceleration

$\ddot{x}$, $\dot{x}$, and x = relative acceleration, velocity, and displacement at the equivalent mass (relative to base).

The above formulation is the same as that used in the original Q-Model [25]. It should be noted that this equation is different from equation of equilibrium for a typical "single-degree" oscillator in that the mass on the right-hand side of the equation is the total mass, while the mass on the left-hand side is the equivalent mass which is smaller than the total mass. This difference should be accounted for during integration by either using the total mass on the right-hand side, or by using the equivalent mass on the right-hand side and amplifying the base acceleration by the ratio of total mass over equivalent mass.

The base moment versus displacement at equivalent height relationship forms the primary curve upon which the hysteresis model operates. The displacement at equivalent height is found from a linear interpolation of displacements at adjacent floors.

A damping factor of two percent is used, and Eq. 2.4 is integrated using the Newmark's β method [17] to determine the displacement history at the equivalent height, and base moment history. Displace-

ments at different floors can be obtained using the assumed displaced shape.

$$D_i = (\phi_i/\phi_e)D_e \qquad (2.5)$$

where D_e = displacement at equivalent height

D_i = displacement at floor i

ϕ_e = normalized displacement at equivalent height

ϕ_i = normalized displacement at floor i

A step-by-step procedure for the Q-Model(L) analysis is presented in Appendix C.

CHAPTER THREE

STRUCTURES AND DESIGN METHODS

3.1 Introductory Remarks

Three groups of reinforced concrete structures were studied. The first group consisted of four small-scale test structures for which measured data from dynamic testing were available. The second group included several ficticious small-scale structures similar to those in the first group. In the third group was an eight-story full-scale reinforced concrete frame with approximately 67 percent setback at the upper five stories. No experimental data were available for structures in the second and third groups.

Part of this chapter provides a brief description of design and experimental testing of the structures in the first group. Detailed information on these structures may be found in Ref. 16. This chapter also presents the design method and information about the assumed material properties, geometry, and reinforcement distribution of the structures in the second and third groups.

3.2 Test Structures

This group consisted of four small-scale reinforced concrete structures tested at the Newmark Civil Engineering Laboratory at the University of Illinois at Urbana-Champaign by Moehle and Sozen [16]. The main purpose of the experimental investigation was to determine the effect of abrupt change of stiffness on the dynamic performance of structures.

(a) Structural Properties - Each structure was composed of two identical frames placed parallel to each other on the University of Illinois shake table platform. Three of the structures had a central shear wall which was connected to "floor" levels by hinged links.

Different wall heights were used for different structures, providing the opportunity to study the effect of wall cut-off point on seismic performance of structures (Fig. 3.1). The structure without shear wall was called FNW, and the ones with one-, four-, and nine-story walls were called FSW, FHW, and FFW, respectively. The shear walls provided for approximately 75 percent of lateral stiffness during the elastic stage. Beam, column, and wall dimensions were 38 x 38, 38 x 51, and 38 x 203 mm, respectively. The measured material properties are shown in Table 3.1.

The structures were designed using the Substitute-Structure method [33]. Nonlinearity of the response is taken into account in this method through a pre-assigned damage ratio (generally comparable to rotational ductility factor) which can be different for different structural elements. For the test structures, the damage ratios were chosen as one for columns, three for walls, and six for beams [16]. These values were chosen to arrive at "weak-girder" structures. To insure that yielding would be limited to beams, the columns were overdesigned by approximately twenty percent.

Floor masses were simulated by concrete blocks, weighing approximately 465 kg, attached to the frames at the intersection of beams and columns through hinged connections. As a result, the beams were not subjected to any dead loads other than their own weights, and the beam forces were effectively those caused by dynamic lateral loads. Yielding in beams, therefore, was limited to beam ends. The reinforcement in all elements was symmetrical (Fig. 3.2). A considerable amount of shear reinforcement was provided to avoid shear failure. The longitudinal steel ratios are shown in Fig. 3.2. The values for beams and walls represent the steel area per face divided by width and effective depth,

and the values for columns are the total steel area over column gross section. The concrete cover on shear reinforcement was 5 mm for all cases but on vertical legs in beams where the cover was 8 mm.

(b) Dynamic Testings - The structures were subjected to extensive dynamic testings in the direction of their planes. The tests included earthquake simulations, steady state motions, and free vibrations. Of relevance to this study were the first earthquake runs which are described here.

The north-south component of the El Centro 1940 earthquake acceleration was simulated. The maximum acceleration was normalized to approximately forty percent of gravity acceleration. This value had been used as the maximum acceleration of the design earthquake. Because the structures were of small scale, their period was shorter than that of full-scale structures with comparable configuration. Therefore, the earthquake time coordinate was lapsed by a factor of 2.5. The test data collected included floor displacement histories relative to base, floor absolute acceleration histories, and base acceleration history. The latter was measured because the base acceleration acting on the structure was not precisely the same as the simulated earthquake.

3.3 Hypothetical Small-Scale Structures

Several artifical small-scale structures were generated for the purpose of parametric studies. These structures were identical to the test structures. The difference between the test structures and the hypothetical structures was in geometric configuration, or in seismic design method, or both. The ones with different geometries consisted of three structures with wall cut-off points other than those of the test structures (Fig. 3.3). The wall in these structures was discontinued at

level three (FW3), five (FW5), and seven (FW7). The cross-sectional dimensions and reinforcement distribution were the same as those of the test structures with wall.

To determine the influence of design method on the dynamic response, structures FNW and FFW were redesigned using the Uniform Building Code [14] to compute earthquake forces. The new buildings were called UFNW and UFFW, with "U" standing for UBC.

Other structures in this group were four frame-walls, each with a different wall width (Fig. 3.4). These structures were named as UFW100, UFW150, UFW250, and UFW300, with the numerals indicating the wall width in terms of millimeter. The wall extended over the full height of each structure.

The earthquake forces for the structures were found using the UBC. Modifications were made to account for the fact that the structures were of small scale.

According to the UBC provisions, the design lateral forces are found from

$$V = Z\ I\ K\ C\ S\ W \tag{3.1}$$

where $C = 1/15\sqrt{T}$

I = Occupancy importance factor

K = factor related to ductility of the structure

S = Coefficient related to soil-structure interaction

T = fundamental elastic period of vibration

W = effective gravity load

and Z = seismicity zoning coefficient.

To determine the fundamental period, the UBC provides three alternative equations. One of these is related to the overall dimensions of

the structure as follows:

$$T = 0.05\ h_n/D^{\frac{1}{2}} \qquad (3.2)$$

where D = dimension of the structure in the direction of vibration (feet)

h_n = height of the top floor from base (feet)

The period from Eq. 3.2 was found equal to 0.217 sec for the small-scale structures. This equation assumes the same period for all of the small-scale structures. To determine how the above result compares with a more accurate estimate of the fundamental period, a frequency analysis was carried out for structure UFNW and the period was found equal to 0.239 sec. Because this value is close to 0.217 obtained from Eq. 3.2, and to simplify the computations, Eq. 3.2 was used for all the structures in this group.

It was assumed that the structures in this group are in zone four (Z=1). The importance factor was taken equal to 1. Based on Table 23-I of the UBC, the "K" factor was assumed equal to 0.67 for UFNW and equal to 0.8 for all other structures in this group. An "S" value of 1.5 was used. The upper limit on the "CS" value given by the UBC is 0.14 for full-scale structures. Because "C" is inversely proportional to the square root of structural period, and because the period of the small-scale structures is approximately forty percent of the period of full-scale structures with similar configuration, the upper limit on "CS" for the small-scale structures should be:

$$CS = 0.14\ (1/0.4)^{\frac{1}{2}} = 0.22$$

With T = 0.217 and S = 1.5, the value of "CS" was found equal to 0.215 which is less than the upper limit. The design lateral force (Eq.

3.1) was found equal to 0.144W for UFNW and 0.172W for other structures. Floor weights were assumed the same for all the structures. The lateral forces are listed in Table 3.3.

The factored design forces were controlled by Eq. 9.2 of the ACI Code [2] as follows:

$$U = 1.05D + 1.275L + 1.403E \qquad (3.3)$$

where U = factored load

D = dead load

L = live load

E = earthquake load

With a live load of zero, each structure was analyzed for the above loads using program SAP IV [6] and the internal forces were found. The reinforcement pattern used in these structures was similar to that used in the test structures. For example, because all the beams in each frame-wall test structure has the same reinforcement, the steel distribution in all of the beams in the hypothetical frame-wall structures was taken the same. This was done because it was not the intention of this study to examine the effect of different steel patterns. The resulting design moments and forces are listed in Table 3.4.

Using the material properties listed in Table 3.1 and the design moments, reinforcement was found for different elements. The material properties used for UFNW were the same as those for FNW, and the values for all other hypothetical small structures were the same as those for FFW. The steel distribution is presented in Table 3.5. It can be seen that the UBC design method generally led to structures with larger reinforcement than those obtained using the Substitute-Structure method

(Fig. 3.2).

3.4 Structure with Setbacks

An eight-story reinforced concrete frame with sixty seven percent setbacks was analyzed in this study to determine the reliability of the analytical models in response prediction of this class of structures. The frame was called EFS for Eight-Story Frame with Setbacks.

The dimensions of the frame and cross sections are shown in Fig. 3.5 and 3.6, and the assumed material properties are shown in Table 3.2. Floor weights were taken equal to 200 kips (890KN) at the lower three floors and 80 kips (356 KN) at the upper floors.

The structural dimensions and the size of the members were taken within the customary ranges. To obtain a reasonable distribution of reinforcement, an approximate estimate of lateral forces was found using the UBC, even though the provisions of this code do not generally apply to structures with more than 25 percent setbacks. A more rational design would have been based on a dynamic analysis of the frame. However, the intent of the study on this frame was not to investigate the effect of design method; rather, the intent was to evaluate the Q-Model for a structure with setbacks. Based on the UBC, the design base shear is calculated from Eq. 3.1. It was assumed that the building is located in an area with high seismicity (zone 4).

The period of the structure with gross section properties was determined using a computer program, and was found equal to 1.48 sec. An importance factor of one, and a "K" factor of 0.67 was used. The factor "S" was taken equal to 1.5. The resulting base shear was found equal to 0.055 W. The UBC provisions require a concentrated load to be applied at the top floor if certain conditions exist. However, for the

structure considered here, the effect was negligible. The total lateral load was distributed among floors using the provisions of the UBC. The live load was set equal to zero, and the floor weights were assumed to be distributed uniformly. The factored design moments were found and reinforcement was designed using the material properties listed in Table 3.2, and the method described by the ACI Code (Fig. 3.6). For convenience in the later stages of the study, the beam reinforcement was assumed symmetrical. Because the steel distribution appeared to be reasonable, no refinement in the seismic design forces was made and the design was considered final.

CHAPTER FOUR

EFFECT OF PARAMETERS ON Q-MODEL RESPONSE

4.1 Introductory Remarks

The approach used in the Q-Model (or Q-Model(L)) involves a few parameters. To obtain some of these parameters, different analysts may use different methods and idealizations, causing a variation in the values used in the analysis. To determine the degree of sensitivity of the response to moderate changes in these parameters, a parametric study was carried out. This chapter presents the parameters and the results of the study.

4.2 Location of Wall Inflection Point

The method used in the Q-Model to obtain the primary moment-deflection curve involves a nonlinear static analysis of the multistory structure. As it was mentioned in Sec. 2.2, the height of wall inflection point from the base is estimated by the analyst. To determine the effect of this height on the primary curve, structure FFW was analyzed using different wall inflection point heights, ranging from one-half of the first story height to the full height of the structure. A set of monotonically increasing lateral loads were applied in fifty increments, and base moment was plotted in terms of the top-level displacements (Fig. 4.1). It should be noted that the wall in this structure provided for approximately 75 percent of lateral stiffness. Therefore, lateral displacements were mainly controlled by the wall.

It can be seen in Fig. 4.1 that the curve changed only slightly as a result of change in inflection point location. The curve corresponding to inflection point at mid-height of the first story showed the

largest deviation from the other curves. The results for all other cases were very close. By examining the wall moments after each load increment, it was found that the exact inflection point position slightly varied as cracking and yielding developed in different elements. For the case when only minor cracks had developed the exact point was at one-third of the total height. In the vicinity of the "knee" point (apparent yield point), the height was 0.37 of the total height, reducing to 0.29 for the loads causing a top displacement equal to two percent of the structural height.

A reasonable estimate of the height of inflection point would be between one-third to full height of the wall. For this range, it can be seen that the location of inflection point made little difference in the primary curve.

4.3 Damping Factor

A viscous damping factor of seven percent has been recommended and widely used for dynamic analysis of reinforced concrete structures in the pre-yielding range [18]. A seven percent damping factor is relatively large, but because structural elements may be cracked in the pre-yielding range, to account for the energy absorbed by friction between the aggregates, this damping factor is justified. In structures which undergo yielding, much of the input energy is dissipated through hysteretic damping, and a smaller damping factor is more appropriate. To determine the influence of damping on the displacement response, the Q-Model was used to analyze structure FHW based on different damping coefficients. The study was carried out for both the elastic and inelastic ranges. The responses were judged based on their agreement with the measured data.

Figure 4.2 shows the top-level displacement response for FHW forced to remain elastic while the damping factor was varied. As it would be expected, the elastic responses showed poor correlation with the experimental data. The response with zero percent damping showed the largest deviation. During the first 1.5 seconds, when no major yielding had yet occurred and the structure was indeed elastic, close correlation was observed for all values of damping. It can be concluded that: (1) the response history could not be predicted well using an elastic analysis with cracked stiffness, regardless of the damping factor, and (2) amplitudes, frequency content, and waveforms of the response based on an elastic analysis are very sensitive to the damping factor.

Figure 4.3 presents the top-level nonlinear displacement histories for different damping factors. It can be seen that the inelastic responses were considerably better than the elastic responses. Displacements found based on two and five percent damping factors were in closer agreement with the measured curves. As the damping factor was varied, the calculated response histories changed slightly, indicating that the inelastic response is not very sensitive to the damping factor.

To obtain an overall evaluation of the responses, the displacement maxima and a factor called the "Performance Index (PI)" were plotted (Fig. 4.4). The PI is a simple index representing the closeness of the calculated and measured results and is found from

$$PI = 100(1 - A_1/A_2) \qquad (4.1)$$

in which

A_1 = area in between calculated and measured responses,

and A_2 = area in between measured response and zero displacement axis.

A response with PI = 100 is in perfect agreement with the measured data, while a response with a negative PI has a considerable deviation from the measured response.

It is evident in Fig. 4.4.a that the elastic maximum displacement was considerably more sensitive than the inelastic response. The PI values for the elastic cases were also affected significantly by the change in the damping factor (Fig. 4.4.b). The poor correlation of elastic responses with the measured curves is indicated by the negative PI's. The PI was stable for the nonlinear responses with damping factors ranging from two to eight percent.

In summary, the choice of damping factor had little effect on the nonlinear response as long as a damping factor of between two to eight percent was used. It should be noted that this observation was made for a physical model structure with no "non-structural" elements. Furthermore, the structure developed significant nonlinearity (maximum displacement of about 2.5 times the yield displacement). Response of structures with non-structural elements and with limited nonlinearity is more sensitive to the damping factor.

4.4 Elastic Stiffness

Elastic stiffness is referred to the slope of the line connecting the origin to the apparent yield point of the primary curve (Fig. 2.2). For a Q-Model analysis, the moment-deflection curve obtained from a nonlinear static analysis needs to be idealized by a bilinear curve. The choice of the breakpoint has an effect on the elastic stiffness. To determine the effect of slight variations in the stiffness on response,

structure FHW was analyzed assigning different values of elastic stiffness. First, the result from the static analysis was idealized by a bilinear curve using judgement. The response obtained based on this curve is called the reference case, and is shown in Fig. 4.5. Four other cases were studied using elastic stiffnesses equal to 90, 95, 105, and 110 percent of the stiffness used in the reference case (k_o). The post-yielding slope of the primary curve and yield moment were kept constant. A damping factor of two percent was used for all cases.

Figure 4.6 shows the response histories and Fig. 4.7 shows the maximum displacements and the PI's. No significant changes could be observed as the initial stiffness changed. The response history for the case with 110 percent of reference stiffness was in closer agreement with the measured curve. This case also had the highest PI. However, with respect to maximum displacement, the case with 90 percent of reference stiffness had the best agreement. Nevertheless, the results for different cases were close, suggesting that $\pm$ 10 percent variation in the elastic stiffness is not likely to cause any drastic changes in the response. It should be noted that this observation may not true for earthquakes with "sharp" peaks in their response spectra in the range close to effective period of structure [25].

4.5 Post-Yielding Stiffness

The slope of the primary curve beyond the yield point is established by the analyst through the process of idealization of the calculated curve for a Q-Model analysis, and found from Eq. 2.1 for a Q-Model(L) analysis. To determine the slope used in the Q-Model, the knee point is connected to a point on the calculated curve with displacement equal to five times the displacement at the knee point. In

the Q-Model(L), the slope is a function of elastic slope and strain hardening slope in stress-strain relationship for steel. Both these approaches are arbitrary, and have been used because they are simple and yield satisfactory results. Questions may be raised as to what effects changes in these slopes may have on the response. To determine the effects, structure FHW was analyzed six times, with the ratio of post-yielding slope over the elastic slope ranging from zero to 0.3. The ratio was 0.08 for the reference case (Fig. 4.5). A damping factor of two percent was used in all the analyses. The response histories are presented in Fig. 4.8, and the maximum responses and the PI's are shown in Fig. 4.9, with "p" indicating the slope ratio. With respect to the displacement histories, it can be seen that slightly closer agreement with the measured response was evident in the high-amplitude ranges as "p" increased to 0.2. However, the effect was the opposite in the low-amplitude ranges (between T = 3 to 5 sec.). All the calculated curves had the same general waveforms. The maximum calculated displacement became slightly closer to the measured value as "p" increased up to 0.2 (Fig. 4.9). The variation in "p" seemed to have little effect on the overall PI's.

The above observations suggest that small variations in the post-yielding slope are not likely to have any pronounced effect on the displacement response.

4.6 Yield Base Moment

In the Q-Model, the "yield" point of the primary curve is a point on the calculated moment-deflection curve, chosen by the analyst. In the Q-Model(L), the yield point depends on the yield moment for structural elements. Depending on the idealizations and assumptions

used in finding the yield point, there may be variations in the magnitude of yield base moment. To study the influence of the yield base moment on the response, structure FHW was analyzed four times, each time with a different yield value ranging from 80 percent of the yield moment in the reference case to 120 percent. The yield moment for the reference case was found using the procedure described in Sec. 2.4.

Figure 4.10 shows the response histories for different cases. The response for the reference case is presented in Fig. 4.5. These curves show that the correlation improved as the yield base moment increased. However, the curves for different cases were identical qualitatively. The case with 120 percent of the reference base moment showed excellent agreement with the experimental data. With respect to the maximum responses, increase in yield moment again improved the results (Fig. 4.11). The change and improvement in the calculated values is very clear in the plot for performance indeces. As the yield moment increased from 80 percent of the reference yield moment to 120 percent of that value, the PI almost doubled. Based on the foregoing observations, it may be stated that the response is somewhat sensitive to the yield base moment, and special care should be exercised in determining this value.

CHAPTER FIVE

RESPONSE OF TEST STRUCTURES

5.1 Introductory Remarks

This chapter describes the results of the analyses of the test structures based on the Q-Model and the Q-Model(L). The analytical results are judged based on their agreement with the measured data. These comparisons were made to determine the reliability of the models before the parametric studies were undertaken.

5.2 Results Based on the Q-Model

The earthquake response of the test structures (Sec. 3.2) was determined using the Q-Model (Sec. 2.4). Program LARZ2 was used to determine the overall moment-deflection curve for each structure. The input to this program includes moment-curvature values at cracking, yielding, and a point beyond the yielding. The moment-curvature values were found using a computer program. No axial loads were considered for beams and walls, while an average axial dead load based on a 460 kg mass at each level was used for columns (Fig. 5.1). The measured material properties (Table 3.1) were used. The moment-curvature values are listed in Table 5.1. Gravity effects and bond slip rotations were ignored in the static analysis, but were considered at a later stage in Q-Model analysis.

The calculated moment-deflection curves and the idealized curves (fine dashed lines) are shown in Fig. 5.2. Visual judgement was used to idealize the curves. For each structure, the displacements at the "knee" point were found, normalized with respect to the top-level displacement, and were used as the displaced shape (Table 5.2). The properties of the equivalent single-degree systems are listed in Table 5.2.

The displacement responses at the top level of each structure for the first earthquake runs were found using program LARZAK [26], and were surperimposed on the measured response histories (Fig. 5.3).

The comparison of the calculated and measured top-level responses is adequate to evaluate the model because both the measured and calculated responses for other levels are similar to those at the top levels. The displacements at the time of maximum top-level displacements and story drifts are presented in Fig. 5.4.

The response histories from the Q-Model analyses are shown at the top of Fig. 5.3. It can be seen that for all four structures the calculated curves were in close agreement with the measured data. The correlation for the first half of the response was better than the correlation for the second half. During the low-amplitude responses (between the third and fifth sec), the analytical results deviated from the experimental responses for structure FSW. However, the Q-Model was able to predict the same type of waveform and amplitude as the measured data. Analytical results showed lower amplitudes than the experimental values after the fifth sec. for all structures. This was particularly pronounced for FNW, the structure with no wall. One possible explanation for the differences is that the test structures actually had lost their hysteretic energy dissipation capacity significantly by the fifth sec, whereas the Q-Model continued to dissipate the input energy through the hysteresis model even after the fifth sec. As a result, the model did not need to develop large displacements. This explanation is supported by the narrow measured hysteresis loops for amplitudes between $\pm$ 15 mm (Fig. 5.5).

In terms of maximum displacements and story drifts, the correlation between the analytical and experimental data was reasonably good

(Fig. 5.4). The correlation was best for FSW and FHW.

5.3 Results Based on the Q-Model(L)

The test structures were also analyzed using the Q-Model(L) described in Sec. 2.5. To carry out the limit analyses, the yield moments listed in Table 5.1 were used as the plastic moments. Several yield mechanisms were considered for each structure. Because the columns had higher yield points than the beams, plastic hinging in columns was limited only to the points needed to satisfy compatibility of deformations. Floor loads were taken proportional to floor mass and height from the base. The loads had a triangular distribution due to the assumed equal floor masses.

Figure 5.6 shows the results of the limit analyses. These results are comparable with those reported in Ref. 16 but show smaller collapse loads because the plastic moments used in that study were larger than the element yield moments used in the present work.

Each structure was analyzed for the collapse load, and the floor displacements were found and normalized with respect to the top-level displacement to obtain the deflected shapes. The properties of the equivalent SDOF systems are listed in Table 5.3. It can be seen that the SDOF system properties are very close to those of the Q-Model.

The dynamic analysis was carried out for the first six seconds of the measured first earthquake acceleration data. The response histories and maximum responses, designated by Q-Model(L), are shown in Fig. 5.3 and 5.4. The closeness of the properties of equivalent systems based on the Q-Model and those based on the Q-Model(L) was an indication that the two models would yield identical results. This can be observed in Fig. 5.3 and 5.4. Close agreement with the experimental data during the first five seconds is evident. Between the fifth and sixth second, the

amplitudes of the calculated curve were smaller than those of the measured data except for FSW. In terms of maximum floor displacements and story drifts, the results from the Q-Model(L) showed better or equal agreement with the experimental data. It can be concluded that the overall performance of the Q-Model(L) was at least as satisfactory as that of the Q-Model.

5.4 Discussion

In Sec. 5.3 it was seen that the Q-Model(L) provided a considerably simpler alternative to the original form of the Q-Model in terms of construction of the primary curves, while the results were very similar to those found from the Q-Model. The method used (limit analysis) in the Q-Model(L) to form the moment-deflection curve is known to most structural engineers and requires relatively small amount of computation. An experienced designer would need to try only a few collapse mechanisms in order to determine the minimum collapse load. It is also worthwhile to notice that the curves of the type found in Fig. 5.6 consist of a relatively flat portion for most parts. Therefore, an estimate of the collapse load can be obtained without any significant effort.

The only element strength property needed in Q-Model(L) is the yield point (taken the same as the ultimate point defined by the ACI Code [2]) which can be found using routine methods or tables and charts available in most structural engineering offices. On the other hand, for a Q-Model analysis, the complete moment-curvature relationship was necessary for each element. Computation of moment curvatures is considerably more involved than finding the yield moment alone.

To determine lateral displacements due to static loads, the ori-

ginal Q-Model requires a computer program for inelastic analysis of structures. Presently, very few design offices have access to such a program. Furthermore, a majority of engineers with baccalaureate and even masters degrees are not familiar with the nonlinear analysis methods and, even with access to inelastic programs, they do not feel confident to use these programs. In contrast, the Q-Model(L) requires an elastic analysis, for which relatively simple and short computer programs are widely available.

Once the properties of the equivalent SDOF system is determined, both Q-Model and Q-Model(L) use the same dynamic analysis. The computer program for the dynamic analysis, LARZAK [26], is relatively short, and it can be implemented on small computers.

Based on the foregoing discussion, it is apparent that the Q-Model(L) is a preferred model over the original version in that it incorporates more familiar methods, simpler computations, and simpler structural analysis programs, while it yields satisfactory results.

CHAPTER SIX

RESPONSE OF THE STRUCTURE WITH SETBACKS

6.1 Introductory Remarks

In chapter five, the original and new version of the Q-Model were used for small-scale test structures with abrupt change of stiffness provided by large first-story height and different wall heights. To determine the acceptability of the models for a full-scale structure with stiffness interruption caused by setbacks, the eight-story frame (EFS) described in Sec. 3.4 was studied. While this frame does not represent any "real" structure, it was designed using the current building codes. Because no measured data were available for this structure, the "true" seismic response of the frame was estimated using the MDOF model discussed in Sec. 2.3. The MDOF model results were used to evaulate the response found using the SDOF models. In this chapter, the MDOF and SDOF results are presented and correlation between the responses is discussed.

6.2 Multi-Degree-of-Freedom Model Results

Based on the assumed material properties (Table 3.2), the moment-curvature values and bond-slip rotations were calculated using routine methods (for moment curvature) and the method described in Ref. 34 (for bond slip). The results are listed in Table 6.1. The frame was analyzed for the first fifteen seconds of the El Centro 1940 NS acceleration record normalized to a maximum acceleration of 0.5g. The input base acceleration and calculated displacement histories are shown in Fig. 6.1. The maximum roof displacement was equal to 17.7 in or approximately 1.5 percent of the total height. The frame developed significant nonlinear deformations. The maximum rotational ductility demand

(defined as the ratio of maximum rotation and yield rotation) was 2.5 for beams (at the eighth floor) and 1.5 for columns (at the base).

Comparison of the responses at the top five floors shows that the displacements were generally in phase. The same was true for the second, third, and fourth floor displacements. Comparison of the roof and fourth floor responses reveals that, although "zero-crossings" were close for most parts, they were not quite simultaneous. This suggests that the motion at the upper five floors (the part with setbacks) was slightly out-of-phase with respect to the lower three floors. Further indication of an out-of-phase motion can be observed in the peak points in the top five floor responses.

To study the deflected shape of the frame, displacements near the peaks at about T = 5.5, 10.5, and 12.5 sec were normalized with respect to the top-floor displacements, and were plotted in Fig. 6.2. The curves with the negative sign preceded the ones with positive sign by a few tenths of a second. Based on this figure, it is apparent that in the vicinity of the peaks the deflection was slightly concave at one instance and slightly convex at another. This indicates the presence of an "apparent" second mode.

6.3 Q-Model Results

The MDOF analysis revealed that the displacement response had visible contribution of an apparent second mode, and that the displacement shape was variable especially near the peaks. This could be interpreted that an equivalent SDOF model, utilizing a single deflected shape, might not be successful in response prediction. To explore the problem, EFS was analyzed using both the old and new versions of the Q-Model.

Using the methods described in Chapter Two, properties of the SDOF

systems were found. The lateral loads for the static analyses had the distribution shown in Fig. 6.3. The Q-Model properties are listed in Table 6.2 and 6.3. The displacement histories obtained from different models, were superimposed (Fig. 6.4). Because the fourth floor response shape was somewhat different from the roof response, the response at both floors was considered.

It can be observed that the roof displacement histories found using different models were in general agreement. The SDOF model responses had a slightly shorter effective period. The waveforms and amplitudes were close. The absolute maximum displacement obtained from the Q-Model was seven percent larger than the MDOF result. The Q-Model(L) overestimated the response by nine percent. The time of maximum roof displacement found from SDOF models coincided with the time of the second largest peak in the MDOF response.

The correlation at the fourth floor was not as satisfactory as that at the roof. The response based on the Q-Model(L) appeared to be slightly closer to the MDOF model result. The SDOF models were unable to reproduce the higher mode contributions seen in the MDOF model response between the second and third seconds and at the ninth second. The correlation between the SDOF model results and that of the MDOF model was poor after the twelfth second, indicating that perhaps the simple hysteresis rules incorporated in the SDOF models led to an overall structural stiffness which was not close to what was considered by the more complex hysteresis rules used in the MDOF model [35]. Nevertheless, in terms of the overall response, the SDOF model results were reasonably close to the response from the MDOF model.

The foregoing observations were contrary to the expectation that, because of the presence of an apparent second mode, an equivalent SDOF

model would not work. The assumed displaced shape used in the SDOF models affects all the main properties of the equivalent systems. A closer look at the responses found for the MDOF model (Fig. 6.1 and 6.2) shows that the drastic changes happening in the deflected shape (Fig. 6.2) are only for a few tenths of a second near the peaks. The average of the "plus" and "minus" curves are shown in Fig. 6.5 along with the deflected shapes used in the SDOF models. It can be seen that the average curves were very close to what was used in the SDOF models. This was particularly visible after nonlinear deformations had developed (T = 10.5 and T = 12.5 sec). The success of the SDOF models can be attributed to closeness of the assumed displaced shapes with the average shapes predicted by the MDOF model, and it can be concluded that such an agreement has led to a reasonable estimate of the properties of the equivalent SDOF systems.

The maximum lateral displacements are presented in Fig. 6.6. With respect to the absolute maximum displacements (Fig. 6.6.a), the results from different models are in agreement. The same holds true for response at the time of maximum displacement predicted by the SDOF models (Fig. 6.6.b). However, the correlation at time of maximum response predicted by the MDOF model is not consistent along the height. Excellent agreement was seen for the lower five floors, while at the roof, the MDOF model result was 34 percent larger than the result from the Q-Model(L) and 48 percent larger than that from the Q-Model. It can be seen in Fig. 6.1 that second mode contributions have caused these differences.

The slope of the curves in Fig. 6.6 shows the ratio of story drift and story height, and is representative of drift. No consistent trend is evident in comparing the slopes for the three curves in Fig. 6.6.c.

While very close agreement can be seen in the lower five stories, the slopes at the upper three stories are very different signifying the inadequacy of the SDOF models.

The performance of the SDOF models for EFS may be viewed satisfactory in terms of overall waveforms, amplitudes, and frequency contents, although significant differences were observed in a few instances. It is not certain whether the models would exhibit an acceptable performance if the frame had even more drastic stiffness interruption. Based on the reasonable results obtained for EFS and those for the test structures which were more uniform, it may be stated that the SDOF models are likely to yield acceptable results for planar structures ranging from uniform to irregular with stiffness interruptions of the type and magnitude which existed in EFS. The need to improve the SDOF models to obtain a better estimate of story drifts is evident.

CHAPTER SEVEN

PARAMETRIC STUDIES ON THE TEST STRUCTURES

7.1 Introductory Remarks

The research reported in Ref. 16 was in effect an experimental parametric study. However, due to the usual constraints on experimental works in terms of time and expense, relatively few parameters were considered. To carry out an extensive parametric study without an enormous cost, an analytical approach would have to be used utilizing a reliable analytical model. In Chapters Five, it was shown that both the original and the new versions of the Q-Model were successful in reproducing the response. In this chapter, the results of a sensitivity study utilizing the Q-Model is presented. The parameters considered here were the input earthquake and the wall height. Because the old and new versions of the Q-Model had yielded identical results and because the software necessary for the nonlinear static analysis required in the Q-Model was readily available, only the original version of the Q-Model was used in this part of the study.

7.2 Effect of Base Motion

(a) Earthquake Records - It is generally believed that different earthquakes have different effects on a given structure. The principal characteristics of earthquakes include frequency content, high amplitudes and number of their occurrence, and duration. In order to compare different earthquakes, one method is to compare the effect of the motions on a collection of single-degree-of-freedom elastic oscillators having different periods of vibration. This method leads to the construction of response spectra for displacement, velocity, and acceleration response. To estimate the relative effect of different ground

motions on an elastic multistory structure, the response can be found from the response spectra treating the structure as a SDOF system with a period equal to the fundamental period of the structure. For inelastic structures, because the stiffness changes with time, period is variable and any comparisons made in terms of the effect of different earthquakes would have to be for the expected period range. Another approach is to construct an inelastic response spectrum [18] and determine response based on an expected ductility. In using elastic spectra, even through the use of a period range, one may not necessarily obtain a close estimate of the response, because in construction of response spectra, it is assumed that the structure with certain period is subjected to the entire duration of the earthquake, while the effective period in an inelastic system may be reached after some time, and the inelastic system with the effective period may be subjected to only part of the earthquake.

To determine sensitivity of the response to earthquakes other than the simulated El Centro, structures FNW and FFW were analyzed for six earthquake acceleration records as listed below:

El Centro	1940, NS
El Centro	1940, EW
Taft	1952, N21E
Taft	1952, S69E
Imperial County Building	1979, EW
Bucharest	1977, NS

The intensity of an earthquake may be measured in terms of the maximum acceleration or the Housner spectrum intensity (SI), which is the integral of the velocity spectrum taken over the structural period ranging from 0.1 to 2.5 sec [13]. Because the second measure is

considered to be a better representative of the overall effect of earthquakes on structures, it was used in this study with the exception that the integral limits were changed to 0.04 and 1.0 seconds to account for the fact that the test structures had fundamental periods of approximately forty percent of period of full-scale structures with similar configuration. The earthquake acceleration records were normalized such that the spectral intensity for each case was equal to the SI of the simulated El Centro used in the experimental investigation [16]. The SI for the simulated earthquakes was 330 mm for FNW and 290 for FFW based on two percent damping. The duration was 15 sec in real earthquake time (6 sec of compressed record). The first four seconds of the county building record were deleted because of the very small amplitudes [11]. The maximum accelerations for different records are shown in Table 7.1.

The displacement, velocity, and acceleration response spectra for two percent damping are shown in Fig. 7.1. The fundamental period of the test structures at uncracked stage was approximately 0.2 second. Due to the nonlinear deformations anticipated during each earthquake, it was expected that the effective period would increase to, say, 0.4 sec. It can be seen in Fig. 7.1 that for the period ranging from 0.2 to 0.4 sec, the responses from different earthquakes showed different trends.

(b) Responses - The calculated displacement response histories for FNW are shown in Fig. 7.2. The time coordinate in each record was compressed by a factor of 2.5. The response caused by the original El Centro 40, NS appeared to be very similar to that induced by the simulated El Centro (Ch. 5). The responses due to the El Centro 40 (EW), Taft 52 (N21E), and Taft 52 (S69E), were identical in terms of

both the frequency contents and the displacement maxima. Similarities of this type can also be found in comparing the response due to El Centro 1940, NS, and that caused by the record measured at the Imperial County Building. The response for the Bucharest record did not resemble any other response. Only one high-amplitude wave was developed followed by low-amplitude responses with relatively long periods.

The above observations are also generally true for FFW responses (Fig. 7.3). With respect to the response due to the Bucharest record, the amplitudes were considerably lower than those in the FNW response. The difference can be explained as follows: By the end of the first second of the response, both FNW and FFW had an effective period of slightly over 0.2 second. Structure FFW was initially stiffer (due to the presence of the wall) and at the end of the first second was likely to have a period which was shorter than that of FNW. Noting the fact that for the period range of 0.3 and slightly larger, the velocity (and the input energy) increases with increase in the period (Fig. 7.1), the larger response for FNW would be expected.

With respect to the maximum displacements (Fig. 7.4), it can be seen that for FNW the deflections were relatively close. The top-level displacement response ranged from 18 to 25 mm. The response for the El Centro 40, EW, record coincided with the response due to the County Building record. The story drifts for different earthquakes were also identical. A wide scatter was visible in the FFW response maxima. The maximum top-level displacement ranged from 11 mm for the Bucharest record to 25 mm for the El Centro 40, NS record. However, responses from earthquakes other than Buchrest had a much smaller range. The response for the Taft N21E acceleration coincided the response due to the El Centro 40, EW.

The above observations suggest that different ground motions had generally different effects. It appeared that minor difference between the effective period of FNW and FFW caused a relatively large difference in the response due to the Bucharest record. In contrast, the difference in period did not have any significant influence on the response from El Centro NS. By comparing the displacement maxima from different earthquakes and the measured response (due to a simulated El Centro 40, NS), it can be also concluded that FNW and FFW did not develop any excessive deflections under ground motions other than the design earthquake.

The variations in the responses caused by earthquakes with the same SI suggest that SI is not necessarily a measure of effect of an earthquake on a given building. Comparison of the response due to Taft (N21E) and El Centro (NS) shows that, although the two records had approximately the same peak ground acceleration (PGA), the maximum response due to El Centro was more than 30 percent larger than that due to Taft. It appears that neither SI nor PGA alone are representative of severeness of the effects and other factors need to be considered.

7.3 Effect of Wall Height

In the experimental investigation reported in Ref. 16, three frame-wall structures were tested, one with a wall extending over the entire height of the structure, one with a single-story wall, and one with a four-story wall. The steel distribution was the same for all of the structures. There were minor variations in concrete compressive strength for different structures. Experimental results indicated that the location of wall cutoff point had a small effect on the overall response.

To determine whether the above observation would hold true for structures with walls discontinued at levels other than those considered in the experimental research, four hypothetical structures were generated and analyzed. The structures were named FW1, FW3, FW5, and FW7, with the numeral indicating the level at which the wall was discontinued. Structure FW9 was the same as FFW with respect to the dimensions, material properties, and reinforcement distribution. The material properties used for the other structures were the same as those of FFW. Structure FW1 was identical to FSW in terms of dimensions and reinforcement, but it had slightly different concrete properties. All the structures were analyzed for the simulated El Centro measured at the base of FFW during the first earthquake run. The original version of the Q-Model was used for the analyses. The Q-Model properties are listed in Table 7.2 and 7.3.

Figure 7.5 shows the response histories for different structures. It can be seen that the responses were identical in terms of waveforms and frequency contents. The fact that the frequency contents were very close to each other indicates that the point of wall discontinuity did not have any visible effect on the overall structural stiffness. This is despite the fact that the wall for each structure was carrying approximately 75 percent of base shear.

With respect to the maximum deflections and drifts (Fig. 7.6), the responses for different structures were close. Structure FW1 showed smaller first story drift due to the restraining effect of the first story wall. Comparison of the deflection of FW1 and FW3 shows a visible variation in the displaced shape caused by the increase in the height of the wall from 458 mm to 916 mm. In contrast, no significant difference can be seen in the deflected shapes for FW3, FW5, and FW7.

This suggests that the extra wall over the third level provided in FW5 and FW7 did not have any beneficial effects in controlling the displacements. The structure with a nine-story wall (FW9) had the largest deflections among all the structures. The deflections at the upper three levels were larger because of the fact that, to satisfy displacement compatibility, upper story walls in relatively tall walls tend to exert forces on the rest of the structure and cause more deflections.

The foregoing observations suggest that, as long as a shear wall was provided in the lower part of the structure, the deflections were controlled and a reasonably uniform distribution of story drifts could be achieved. It is worthwhile to note that these walls were connected to the frames through hinged links. It is not clear whether the above conclusion would be true for walls which are connected to the rest of the structure by moment resisting elements.

CHAPTER EIGHT

PARAMETRIC STUDIES ON THE HYPOTHETICAL STRUCTURES

8.1 Introductory Remarks

In Chapter Seven, the effect of different earthquakes on the structures designed based on the Substitute-Structure method [33] was studied. To determine the effect of different ground motions on structures proportioned using the UBC design procedure [14], the structures described in Sec. 3.3 were analyzed for a collection of earthquakes. Those structures in this group which had different wall widths were also studied to identify the effect of wall stiffness on the seismic response. Only the original version of the Q-Model was used. This chapter presents the results of these studies.

8.2 Effect of Base Motions

(a) Simulated Earthquakes - Structures UFNW and UFFW were analyzed for the earthquakes listed in Table 7.1, in addition to the simulated El Centro records measured in the experimental testing of FNW and FFW. The analyses for the latter records were conducted to compare the response of structures designed based on the UBC with the response of those designed using the Substitute-Structure method [33]. The Q-Model properties are listed in Table 8.1 and 8.2.

The response histories for the simulated earthquakes are shown in Fig. 8 with broken curves representing the measured responses of FNW and FFW. The major difference between the analytical and experimental results is in the effective periods. During the first 1.3 seconds no significant yielding occurred and stiffness was controlled by gross section properties which were the same for the hypothetical and the test structures. As a result, the analytical and experimental results

were close. However, after some of the elements yielded, the hypothetical structures had a shorter average period or a larger average stiffness caused by their generally higher steel ratio. Both FNW and UFNW had an effective period of slightly over 0.3 second with FNW period being somewhat larger. Beyond T = 2.3 sec, UFNW experienced several low-amplitude cycles while FNW continued to develop large peaks. The difference can be explained by considering the velocity response spectra for the simulated earthquake (Fig. 7.1). For periods of slightly larger than 0.3, the velocity spectra is steep, and the velocity increases significantly with minor increases in the period. Because the period of FNW was longer than the period for UFNW, FNW developed relatively larger peaks. The absolute maximum displacements for the two structures were close.

The response of UFFW was relatively close to that of FFW. The apparent period of UFFW was shorter than the period of FFW due to the higher steel ratio in UFFW. With respect to the absolute maxima, FFW experienced a twenty percent larger displacement.

(b) Other Earthquakes - The displacement response of UFNW for a collection of earthquakes is shown in Fig. 8.2. The ground motion accelerations were normalized such that the spectral intensity (SI) for each case was the same as the SI for the measured base acceleration in dynamic testing of FNW. Except for the response due to the Bucharest record, the response histories generally appeared identical. The structure passed its apparent yield displacement in all cases but the Bucharest earthquake. The Taft N21E motion caused the highest number of cycles with moderate to high amplitudes. The structure was not excited significantly by the Bucharest record, and it remained essentially elastic throughout the response. Comparison of this response with that

for FNW (Fig. 7.2) indicates that the larger amount of steel in UFNW prevented any significant yielding and kept the period in a range which was not sensitive to the Bucharest earthquake.

The above observations are also true for structure UFFW (Fig. 8.3), except for the points regarding the Bucharest results. Neither FFW (Fig. 7.3) nor UFFW were affected significantly by this earthquake.

The maximum displacements and story drifts are shown in Fig. 8.4. It can be seen that, except for the deflection due to the Bucharest record, the maximum deflections caused by different earthquakes were close. The same is true for story drifts. Because the maximum deflection is a representative of the maximum ductility demand, it can be concluded that, if these structures are properly detailed to withstand one of these earthquakes, they are likely to survive the others.

8.3 Effect of Wall Stiffness

Small-scale structures with full-height wall having different widths (Sec. 3.3) were used to identify the influence of wall stiffness on the seismic response. These structures, namely UFW100, UFW150, UFFW, UFW 250, and UFW 300, were designed using the UBC provisions and assuming material properties the same as the measured values for FFW. The numeral in each name indicates the wall width in terms of millimeter. Structure UFFW had a wall width of 203 mm, the same as the wall width for FFW.

The wall widths presented a variety of lateral stiffness distributions between the wall and the frames in each structure. The ratio of base shear (for a triangular load distribution with maximum at the top level) carried by the wall in the uncracked stage ranged from 34 percent for UFW100 to 87 percent for UFW300. The ratios increased

slightly as the columns and beams started to yield, then dropped slightly as the wall base yielded. Table 8.3 presents the percentage of base shear carried by the wall at three stages of static lateral loading: uncracked stage, the apparent yield point on the moment-deflection curve for the structure, and the case with the top-level displacement equal to two percent of the total structural height.

The Q-Model properties are listed in Tables 8.4 and 8.5. The structures were analyzed for the first six seconds of the base acceleration measured in the first earthquake testing of FFW. The input acceleration was a simulated El Centro, NS, 1940.

Comparison of top-level displacement histories (Fig. 8.5) indicates that the responses had the same general characteristics in terms of frequency content and amplitudes. Number of high-amplitude cycles was the same for different structures suggesting that the demand for the number of load reversals without failure was approximately the same for the structures. All structures showed a series of small amplitudes between T = 3 and 5 sec. With respect to the maximum deflections (Fig. 8.6), considerable variations among the shapes were visible, although the maxima at the upper level of different structures were close. The deflected shape for UFW100 and UFW150 was "bulged," which is the type of deflections expected of frame structures and structures with relatively "soft" walls. The first story drift was the largest for these two structures. No particular beneficiary effect was realized in increasing the wall width from 203 mm (in UFFW) to 300 mm (in UFW300). In terms of the overall response it can be concluded that while the response waveforms and maximum displacements for different structures were close, structures UFFW, UFW250, and UFW300 performed better in that they had considerably smaller first story drifts.

CHAPTER NINE

SUMMARY AND CONCLUSIONS

9.1 Summary of Research

The study presented in this report consisted of two main parts. The first part was the development and evaluation of a simple single-degree-of-freedom (SDOF) approximate model for the nonlinear displacement response calculation of planar reinforced concrete structures subjected to earthquakes. This model is a simpler version of another model, called the Q-Model, which was previously developed and found successful in response prediction of several uniform structures [28]. The new model was called the Q-Model(L) with (L) standing for the limit analysis method used in the process of determining the properties of the SDOF model. The new version was developed with the aim of its eventual use for design purposes. The Q-Model(L) was used for the seismic analysis of a series of "irregular" small-scale and full-scale reinforced concrete frames and frame-wall structures. The "irregularity" in these structures was due to one or more of the following: drastic change in height from one story to the next, discontinued wall, and setbacks. The objective of the first part of the study was to determine whether the simplified modeling is successful for irregular structures as well as uniform structures studied previously [28].

To evaluate the results obtained from the Q-Model(L), four small-scale nine-story three-bay reinforced concrete structures and a full-scale eight-story reinforced concrete structure were analyzed. All of these structures were idealized as planar systems. The small-scale structures were those tested by Moehle [16] using the shake table at the Newmark Civil Engineering Laboratory, University of Illinois. One of these structures comprised only two parallel frames, while the

others had walls discontinued at different levels. The measured displacement histories of these structures for a design simulated El Centro were considered as the exact response and used as the basis to evaluate the analytical results.

The full-scale eight-story frame was generated for the purpose of this study and did not represent any actual structure. This frame had three equal spans in the lower three stories, and only the middle span extended over the entire height providing a 67 percent setback in the upper five stories. A reasonable reinforcement distribution was obtained based on the provisions of the Uniform Building Code [14] even though the UBC requirements are not strictly developed for irregular structures. The ACI Code was used for the final design [2]. Because there were no experimental data available for this frame, the "true" nonlinear response was estimated using a multi-degree-of-freedom (MDOF) analytical model [26]. The structure was analyzed for the north-south component of El Centro 1940 record using both the original and the new versions of the Q-Model, and the results were studied in relation to the "true" response.

The second part of the study presented here was aimed at determining the influence of different parameters on the nonlinear seismic response of planar structures. Initially, a study was conducted to identify the sensitivity of the Q-Model response to slight changes in the assumptions made in finding the Q-Model properties. Parameters considered were damping factor, elastic stiffness, post-yielding stiffness, and base moment at apparent yielding of the structure. This study was carried out on one of the small-scale test structures.

The parametric study on different structures followed the initial

part and included the following variables: design method, input earthquake, wall cutoff point, and wall stiffness relative to the total structural stiffness.

The design methods were the Substitute-Structure method and the Uniform Building Code Procedure. The input earthquakes were both components of El Centro 1940, both components of Taft 1952, east-west component of the 1979 earthquake measured at the ground floor of the Imperial County Services Building, and the north-south component of Bucharest 1977. The wall cutoff points were chosen at alternate levels starting with level one. The wall stiffness was varied by changing the wall width in a structure with a wall extended over the total height of the structure. The wall width was varied from 100 mm to 300 mm providing wall-to-structure stiffness ratios ranging from 34 to 87 percent for the uncracked stage. To assess the effect of these parameters, response characteristics such as amplitudes, waveforms, frequency contents, number of moderate and large amplitudes, maximum deflections and maximum story drifts were considered.

9.2 Observations

In the course of the study presented in this report, the following important points were noted.

(a) SDOF Modeling

1. The earthquake response of four small-scale two-dimensional physical models and a full-scale hypothetical planar frame was successfully estimated using a simple nonlinear "single-degree" model.

2. The Q-Model(L), through the use of limit analysis method, provided an analytical tool which was simpler than the original version of the Q-Model.

3. With respect to the test structures, the fact that the structures were irregular in the plane did not appear to require any particular modification in the Q-Model.

4. For the full-scale frame (Sec. 3.4), the setbacks led to a displacement response with significant contribution from the second mode of vibration. Such behavior contradicted the assumption of a single deflected shape utilized in the Q-Model. As a result, the Q-Model failed to yield accurate relative story displacements. However, the overall displacement response was calculated reasonably well using the Q-Model.

(b) Effect of the Q-Model Properties

In the course of finding the effect of different modeling parameters on the Q-Model response, it was noted that the results were insensitive to the damping factor as long as the system developed significant nonlinearity. In addition, it was found that the response was not affected by slight variations ($\pm$ 10 percent) in the elastic and post-yielding stiffness of the displacement-moment curve. The response was somewhat sensitive to the magnitude of the moment at the break point (the apparent yield point) in the displacement-moment curve.

(c) Parametric Studies

1. In comparison of structures designed based on the provisions of the Uniform Building Code and those designed using the Substitute-Structure method, it was found that the former required a slightly larger amount of steel. The seismic responses of the two groups were similar.

2. Different base motions with the same spectrum intensities led to responses with no consistent trend. No correlation was observed between the maximum acceleration and spectrum intensities. There was

also no correlation between the maximum displacement response and either of the maximum acceleration or the spectrum intensity (Table 7.1). Earthquakes causing similar maximum deflections led to responses with different number of high amplitudes (Fig. 7.2, 7.3, 8.2, and 8.3).

3. Responses of structures with different wall heights were generally identical. One-story and three-story walls appeared to provide sufficient resistance against excessive story drift at lower stories. The structure with a nine-story wall experienced the largest total deflections.

4. The maximum top-level deflections for structures with different wall widths were close. Deflected shape for the structure in which the wall provided for about fifty percent of lateral stiffness was dominated by a frame type of deflection (somewhat bulged at lower floors). Increase in the wall width from 203 mm (in FFW) to 300 mm (in UFW 300) did not have any significant effect on the structural deflection.

9.3 Conclusions

Based on the study presented in this report, several statements may be made as follows. The conclusions are separated into three groups regarding: (1) the modeling method, (2) properties of the Q-Model, and (3) the parametric studies.

(a) SDOF Modeling

The test structures described in Chapter Three were effectively two-dimensional irregular systems subjected to one horizontal component of an earthquake simulated in the strong direction of the structures. For these structures, both the original and the new versions of the Q-Model led to results in reasonable agreement with the experimental data. The Q-Model was previously found successful for a series of

uniform two-dimensional systems. The success of the Q-Model suggests that the model is likely to produce acceptable results for other similar structures, uniform or irregular, subjected to seismic loading in their planes.

Two important points deserve attention, one about the structures and the other concerning the earthquakes. With respect to the test structures, it should be noted that the "irregularity" in the structures was somewhat limited and confined to a symmetric type. More research is needed to determine the extent to which an approach similar to the Q-Model is applicable. Simplified analysis of irregular structures with unsymmetric distribution of mass or stiffness, or both, is also a topic which deserves extensive research.

The earthquakes considered in this study were unidirectional. Real earthquakes have three translation components, two of which are not included in the Q-Model in its present form. Therefore, the Q-Model response should not be considered the "true" response. Nevertheless, compared to the conventional elastic analyses with a set of static equivalent lateral loads and compared to the response spectra method, the Q-Model provides a much more "realistic" approach in displacement response estimation. The Q-Model is not the realistic analytical model; rather, it is a step towards a simplified and realistic model.

The Q-Model response for the eight-story frame (Sec 3.4) exhibited characteristics similar to the response from the multi-degree-of-freedom analysis. The sixty seven percent setbacks at the upper five stories provided a drastic change of mass and stiffness to the extent that the response contained significant contribution from the second mode of vibration. The contribution from the second mode (which is not considered in the Q-Model) led to an unacceptable estimate of the

deflected shape by the Q-Model. Attempts should be made to improve the Q-Model in this respect. The quality of the response for the eight-story frame, however, suggests that the Q-Model in its present form can be the starting point.

(b) Effect of the Q-Model Properties

The Q-Model response does not appear to be significantly affected by slight variation in the Q-Model properties. This conclusion is reached for a structure which experienced maximum deflections of approximately 2.5 times the displacement at the apparent yield point of the structure (Chapter Four). While this conclusion may be valid for earthquakes with broad-band spectra, it is not applicable to earthquakes which are sensitive to slight variations in the period of the structure [25]. Among the parameters studied, the apparent yield base moment appears to be the one with somewhat pronounced effect.

(c) Parametric Studies

The effect of an earthquake on a structure is defined in terms of maximum displacement (and the maximum ductility demand), maximum story drifts, and the number of yielding cycles it produces at joints. The study presented here showed that neither the peak ground acceleration (PGA) nor spectrum intensity can be a measure of these effects (Sec. 7.2). Earthquakes with PGA of 0.26g and 0.36g appeared to have identical effects, while other earthquakes with the same spectrum intensity led to totally different results.

With respect to the effect of wall cutoff point on the displacement response, the frequency content and waveforms do not appear to be sensitive to this parameter. Presence of the wall at lower few stories reduces the story drifts for structures with "soft" first story. No

beneficial effect is seen by extending the wall over the full height of the structure to control the displacements and drifts at upper stories.

In comparison of the response of structures designed based on the UBC provisions and the Substitute-Structure method, it is noted that the structural responses for the two groups were identical, while the Substitute-Structure method led to a slightly more economical designs.

The study on structures with different wall stiffnesses revealed that increase in wall stiffness to control story drifts was effective only to a certain extent. The structure in which the wall stiffness was seventy five percent of the total stiffness based on gross section properties experienced the least drifts.

LIST OF REFERENCES

1. ACI-ASCE Committee 352, "Recommendations for Design of Beam-Column Joints in Monolithic Reinforced Concrete Structures," ACI Journal, Vol. 73, No. 7, July 1976, pp. 375-393.

2. ACI Committee 318, "Building Code Requirements for Reinforced Concrete," American Concrete Institute, Detroit, Michigan, 1977.

3. Aoyama, H., "Simple Nonlinear Models for the Seismic Response of Reinforced Concrete Buildings," U.S.-Japan Cooperative Research Program in Earthquake Engineering with Emphasis on the Safety of School Buildings, August 1975, pp. 291-309.

4. Aziz, T. S., "Inelastic Dynamic Analysis of Building Frames," Publication No. R76-37, Department of Civil Engineering, Massachusetts Institute of Technology, Cambridge, August 1976.

5. Banon, H., J. M. Biggs, and H. M. Irvine, "Seismic Damage in Reinforced Concrete Frames," Journal of the Structural Division, ASCE, Vol. 107, No. ST9, September 1981, pp. 1713-1729.

6. Bathe, K-J., E. L. Wilson, and F. E. Peterson, "SAP IV, A Structural Analysis Program for static and Dynamic Response of Linear Systems," Earthquake Engineering Research Center, Report No. EERC 73-11, University of California, Berkeley, April 1974.

7. Biggs, J. M., Introduction to Structural Dynamics, McGraw-Hill Book Co., 1964.

8. Clough, R. W. and S. B. Johnston, "Effect of Stiffness Degradation on Earthquake Ductility Requirements," Proceedings, Japan Earthquake Engineering Symposium, Tokyo, October 1966, pp. 195-198.

9. Clough, R. W. and J. Penzien, Dynamics of Structures, McGraw-Hill Book Company, 1975.

10. Derecho, A. T., S. K. Ghosh, M. Iqbal, G. N. Freskakis, and M. Fintel, "Structural Walls in Earthquake-Resistant Buildings, Dynamic Analysis of Isolated Structural Walls, Parmetric Studies," Portland Cement Association, March 1978.

11. Haroun, M., "Corrected Accelerograms and Response Spectra, Imperial Valley Earthquake of October 15, 1979," Earthquake Engineering Research Laboratory, California Institute of Technology, March 1980.

12. Hodson, K. E., "Simplified Inelastic Analysis of Reinforced Concrete Frame-Wall Structures Subjected to Earthquakes," Thesis, submitted in partial fulfillment of the degree of Master of Science, Graduate School, University of Nevada, Reno, Nevada, May 1982.

13. Housner, G. W., "Behavior of Structures During Earthquakes," Journal of the Engineering Mechanics Division, ASCE, Vol. 85, No. EM4, October 1959, pp. 108-129.

14. International Conference of Building Officials, Uniform Building Code, Whittier, California, 1979.

15. Lybas, J. M. and M. A. Sozen, "Effect of Beam Strength and Stiffness on Dynamic Behavior of Reinforced Concrete Coupled Walls, Civil Engineering Studies, Structural Research Series No. 444, University of Illinois, Urbana, July 1977.

16. Moehle, J. P. and M. A. Sozen, "Experiments to Study Earthquake Response of R/C Structures with Stiffness Interruptions," Civil Engineering Studies, Structural Research Series No. 482, University of Illinois, Urbana, August 1980.

17. Newmark, N. M., "A Method of Computation for Structural Dynamics," Journal of Engineering Mechanics Division, ASCE, Vol. 85, EM3, July 1959, pp. 69-86.

18. Newmark, N. M., and E. Rosenbluth, Fundamentals of Earthquake Engineering, Prentice-Hall, Inc., 1971.

19. Otani, S., and M. A. Sozen, "Behavior of Multistory Reinforced Concrete Frames During Earthquakes," Civil Engineering Studies, Structural Research Series No. 392, University of Illinois, Urbana, November 1972.

20. Penzien, J., "Elasto-Plastic Response of Idealized Multi-Story Structures Subjected to a Strong Motion Earthquake," Proceedings of the Second World Conference on Earthquake Engineering, Tokyo, Japan, July 1960, Vol. II, pp. 739-760.

21. Penzien, J., "Earthquake Response of Irregularly Shaped Buildings," Proceedings of the Fourth World Conference on Earthquake Engineering.

22. Pique, J. R., "On the Use of Simple Models in Nonlinear Dynamic Analysis," Publication R76-43, Department of Civil Engineering, Massachusetts Institute of Technology, Cambridge, September 1976.

23. Popov, E. P., "Seismic Behavior of Structural Subassemblages," Journal of the Structural Division, ASCE, Vol. 106, No. ST7, July 1980, pp. 1451-1474.

24. Powell, G. H. and D. G. Row, "Influence of Analysis and Design Assumptions on Computed Inelastic Response of Moderately Tall Frames," Earthquake Engineering Research Center, Report No. EERC 76-11, University of California, Berkeley, April 1976.

25. Saiidi, M. and M. A. Sozen, "Simple and Complex Models for Nonlinear Seismic Analysis of Reinforced Concrete Structures," Civil Engineering Studies, Structural Research Series No. 465, University of Illinois, Urbana, August 1979.

26. Saiidi, M., "User's Manual for the LARZ Family, Computer Programs for Nonlinear Seismic Analysis of Reinforced Concrete Planar Structures," Civil Engineering Studies, Structural Research Series No. 466, University of Illinois, Urbana, November 1979.

27. Saiidi, M., "Influence of Hysteresis Models on Calculated Seismic Response of Reinforced Concrete Structures," Proceedings of the Seventh World Conference on Earthquake Engineering, Istanbul, Turkey, September 1980, Vol. 5, pp. 423-430.

28. Saiidi, M. and M. A. Sozen, "Simple Nonlinear Seismic Analysis of RC Structures," Journal of the Structural Division, ASCE, Vol. 107, No. ST5, May 1981, pp. 937-952.

29. Saiidi, M., "Seismic Study of Imperial County Services Building," Proceedings of the 2nd ASCE-EMD Structural Dynamics Specialty Conference, Atlanta, GA., January 1981, pp. 431-444.

30. Saiidi, M., "Hysteresis Models for Reinforced Concrete," to appear in Journal of the Structural Division, ASCE, Vol. 108, No. ST5, May 1982.

31. Saiidi, M., Discussion on "Seismic Response of Reinforced Concrete Frames," Journal of the Structural Division, ASCE, Vol. 108, No. ST2, February 1982.

32. Saul, W.E., J. F. Fleming, and S. L. Lee, "Dynamic Analysis of Bilinear Inelastic Multiple Story Shear Buildings," Proceedings of the Third World Conference on Earthquake Engineering, Auckland, New Zealand, January 1965, Vol. II, pp. 533-545.

33. Shibata, A. and M. A. Sozen, "Substitute-Structure Method for Seismic Design in R/C," Journal of the Structural Division, ASCE, Vol. 102, No. ST1, January 1981, pp. 937-952.

34. Sozen, M.A., "Hysteresis in Structural Elements," Applied Mechanics in Earthquake Engineering, ASME, MMD, Vol. 8, November 1974, pp. 63-97.

35. Takeda, T., M. A. Sozen, and N. N. Nielsen, "Reinforced Concrete Response to Simulated Earthquake," Journal of The Structural Division, ASCE, Vol. 96, ST12, December 1970, pp. 2557-2573.

36. Takizawa, H., "Nonlinear Models for Simulating the Dynamic Damaging Process of Low-Rise Reinforced Concrete Buildings During Severe Earthquakes," International Journal of Earthquake Engineering and Structural Dynamics, Vol. 4, No. 1, July 1975, pp. 73-94.

37. Tansirikongkol, V. and D. A. Pecknold, "Approximate Modal Analysis of Bilinear MDF Systems Subjected to Earthquake Motions," Civil Engineering Studies, Structural Research Series, No. 449, University of Illinois, Urbana, August 1978.

TABLE 3.1 - Material Properties for Test Structures

Concrete

Structure	Compressive Strength, f'_c (MPa)	Tensile Strength (MPa)	Strain at f'_c	Ultimate Strain	Mod. of Elast. (MPa)	Descend. Slope (MPa)
FNW	39.9	3.5	0.003	0.004	20,300	6,000
FSW	37.1	3.1	0.003	0.004	18,000	5,570
FHW	35.9	3.6	0.003	0.004	19,000	5,390
FFW	34.5	3.0	0.003	0.004	18,700	5,180

Steel

Element	Yield Stress (MPa)	Modulus of Elasticity (MPa)	Strain at Start of Strain-Hardening	Strain-Hardening Slope (MPa)
Wall	339	200,000	0.005	1680
Beams and Columns	399	200,000	0.0045	1060

Note: Tensile Strength is based on split cylinder test

TABLE 3.2 - Material Properties for EFS

Concrete	Compressive Strength (f'_c)	4.0 ksi
	Tensile Strength	0.474 ksi
	Strain at f'_c	0.002
	Strain at Ultimate Point	0.003
	Modulus of Elasticity	3,600 ksi
	Descending Slope	300 ksi
Steel	Yield stress	60 ksi
	Modulus of Elasticity	29,000 ksi
	Strain at Start of Strain Hardening	0.00207
	Strain-Hardening Slope	2,900 ksi

See Appendix D for Unit Conversion Factors

TABLE 3.3 - Lateral Forces for Hypothetical Small-Scale Structures

Unit = N

	Level								
Structure	9	8	7	6	5	4	3	2	1
UFNW	1092	981	877	764	657	547	435	328	217
Others	1304	1171	1048	913	784	653	519	392	259

TABLE 3.4.a - Design Forces for UFNW

Element	Axial Force (KN)	Moment (KN-mm)
Level 1-3 Beams	0	165.2
Level 4-9 Beams	0	108.0
First Story Ext. Col's.	4.84	363.7
Story 1-2 Int. Col's	4.84	363.7
All other Columns	3.62	149.6

TABLE 3.4.b - Design Forces for Hypothetical Frame-Wall Structures

Force	UFW100	UFW150	UFFW	UFW250	UFW300
Beam Mom. (KN-mm)	162.6	135.4	113.3	96.9	86.9
Col. Ax. Load (KN)	4.73	4.11	4.15	4.19	5.3
Col. Mom. (KN-mm)	297.6	192.8	159.1	129.7	97.9
Wall Mom. (KN-mm)	1360.	2785.	4300.	5613.	6966.

TABLE 3.5.a. Reinforcement, Ratios (x 100) for UFNW

Element	Beams (Levels 1-3)	Beams (Levels 4-9)	Columns (Ext. Story 1) (Int. Story 1-2)	Other Columns
Reinforcement Ratios	1.47	0.91	1.91	0.61

TABLE 3.5.b. Reinforcement, Ratios (x 100) for Hypothetical Frame-Wall Structures

Element	UFW100	UFW150	UFFW	UFW250	UFW300
Beams	1.47	1.13	0.98	0.85	0.74
Columns	1.52	0.81	0.61	0.61	0.61
Walls	1.50	1.23	1.05	0.85	0.70

TABLE 5.1 - Flexural Properties of Elements in Test Structures

Structure	Element	Crack. Mom. (KN-mm)	Yield Mom. (KN-mm)	Post-Yield Mom. (KN-mm)	Yield Curv. (1/mm) $\times 10^6$	Post-Yield Curv. (1/mm) $\times 10^6$
FNW	Beams (level 4-9)	32.	91.9	94.	92.7	1300.
	Beams (level 1-3)	32.	134.	135.	98.6	1330.
	Columns (Story 6-9)	69.7	162.	170.	64.2	836.
	Columns (Ext. Story 2-5 Int. Story 3-5)	89.	205.	207.	69.	869.
	Columns (Ext. Story 1 Int. Story 1-2)	98.7	346.	354.	75.5	900.
FSW	Beams	27.4	91.	92.1	94.7	1310.
	Columns (Story 6-9)	61.4	161.	167.	65.7	845.
	Columns (Story 1-5)	83.4	208.	209.	71.6	891.
	Wall	783.	4217.	4918.	12.4	169.
FHW	Beams	32.8	91.3	100.	94.2	652.
	Columns (Story 6-9)	71.2	161.	174.	65.2	580.
	Columns (Story 1-5)	93.1	209.	219.	71.	472.
	Wall	937.	4219.	4919.	12.3	169.
FFW	Beams	28.4	91.5	101.	93.7	660.
	Columns (Story 6-9)	63.2	161.	174.	64.9	588.
	Columns (Story 1-5)	85.2	209.	220.	70.6	480.
	Wall	812.	4221.	4921.	12.3	169.

Note: Post-yielding quantities represent values for an arbitrary point beyond yield point.

TABLE 5.2.a. - Normalized Displaced Shapes for Q-Model Analysis of Test Structures

Level	9	8	7	6	5	4	3	2	1
FNW	1.00	0.96	0.95	0.89	0.81	0.71	0.60	0.48	0.34
FSW	1.00	0.98	0.93	0.85	0.74	0.60	0.43	0.25	0.11
FHW	1.00	0.98	0.94	0.87	0.76	0.62	0.48	0.23	0.20
FFW	1.00	0.94	0.87	0.78	0.68	0.57	0.44	0.32	0.19

TABLE 5.2.b. - Q-Model Properties for the Test Structures

Structure	Eq. Mass (Kg)	Eq. Height (mm)	Mom. at Break Pt. (KN-mm)	Disp. at Break Pt. (mm)	Post Yield. Slope (KN-mm/mm)
FNW	3540.	1544.	14500.	7.0	108.
FSW	3340.	1646.	14500.	6.6	214.
FHW	3340.	1606.	16920.	8.3	160.
FFW	3150.	1620.	18130.	8.2	166.

TABLE 5.3.a. - Normalized Displaced Shapes for Q-Model(L) Analysis of Test Structures

Level	9	8	7	6	5	4	3	2	1
FNW	1.00	0.96	0.91	0.83	0.74	0.64	0.53	0.42	0.30
FSW	1.00	0.95	0.88	0.78	0.66	0.52	0.37	0.22	0.10
FHW	1.00	0.95	0.87	0.78	0.66	0.52	0.39	0.25	0.14
FFW	1.00	0.92	0.83	0.73	0.61	0.49	0.37	0.24	0.13

TABLE 5.3.b. - Q-Model(L) Properties for the Test Structures

Structure	Eq. Mass (Kg)	Eq. Height (mm)	Mom. at Break Pt. (Kn-mm)	Disp. at Break Pt. (mm)	Post-Yield. Slope (KN-mm/mm)
FNW	3260.	1570.	12100.	5.2	144.
FSW	3190.	1668.	13630.	6.2	174.
FHW	3170.	1655.	13650.	4.7	192.
FFW	3190.	1661	16090.	5.7	192.

TABLE 6.1 - Flexural Properties of Elements in EFS

Element	Crack. Mom (k-in)	Yield Mom. (k-n)	Post-Yield. Mom. (k-in)	Yield Curv. $(1/in)x10^6$	Post-Yield. Curv. $(1/in)x10^6$	Bond Slip Rot. at Yield $(1/in)x10^6$	Bond Slip Rot. at Post Yield $(1/in)x10^6$
Beams (Fl. 5-7)	506	4546	5400	186	749	19.6	27.6
Other Beams	506	3606	4288	179	827	15.4	21.8
Columns (St. 1-3, Ext.)	1734	6171	8411	127	627	23.4	43.5
Columns (St. 1-4)	2710	9208	11734	145	410	28.9	46.9
Columns (St. 5-8)	1822	7511	10167	132	550	33.3	61.0

Note: Post-yield quantities represent values for an arbitrary point beyond yield point.
Bond-slip rotations before cracking were ignored.
Bond-slip rotations are for unit length of each element.

TABLE 6.2 - Normalized Displaced Shapes for EFS

Level	Roof	8	7	6	5	4	3	2
Q-Model	1.0	0.91	0.80	0.65	0.48	0.33	0.22	0.11
Q-Model(L)	1.0	0.89	0.75	0.58	0.40	0.25	0.15	0.06

TABLE 6.3 - Q-Model Properties for EFS

Parameter	Eq. Mass (kip-mass)	Eq. Height (in)	Mom. at Break Pt. (k-in)	Disp. at Break Pt. (in)	Post-Yield. Slope (k-in/in)
Q-Model	1.74	776	150,000	6.26	6340
Q-Model(L)	1.74	823	142,000	5.19	5490

TABLE 7.1 - Maximum Acceleration for Different Records

Earthquake	Max. Acc. in Original Record (g)	Scaled Max. Acc. (g) FNW	FFW
El Centro N-S	.348	.412	.363
El Centro E-W	.214	.295	.260
Taft N21E	.156	.401	.354
Taft S69E	.179	.405	.357
Bucharest N-S	.206	.155	.136
Imp. County Bldg. E-W	.331	.357	.314

TABLE 7.2 - Normalized Displaced Shapes for Structures with Different Wall Heights

Structure	9	8	7	6	5	4	3	2	1
FW1	1.0	.98	.93	.86	.75	.60	.42	.24	.10
FW3	1.0	.98	.92	.84	.72	.58	.43	.29	.17
FW5	1.0	.98	.93	.86	.75	.61	.47	.33	.20
FW7	1.0	.97	.91	.81	.69	.57	.44	.31	.19
FW9	1.0	.94	.87	.78	.68	.57	.44	.32	.19

TABLE 7.3 - Q-Model Properties for Structures with Different Wall Heights

Structure	Equivalent Mass (kg)	Equivalent Height (mm)	Yield Mom. (KN-mm)	Yield Disp. (KN-mm)	Post Yield Slope (KN-mm/mm)
FW1	3360.	1643.	15710.	6.5	228
FW3	3260.	1613.	15710.	6.1	182
FW5	3320.	1609.	16920.	8.5	164
FW7	3220.	1623.	16920.	7.2	174
FW9	3150.	1620.	18130.	8.2	166

TABLE 8.1 - Normalized Displaced Shapes for Structures Designed Based on UBC

Structure	9	8	7	6	5	4	3	2	1
UFNW	1.0	0.98	0.94	0.88	0.79	0.69	0.58	0.48	0.35
UFFW	1.0	0.94	0.87	0.79	0.69	0.58	0.45	0.32	0.19

TABLE 8.2 - Q-Model Properties for Structures Designed Based on UBC

Structure	Equivalent Mass (kg)	Equivalent Height (mm)	Yield Moment (KN-mm)	Yield Disp. (mm)	Post Yield Slope (KN-mm/mm)
UFNW	3380.	1545.	18795.	8.0	131.
UFFW	3160.	1632.	22821.	8.5	116.

TABLE 8.3 - Percentage of Shear Carried by the Wall in Structures with Different Wall Widths

	Uncracked	Apparent Yield	2 Percent Drift
UFW100	34	31	28
UFW150	59	54	49
UFFW	74	67	59
UFW250	82	69	61
UFW300	87	76	63

TABLE 8.4 - Normalized Displaced Shapes for Structures with Different Wall Widths

Level	9	8	7	6	5	4	3	2	1
UFW100	1.0	0.98	0.94	0.88	0.81	0.72	0.61	0.48	0.33
UFW150	1.0	0.97	0.92	0.85	0.76	0.66	0.54	0.40	0.25
UFW250	1.0	0.92	0.83	0.73	0.62	0.51	0.39	0.27	0.15
UFW300	1.0	0.91	0.81	0.70	0.59	0.48	0.36	0.25	0.14

TABLE 8.5 - Q-Model Properties for Structures with Different Wall Widths

Structure	Eq. Mass (ton)	Eq. Height (mm)	Moment at Break Pt.	Disp. at Break Pt.	Post Yield Slope (KN-mm/mm)
UFW100	3.40	1544.	21480.	8.08	353.
UFW150	3.32	1594.	21480.	8.82	265.
UFW250	3.06	1664.	22150.	6.64	231.
UFW300	3.00	1678.	22150.	6.22	213.

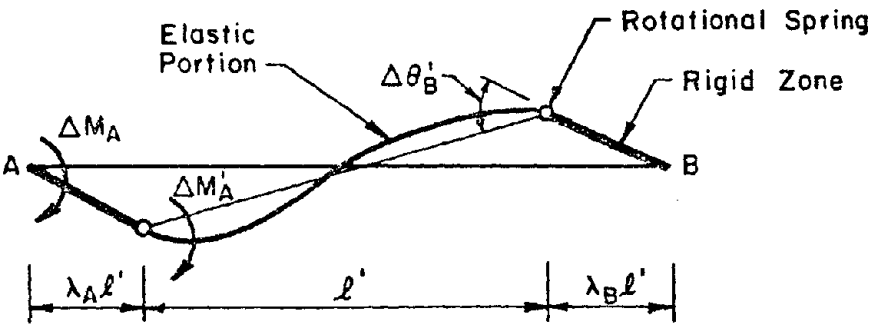

Fig. 2.1 Idealized Structural Element

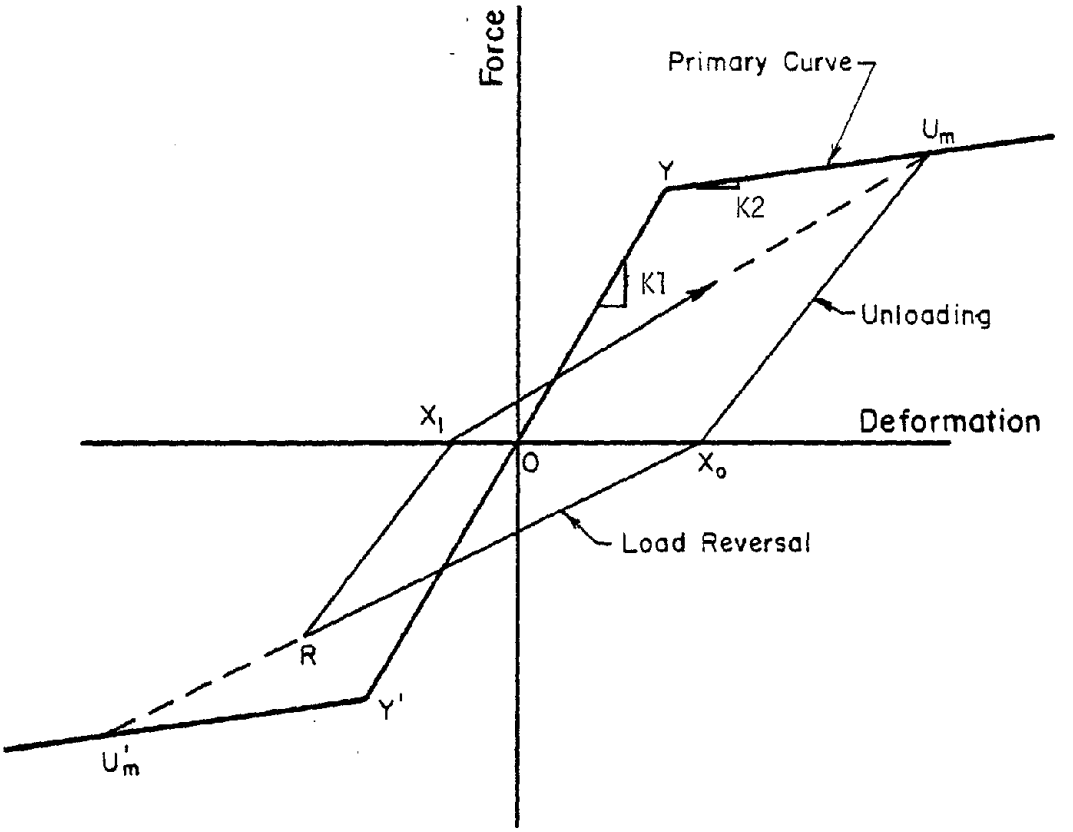

Fig. 2.2 Q-Hyst System

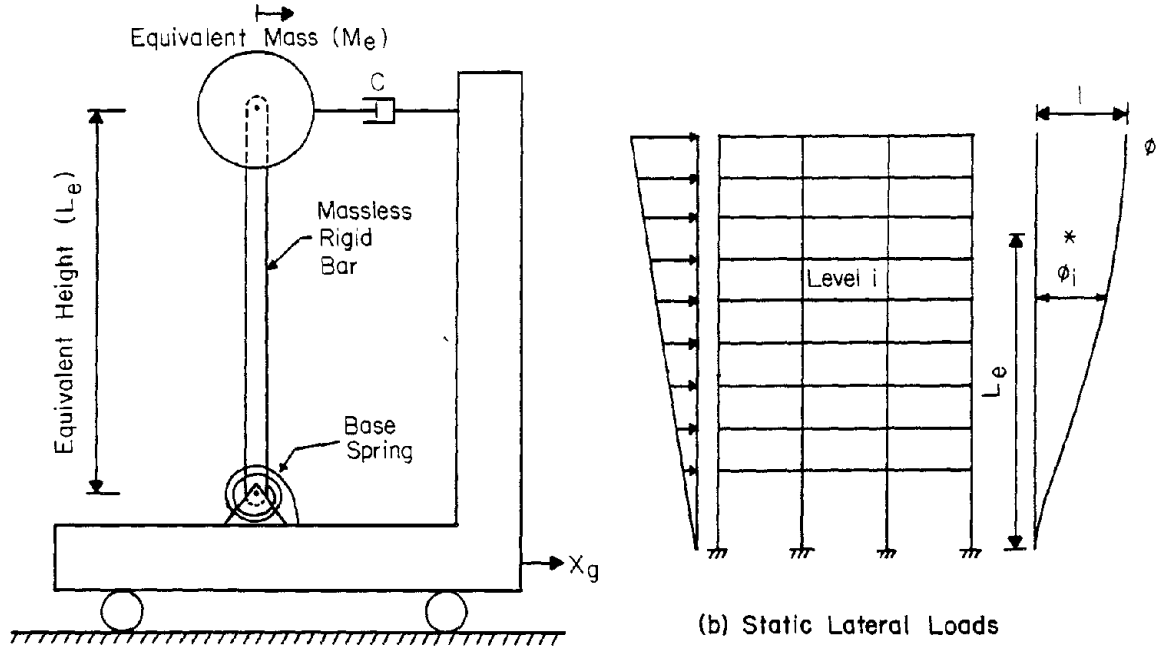

Fig. 2.3 Q-Model and Multistory Structure

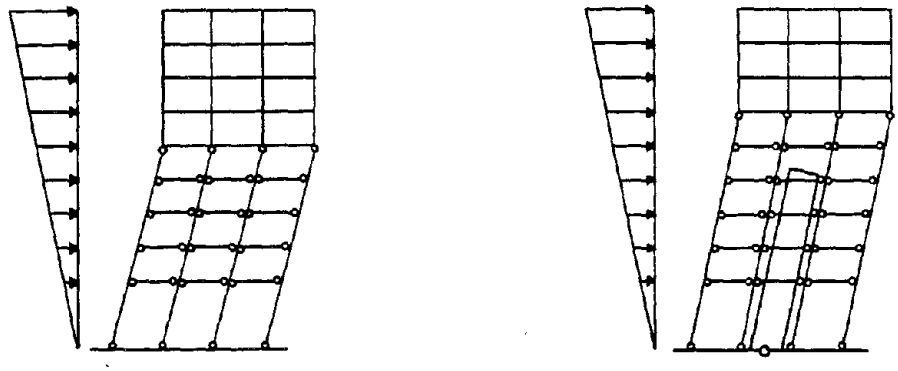

Fig. 2.4 Sample Collapse Mechanisms

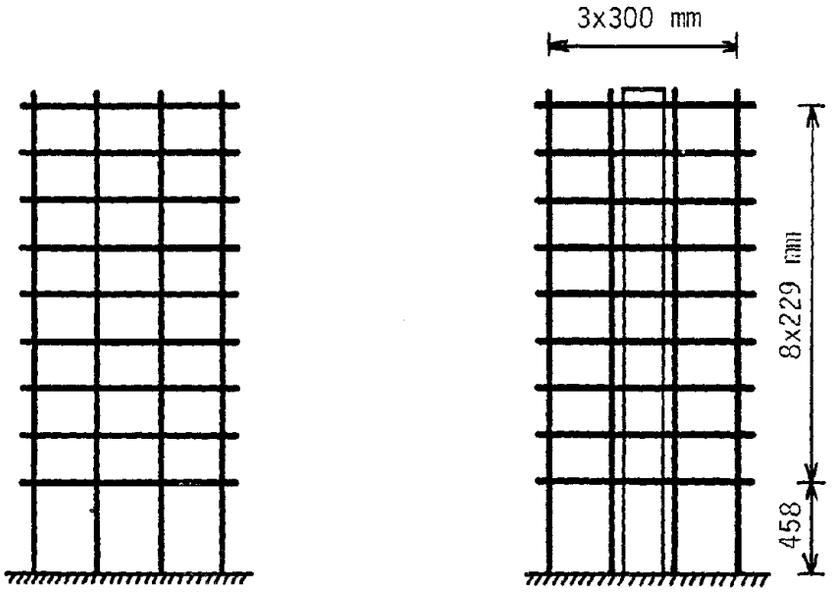

(a) No Wall
FNW

(b) Full-Height Wall
FFW

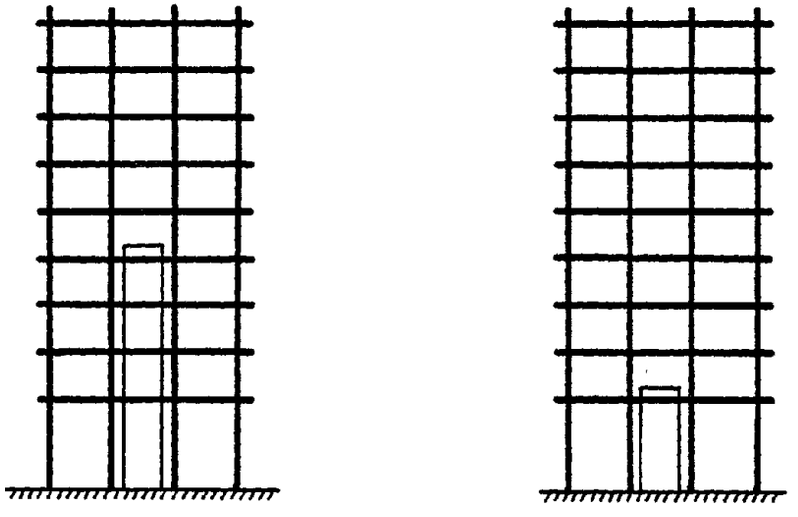

(c) Four-Story Wall
FHW

(d) One-Story Wall
FSW

Fig. 3.1 Elevation of Test Structures

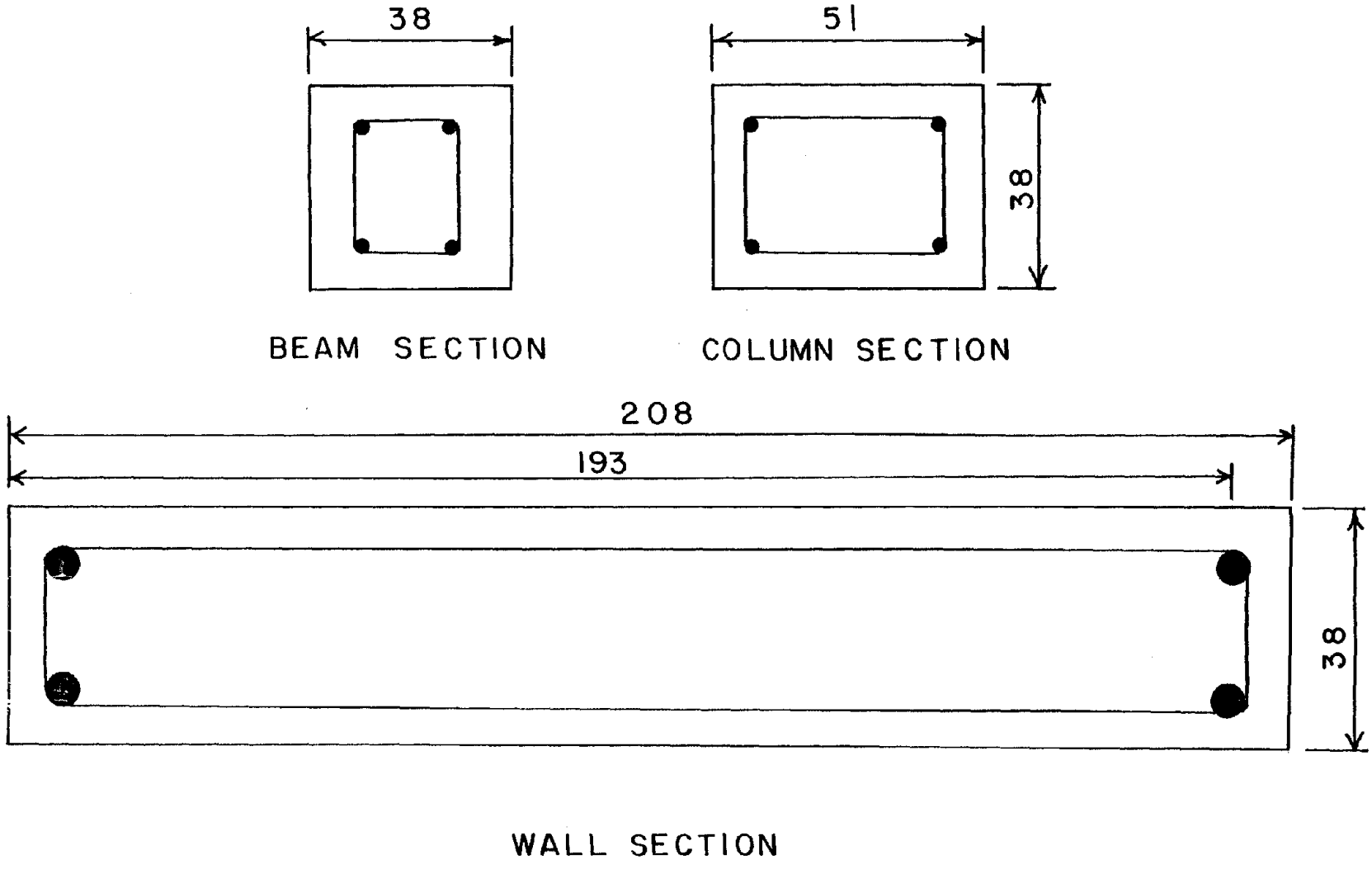

Fig. 3.2.a Reinforcement Detail for Test Structures

REINFORCEMENT RATIOS (x 100)

	FRAME STRUCTURE			FRAME-WALL STRUCTURES		
LEVEL	EXTERIOR COLUMNS	INTERIOR COLUMNS	BEAMS	COLUMNS	BEAMS	WALL
9	0.88	0.88	0.74	0.88	0.74	0.90
8	↑	↑	↑	↑	↑	↑
7	↑	↑	↑	↑	↑	↑
6	↑	↑	↑	↑	↑	↑
5	↑	↑	↓	↑	↑	↑
4	↑	↓	0.74	↑	↑	↑
3	↓	0.88	1.10	↑	↑	↑
2	0.88	1.75	1.10	↓	↓	↓
1	1.75	1.75	1.10	0.88	0.74	0.90

Fig. 3.2.b Reinforcement Schedule for Test Structures (from Ref. 16)

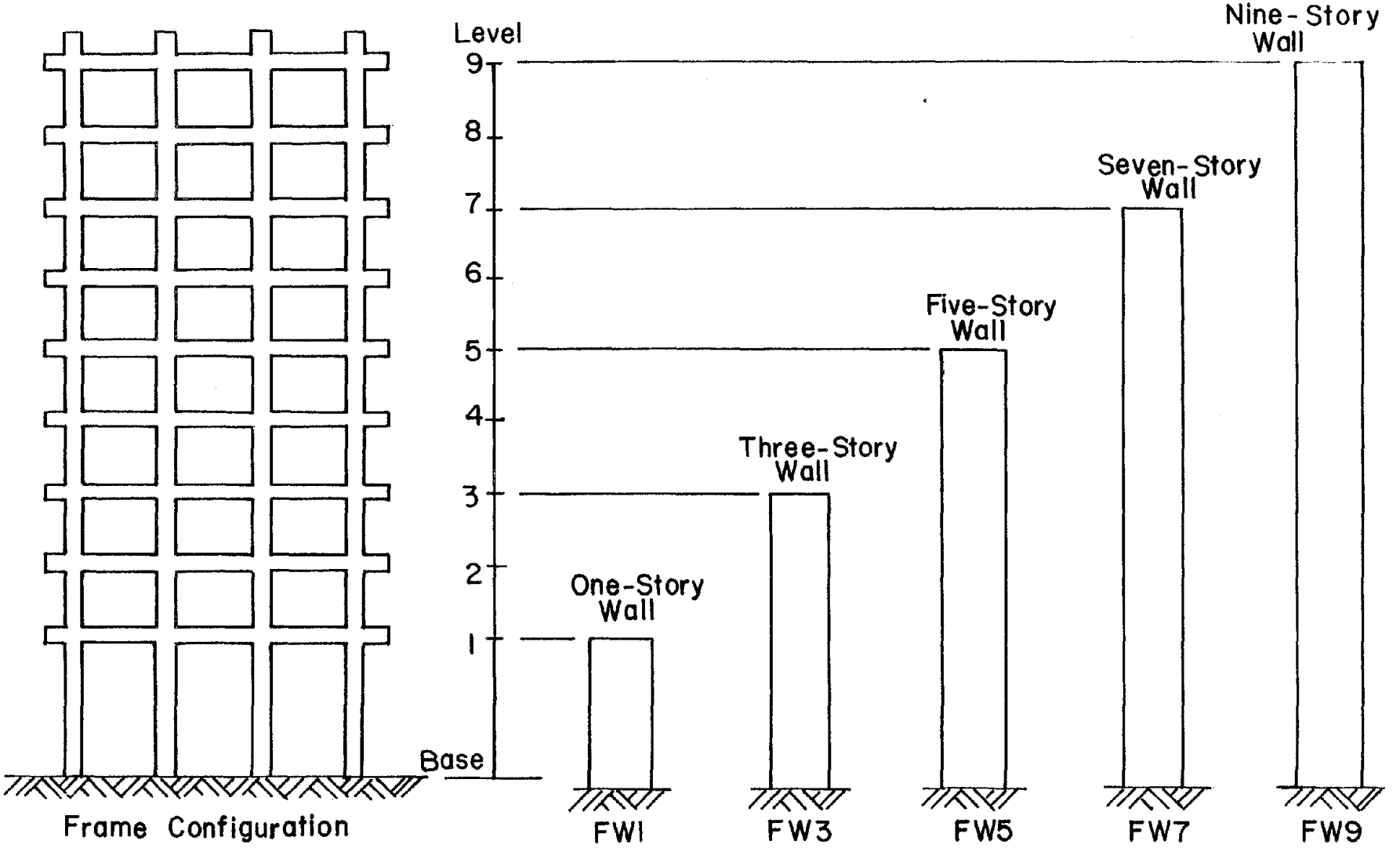

Fig. 3.3 Small-Scale Structures with Different Wall Heights

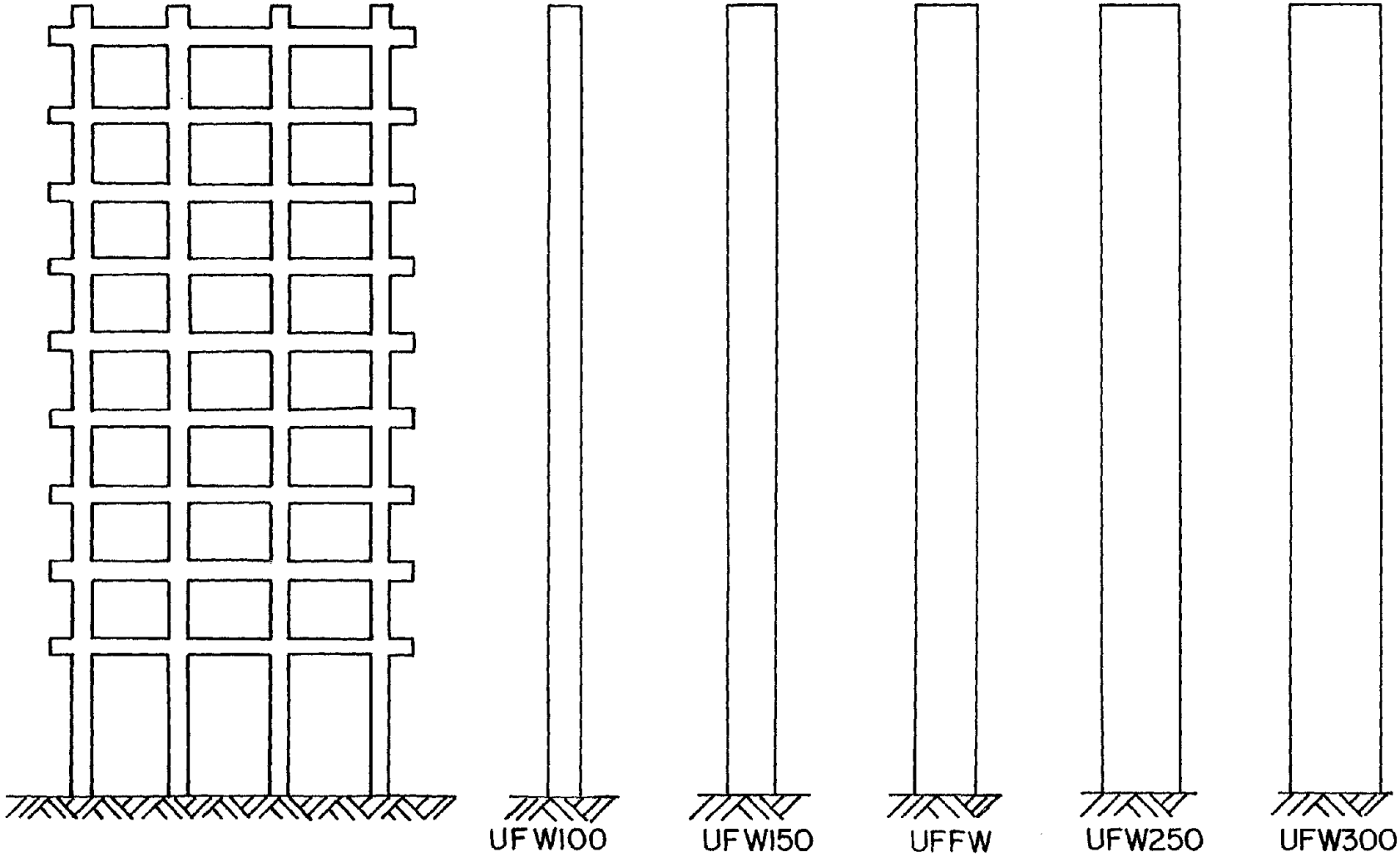

Fig. 3.4 Small-Scale Structures with Different Wall Widths

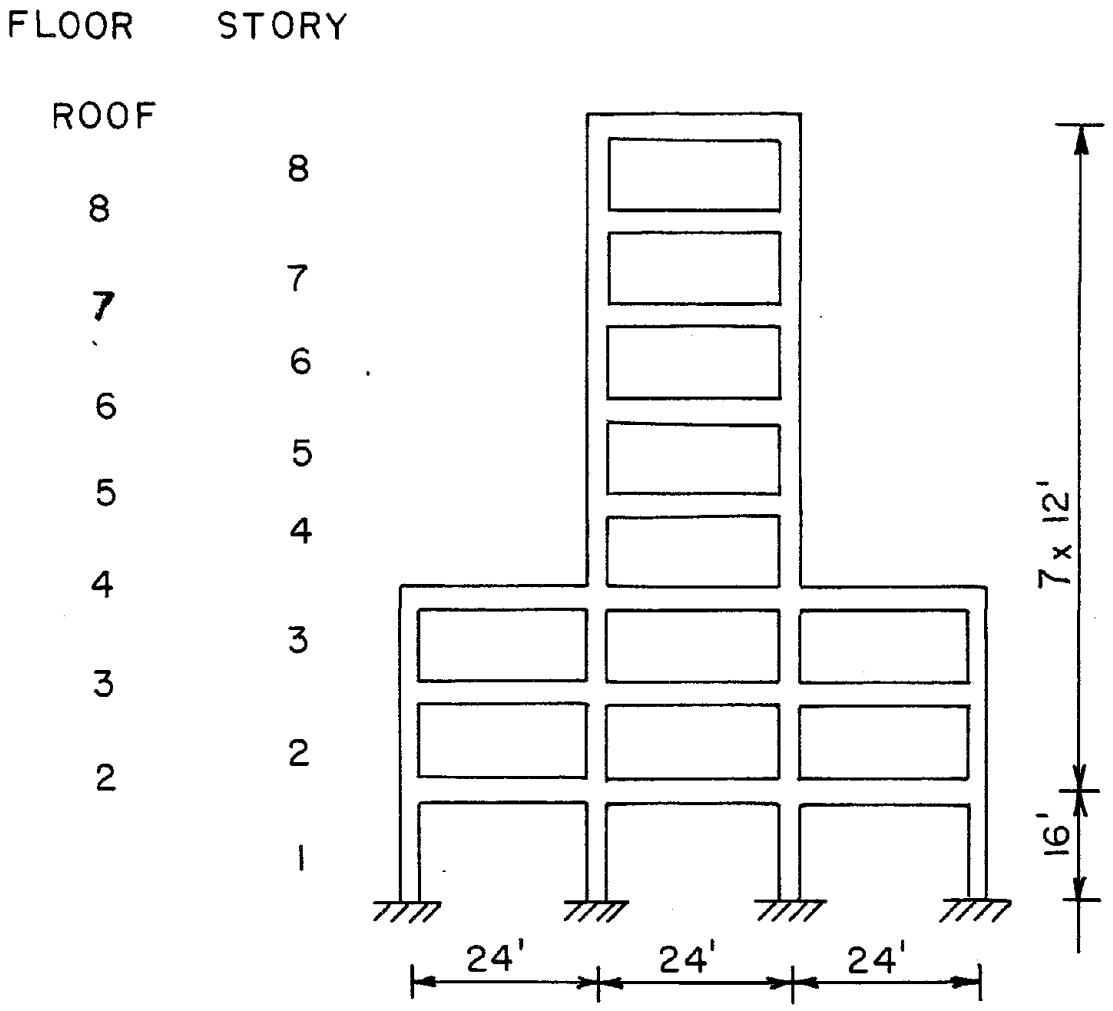

Fig. 3.5 Eight-Story Frame with Setbacks

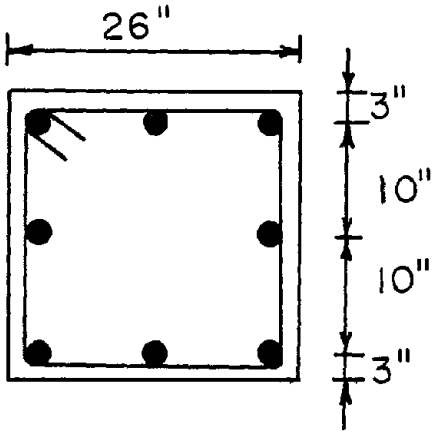

COLUMN SECTION

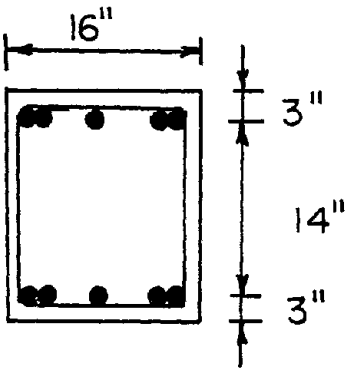

BEAM SECTION

REINFORCEMENT SCHEDULE

Floor/Story		Beams (per face)	Exterior Columns	Interior Columns
Roof	8	5#7	8#9	—
8	7	"	"	—
7	6	"	"	—
6	5	5#8	"	—
5	4	"	"	—
4	3	5#9	"	8#11
3	2	"	"	"
2	1	"	"	"

Fig. 3.6 Eight-Story Frame Reinforcement

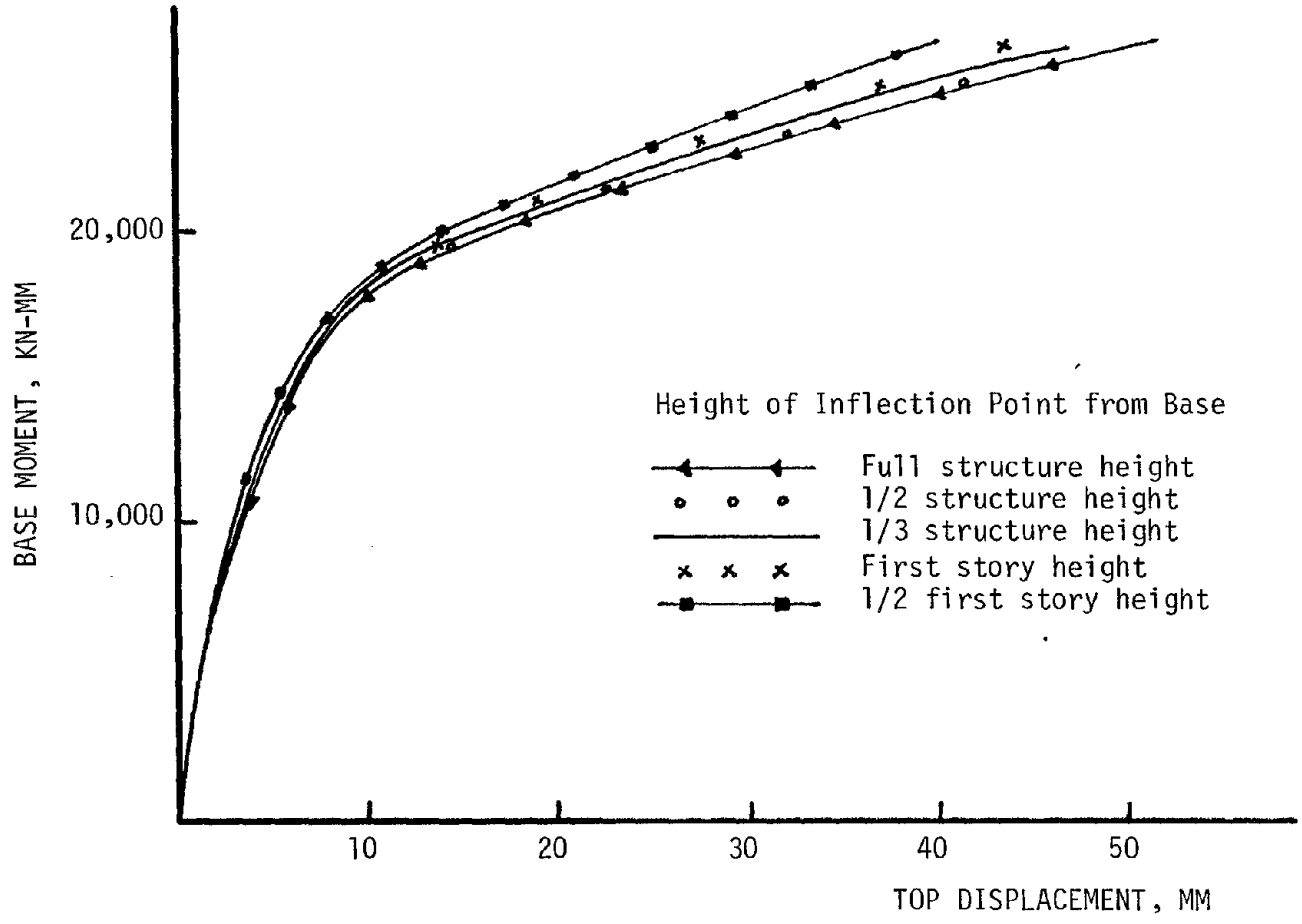

Fig. 4.1 Primary Curves Based on Different Wall Inflection Points

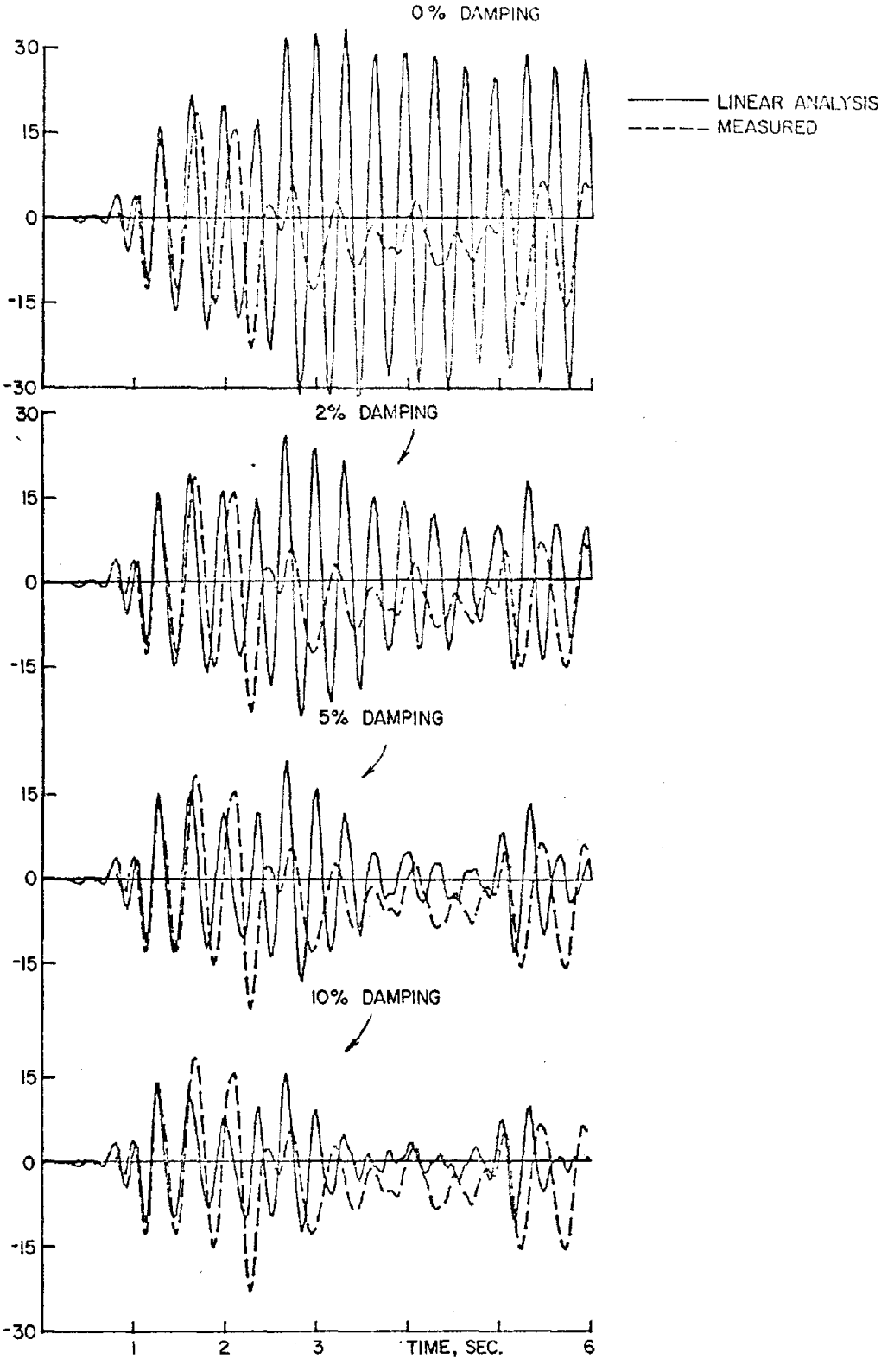

Fig. 4.2 Elastic Top-Level Displacement Based on Different Damping Ratios

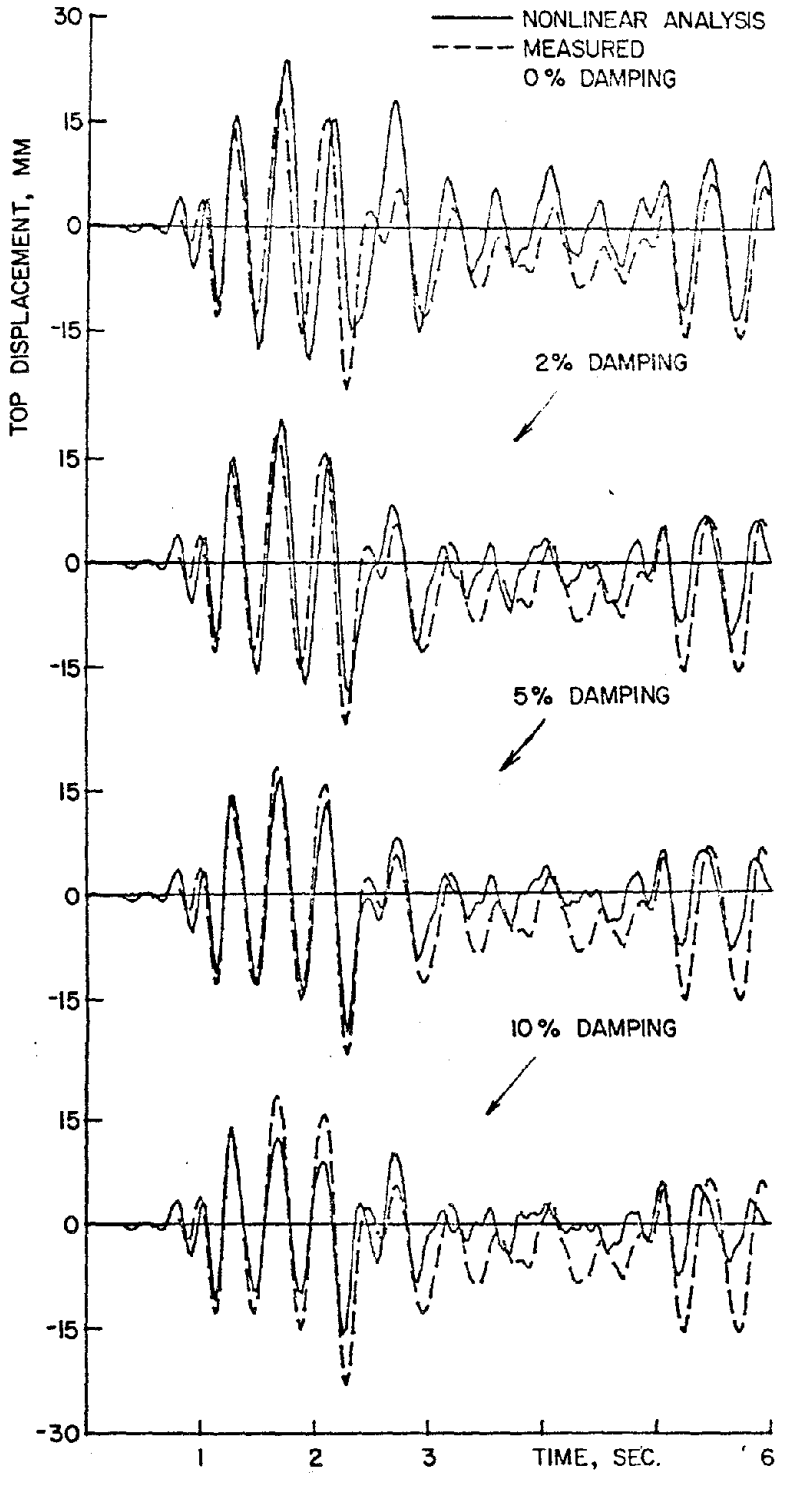

Fig. 4.3 Inelastic Top-Level Displacement Based on Different Damping Ratios

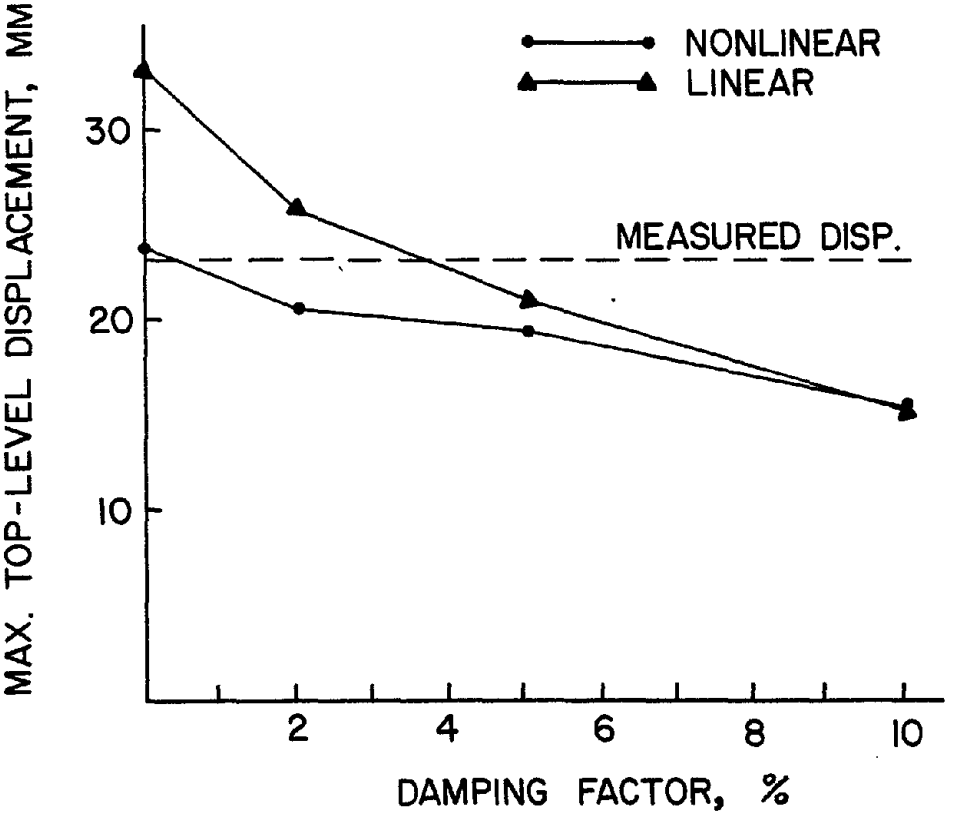

Fig. 4.4.a Maximum Displacements Based on Different Damping Ratios

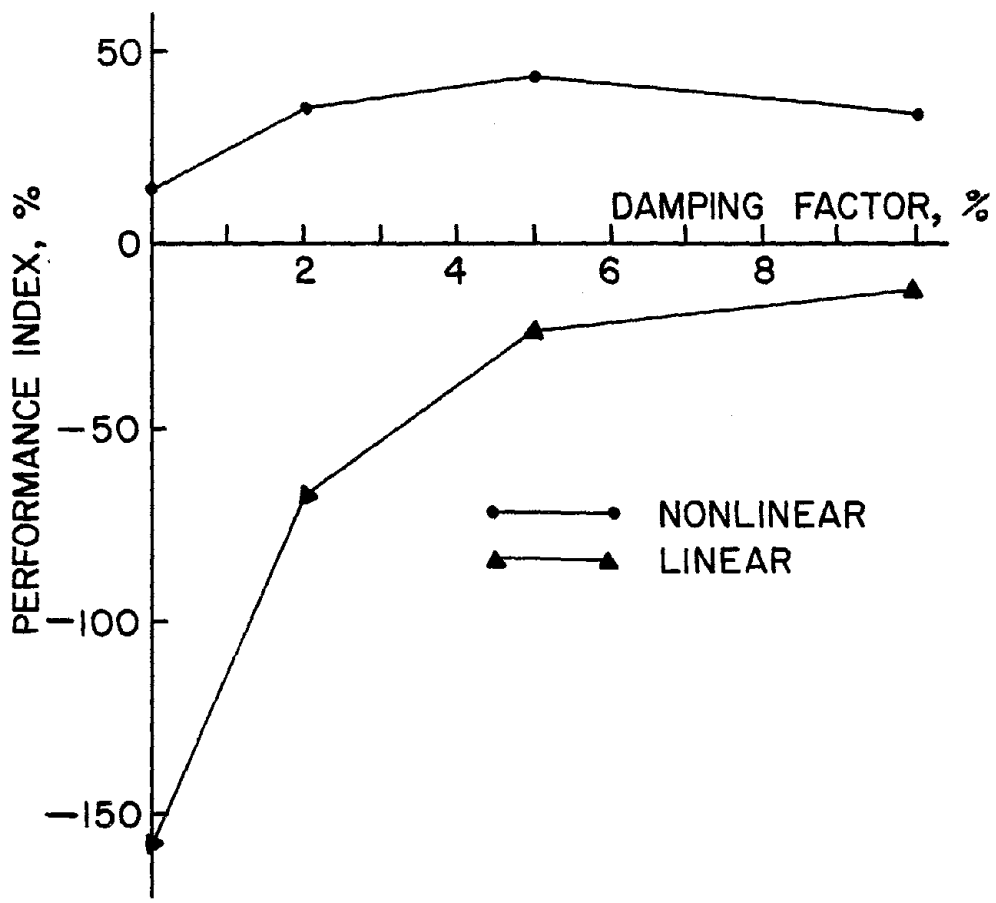

Fig. 4.4.b Performance Indeces for Different Damping Ratios

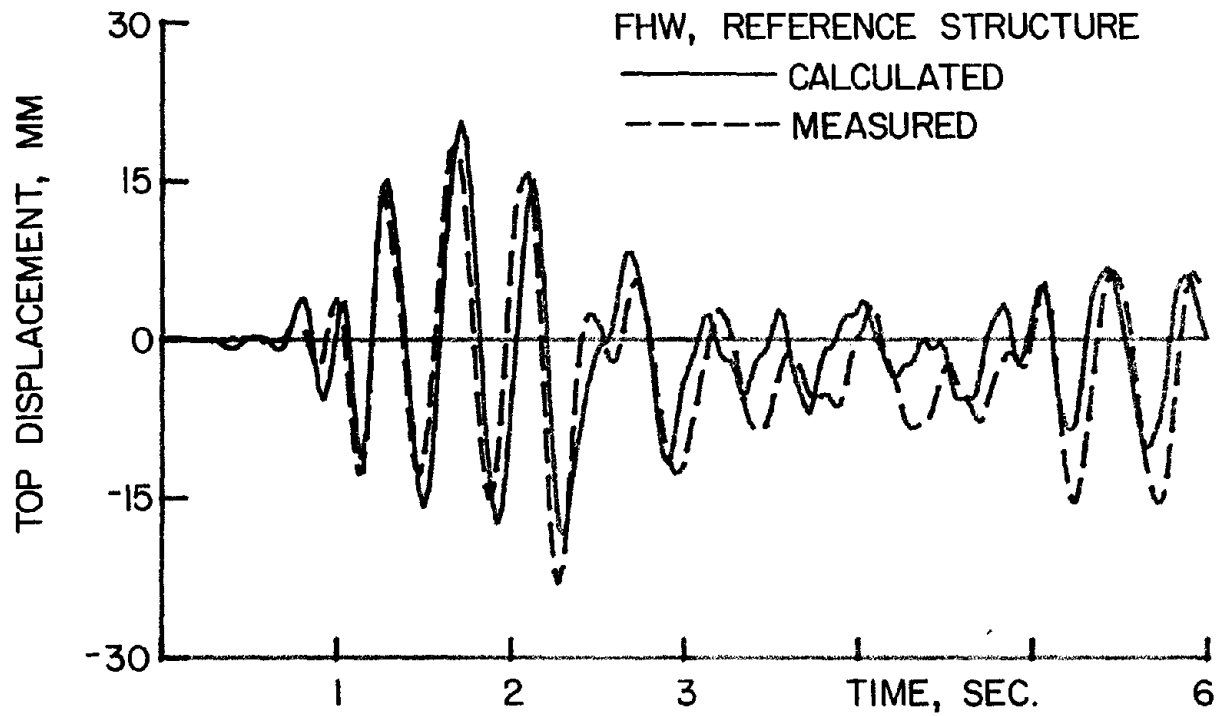

Fig. 4.5 Calculated and Measured Response of FHW

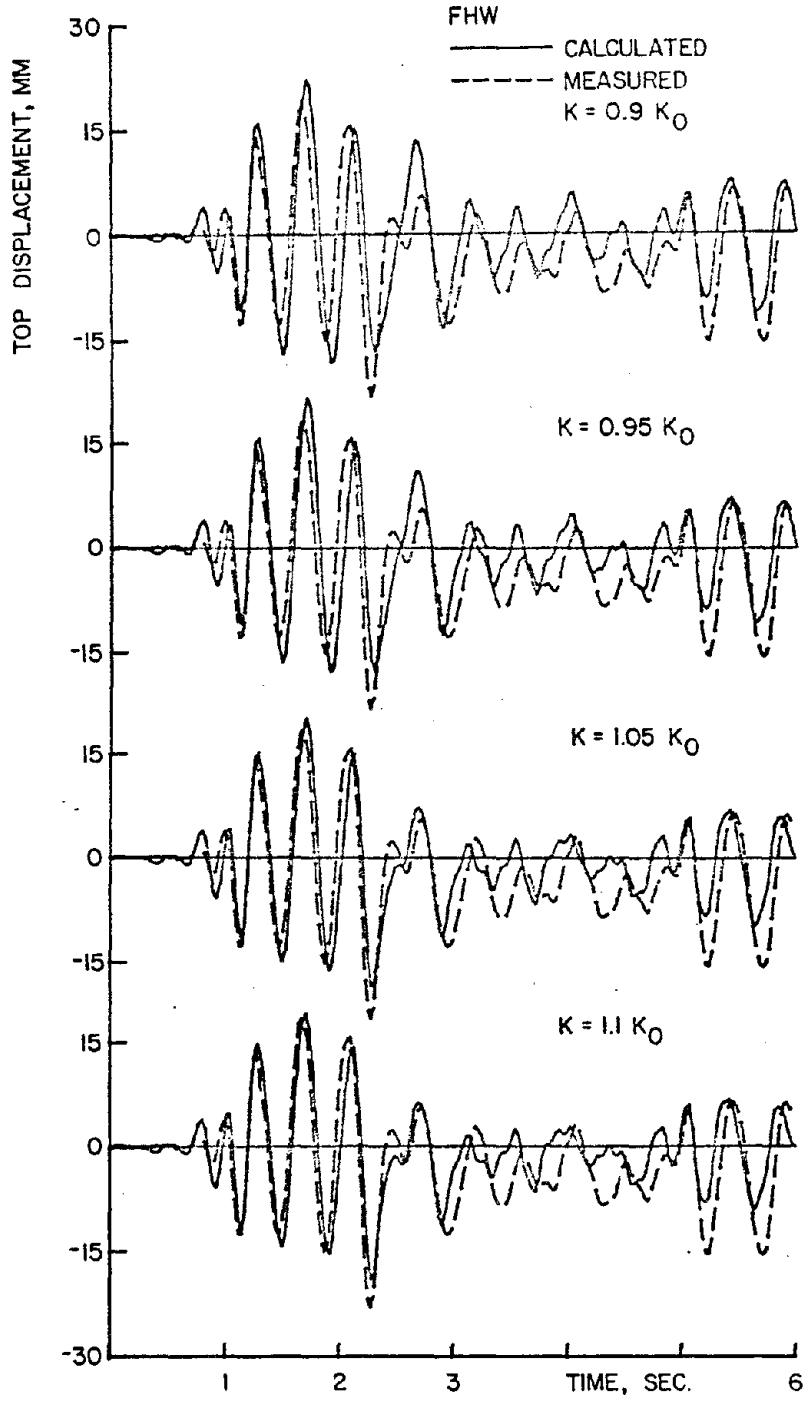

Fig. 4.6 Responses Based on Different Elastic Stiffnesses

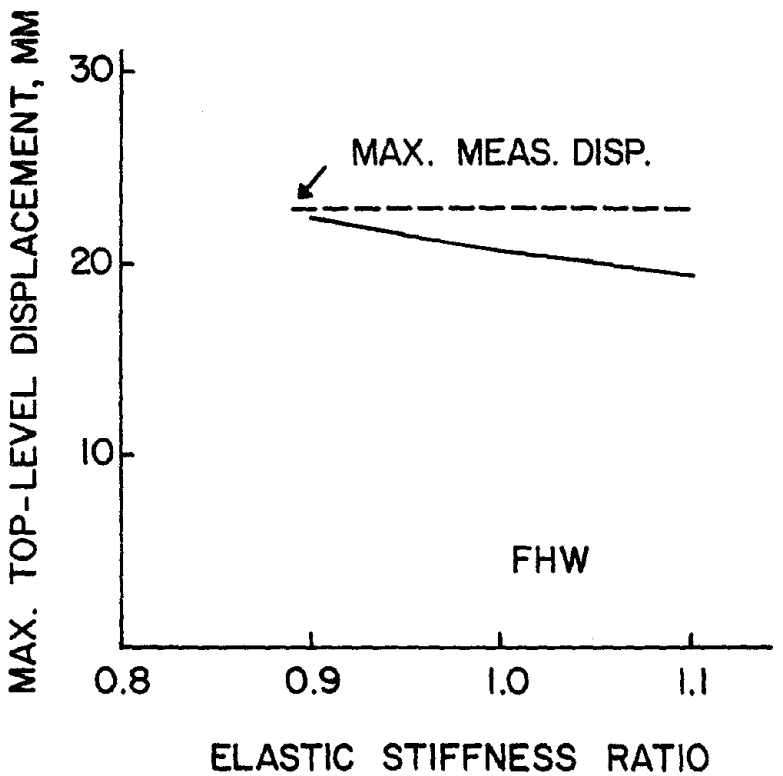

Fig. 4.7.a Maximum Displacements for Different Elastic Stiffnesses

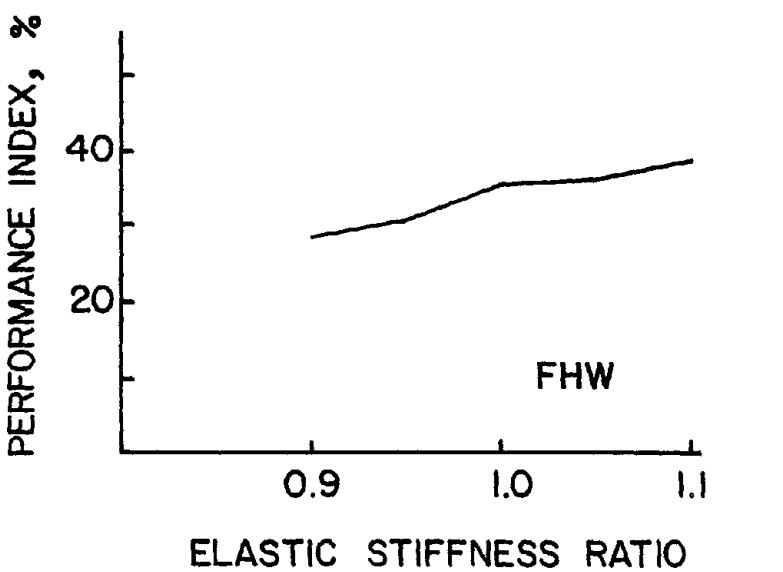

Fig. 4.7.b Performance Indeces for Different Elastic Stiffnesses

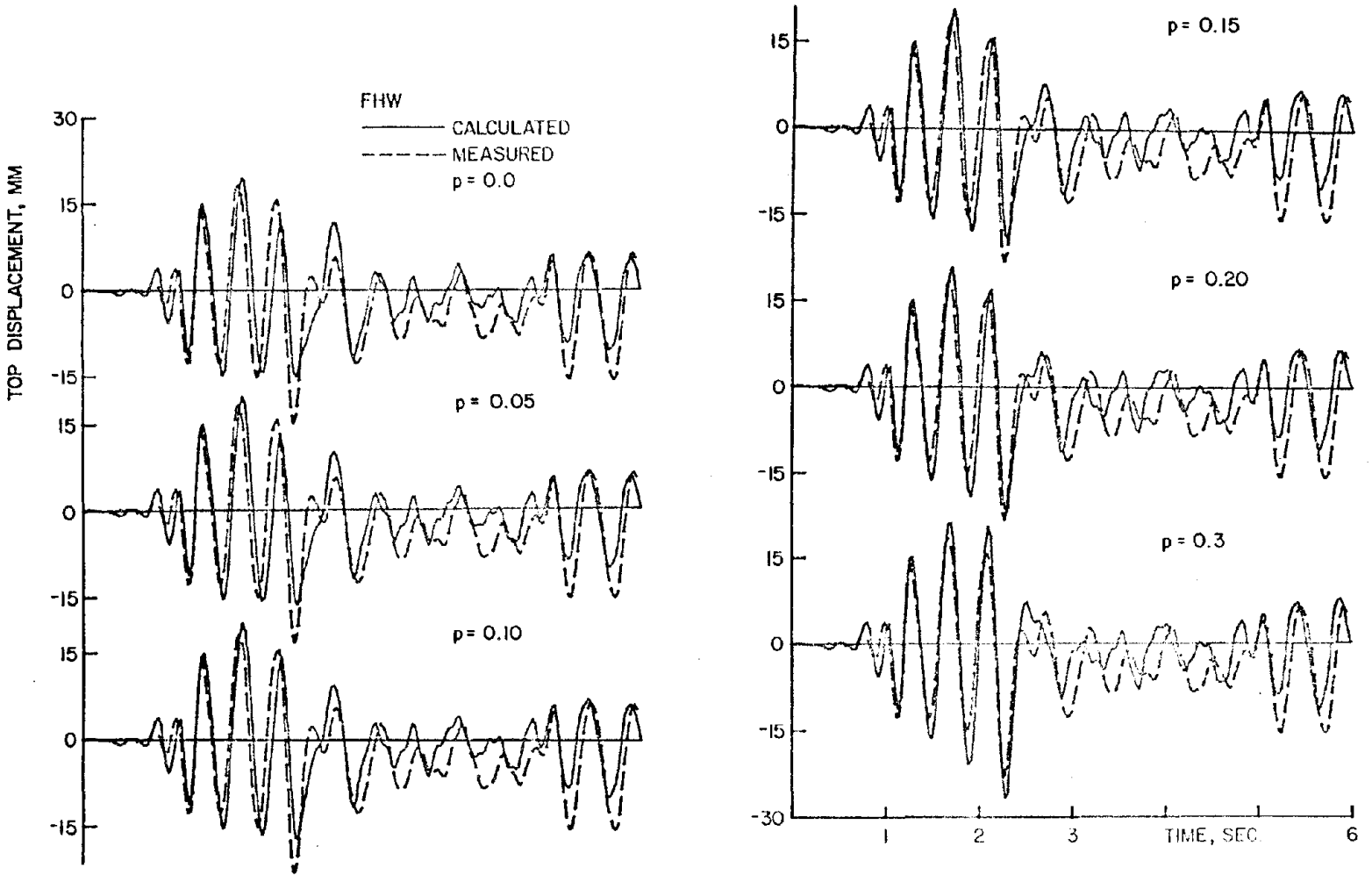

Fig. 4.8 Responses Based on Different Post-Yielding Stiffnesses

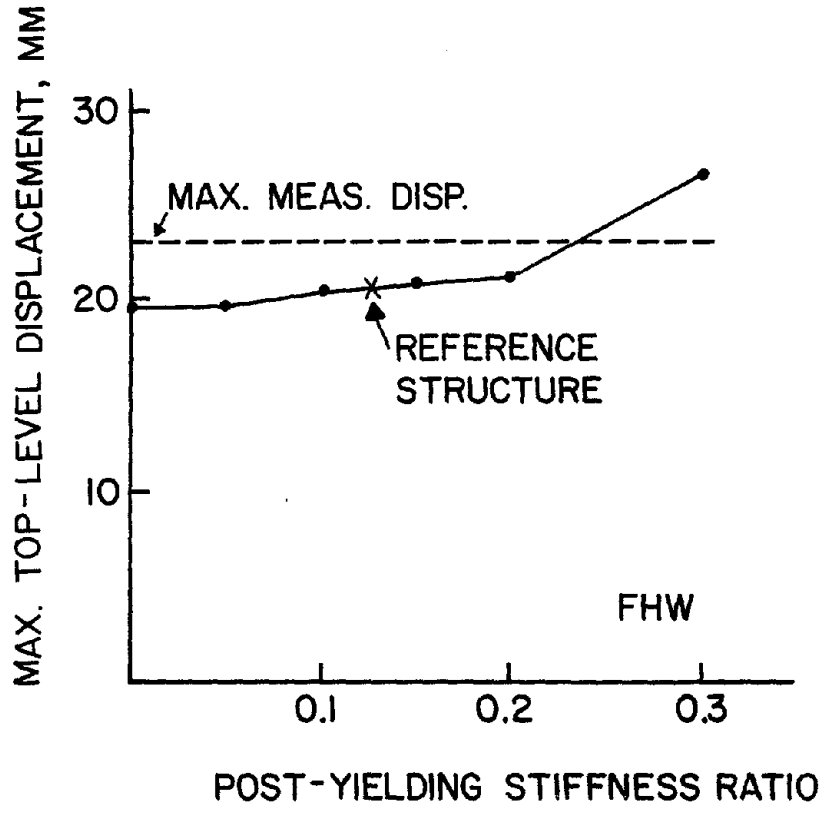

Fig. 4.9.a Maximum Displacements for Different Post-Yielding Stiffnesses

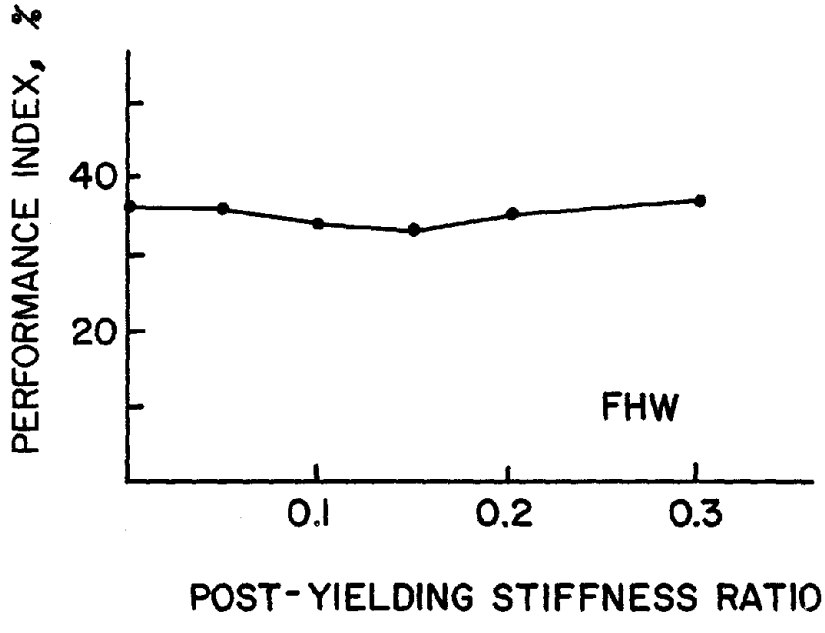

Fig. 4.9.b Performance Indeces for Different Post-Yielding Stiffnesses

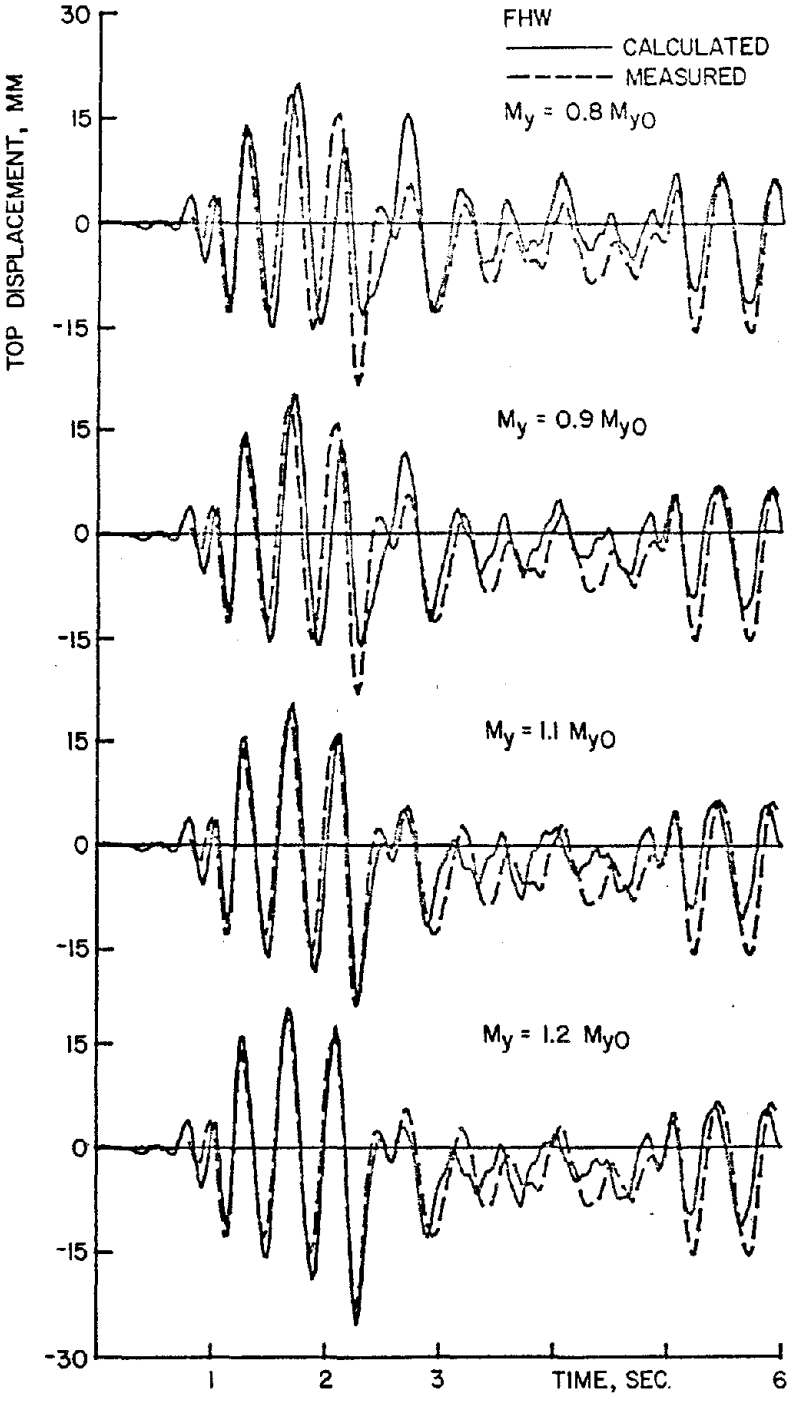

Fig. 4.10 Responses Based on Different Yield Base Moments

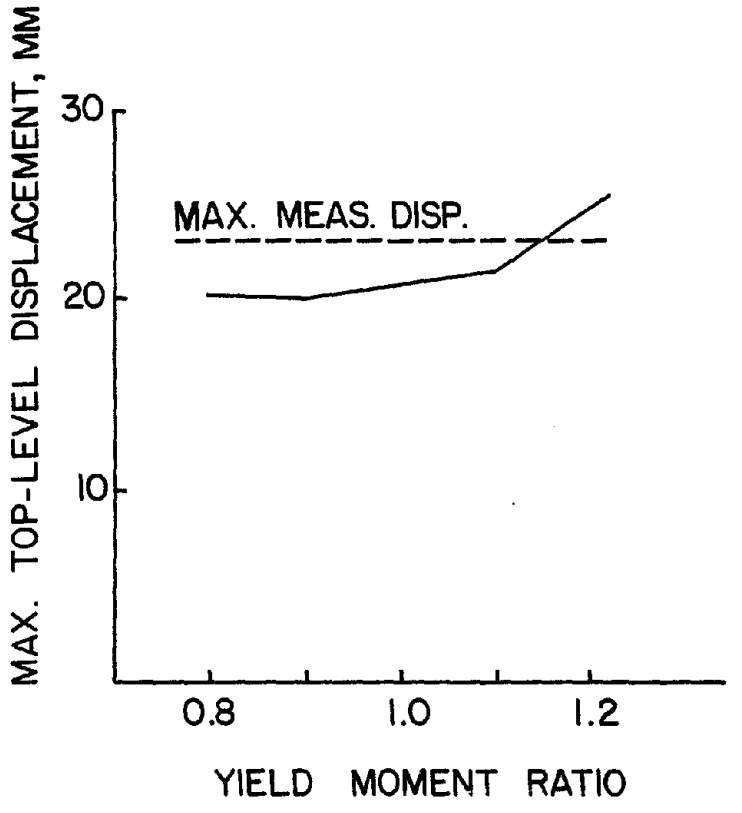

Fig. 4.11.a Maximum Displacements for Different Yield Base Moments

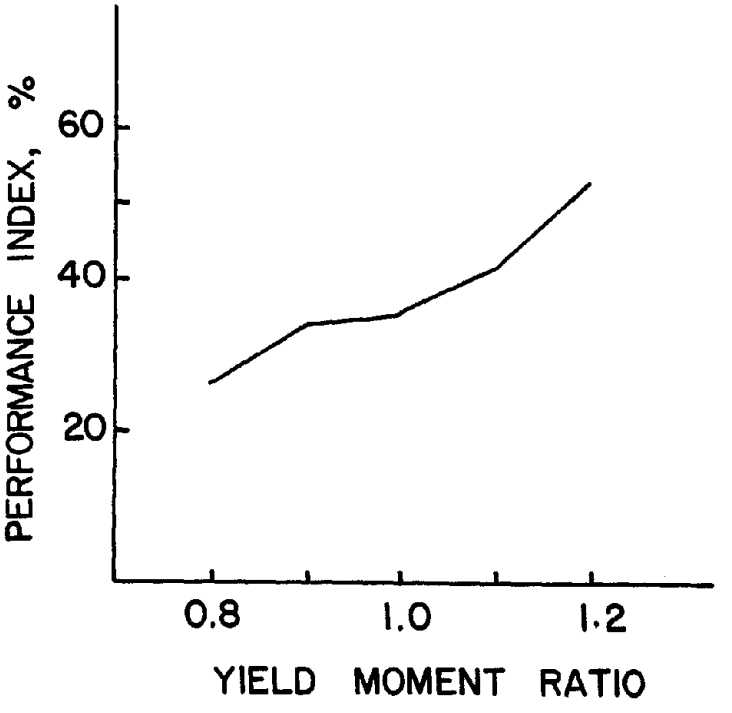

Fig. 4.11.b Performance Indeces for Different Yield Base Moments

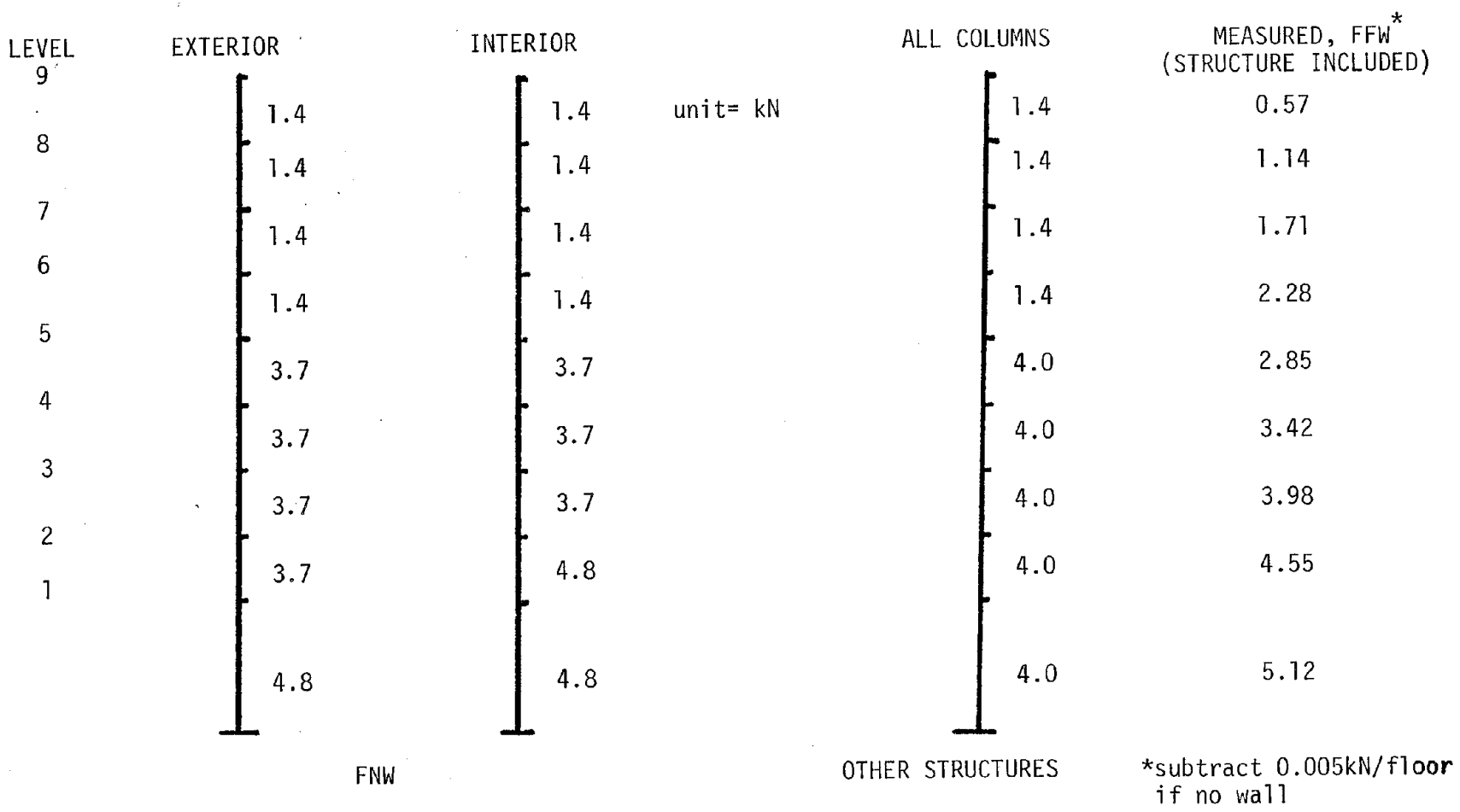

Fig. 5.1 Assumed Column Axial Loads

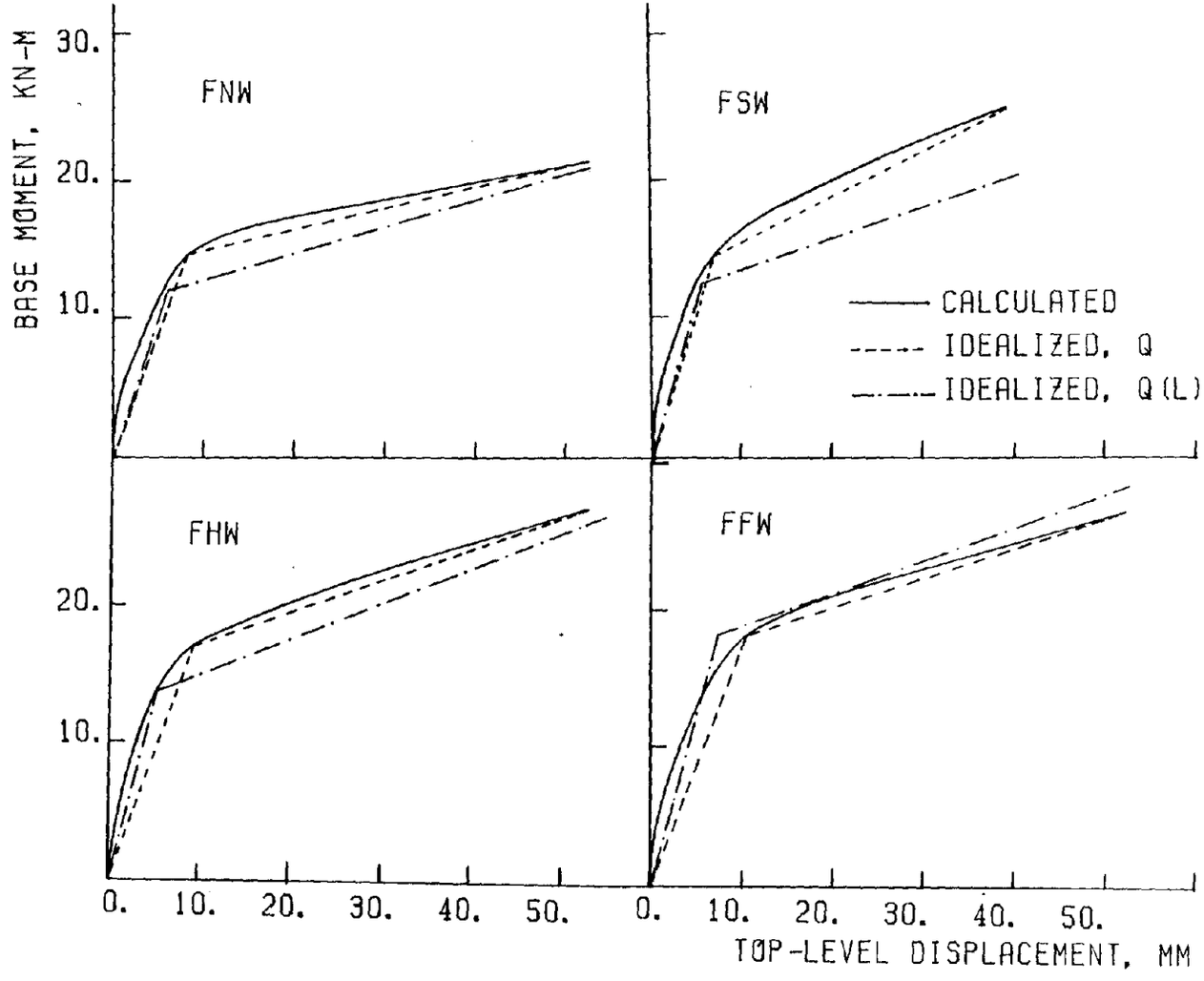

Fig. 5.2 Calculated and Idealized Primary Curves for Test Structures

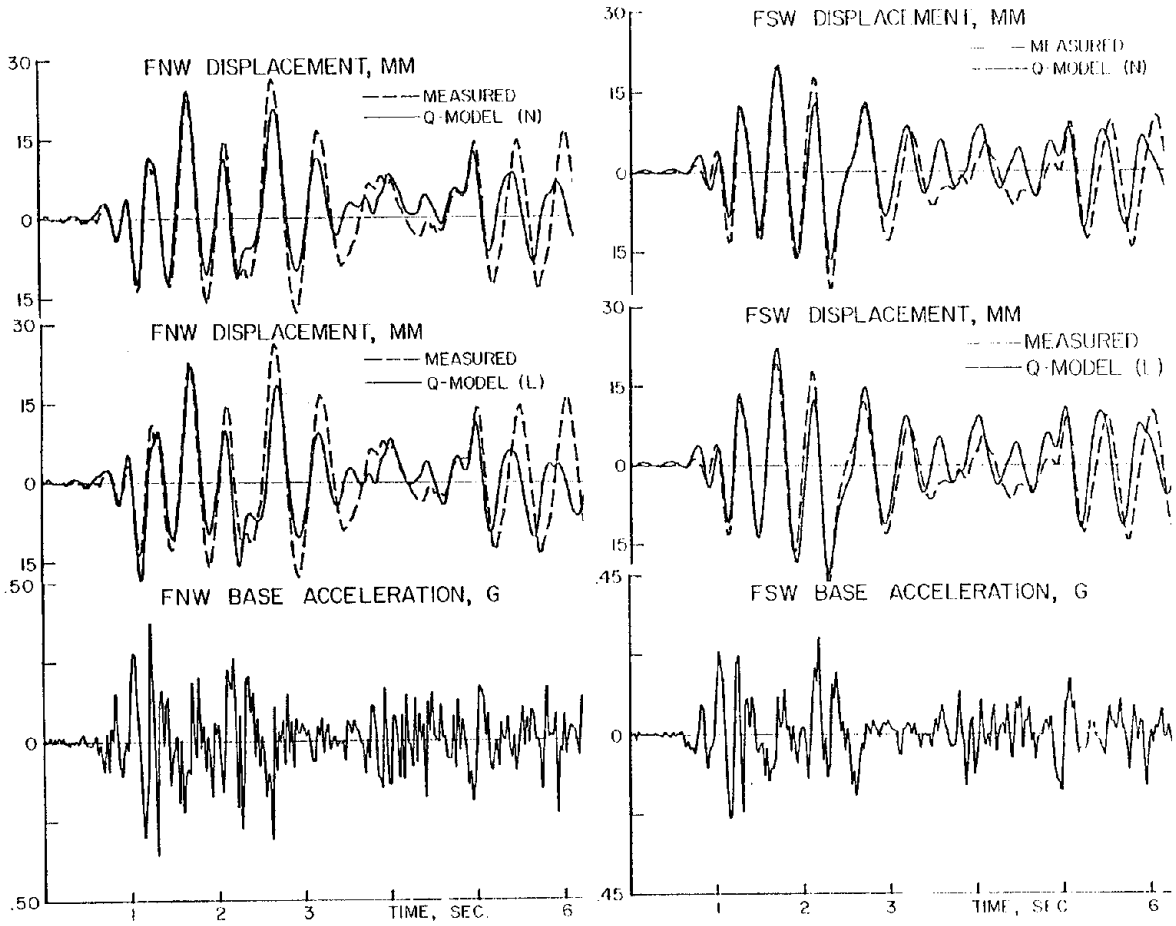

Fig. 5.3 Top-Level Response Histories for Test Structures

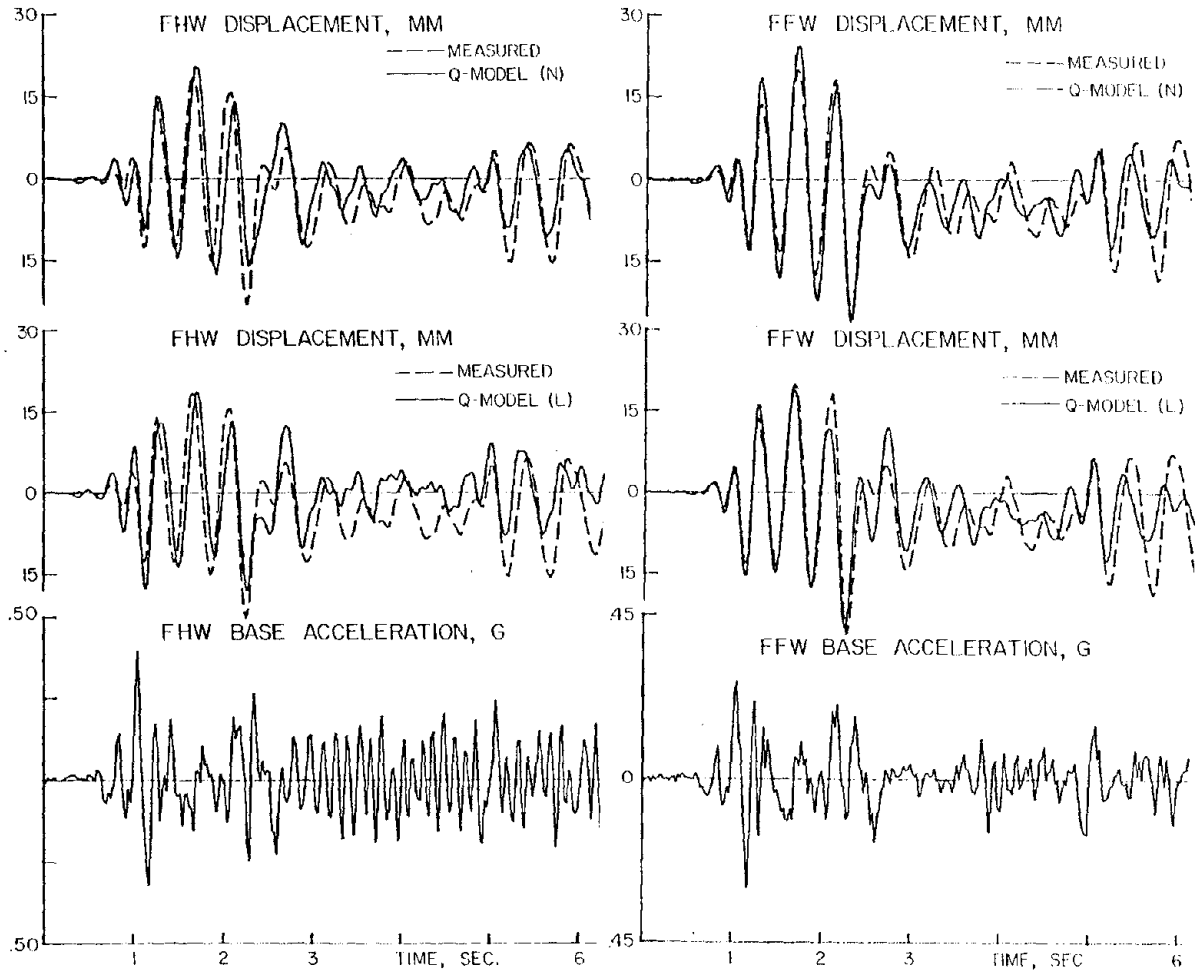

Fig. 5.3 (cont'd) Top-Level Response Histories for Test Structures

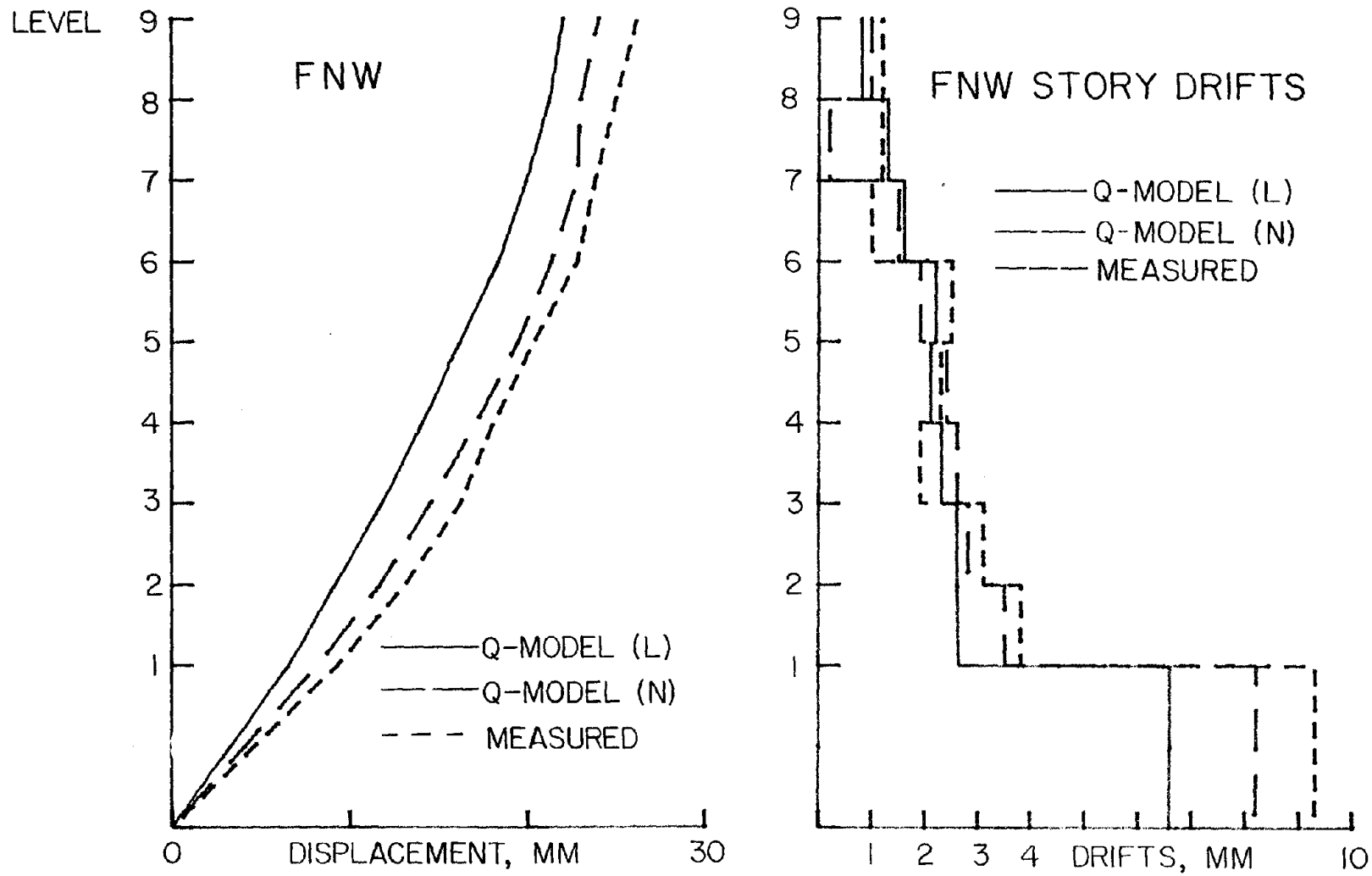

Fig. 5.4 Displacements at Time of Maximum Top-Level Displacement

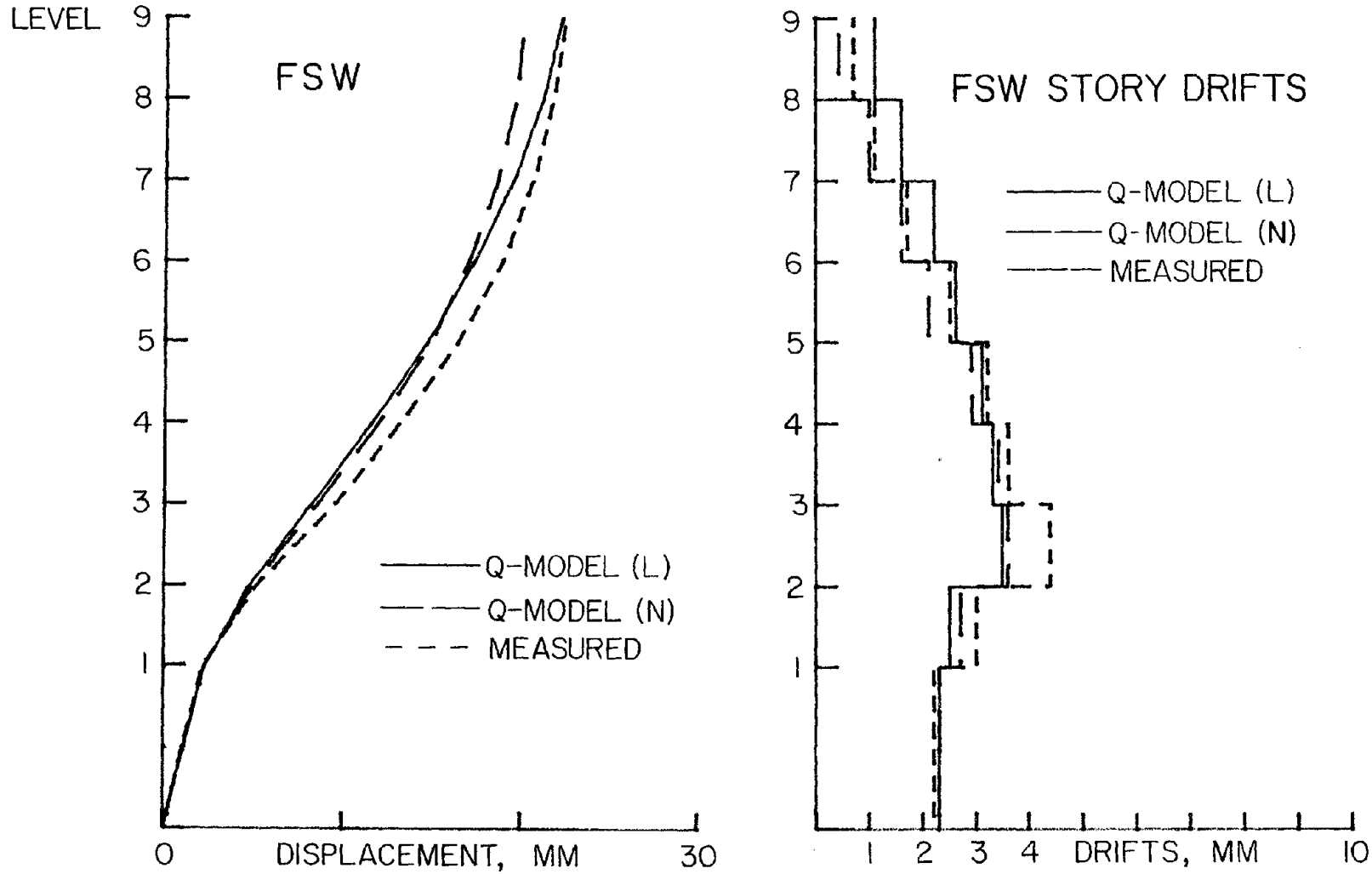

Fig. 5.4 (cont'd) Displacements at Time of Maximum Top-Level Displacement

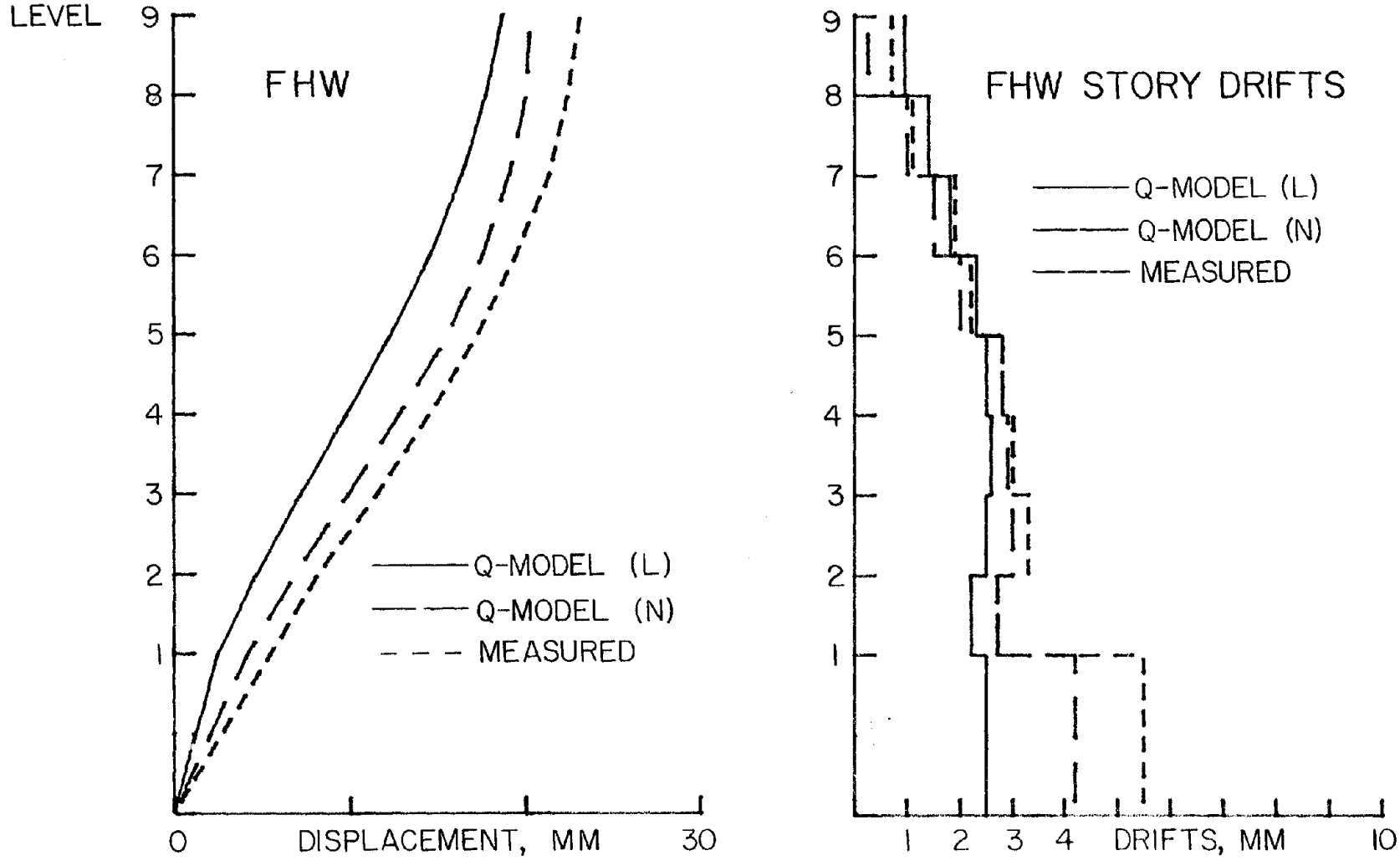

Fig. 5.4 (cont'd) Displacements at Time of Maximum Top-Level Displacement

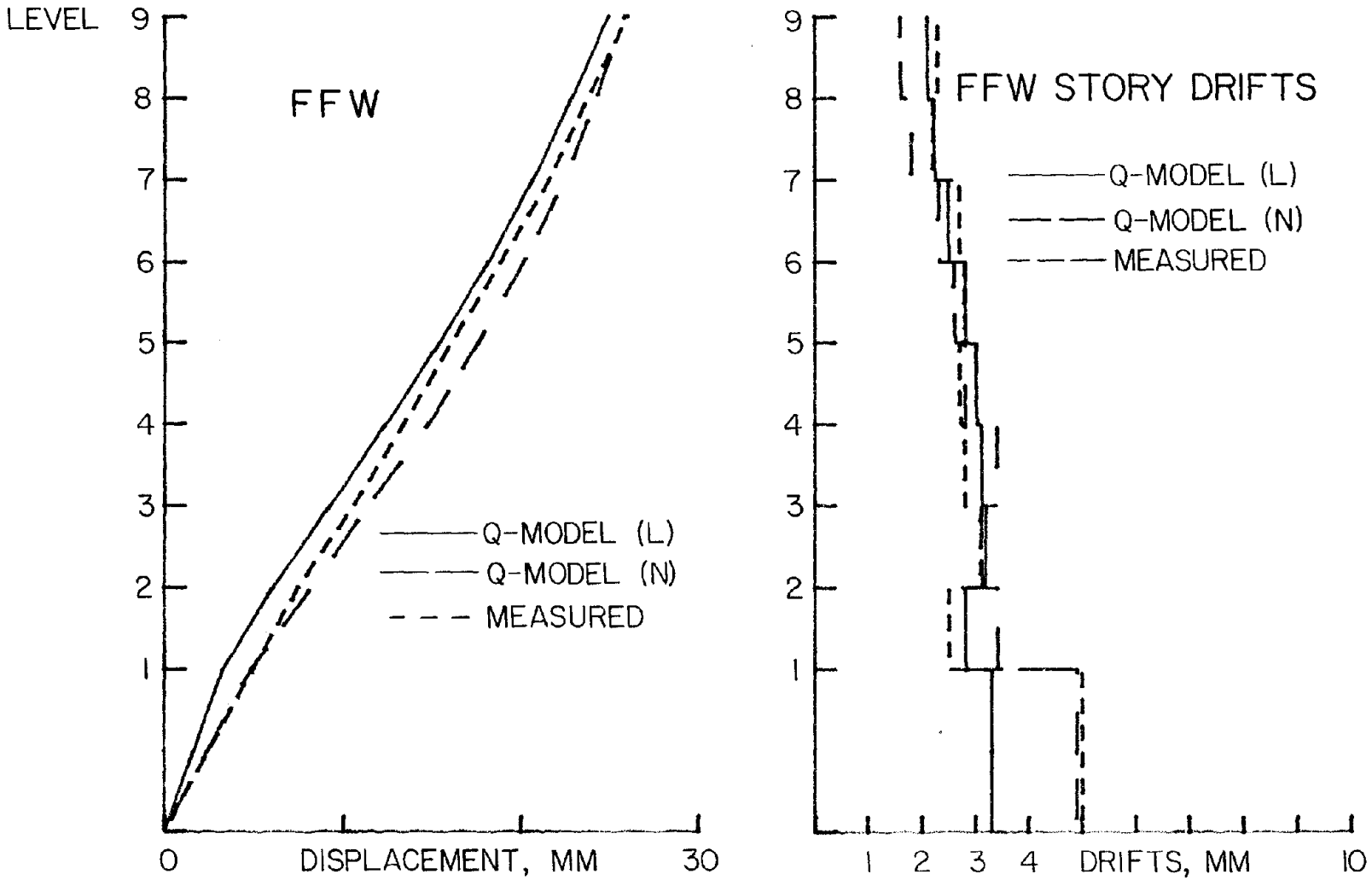

Fig. 5.4 (cont'd) Displacements at Time of Maximum Top-Level Displacement

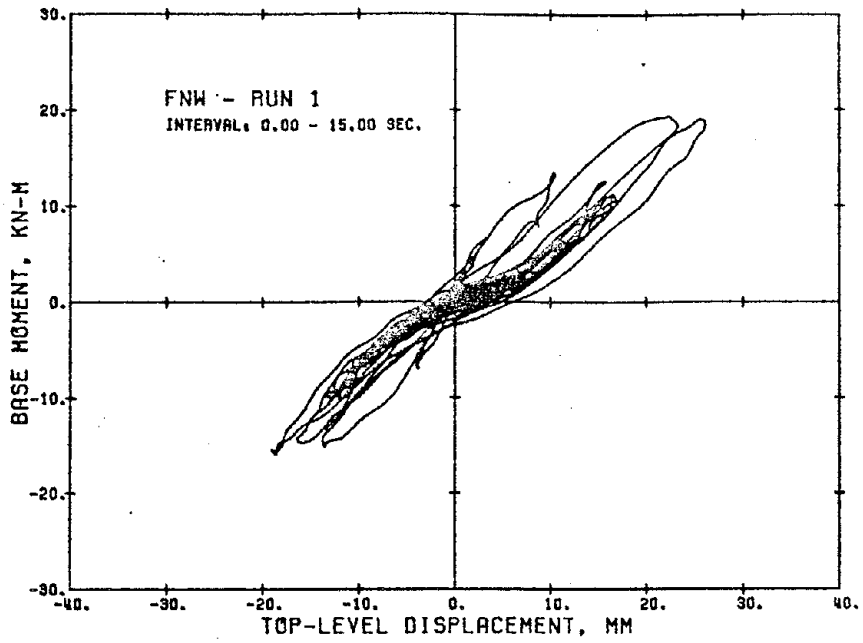

Fig. 5.5 Measured Hysteretic Behavior for FNW (from Ref. 16)

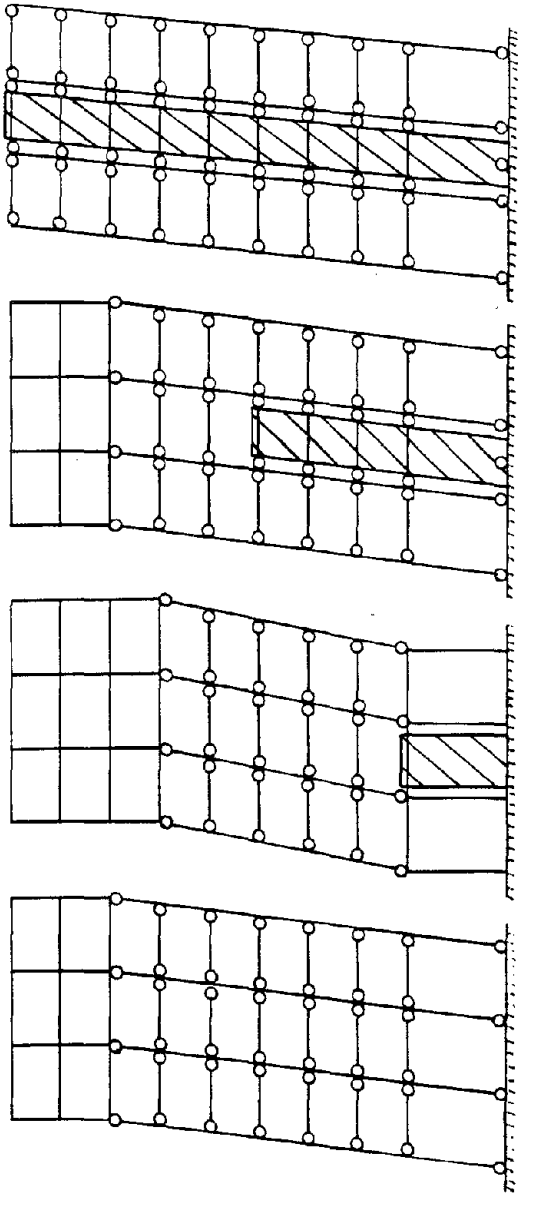

Fig. 5.6 Collapse Mechanisms for Test Structures

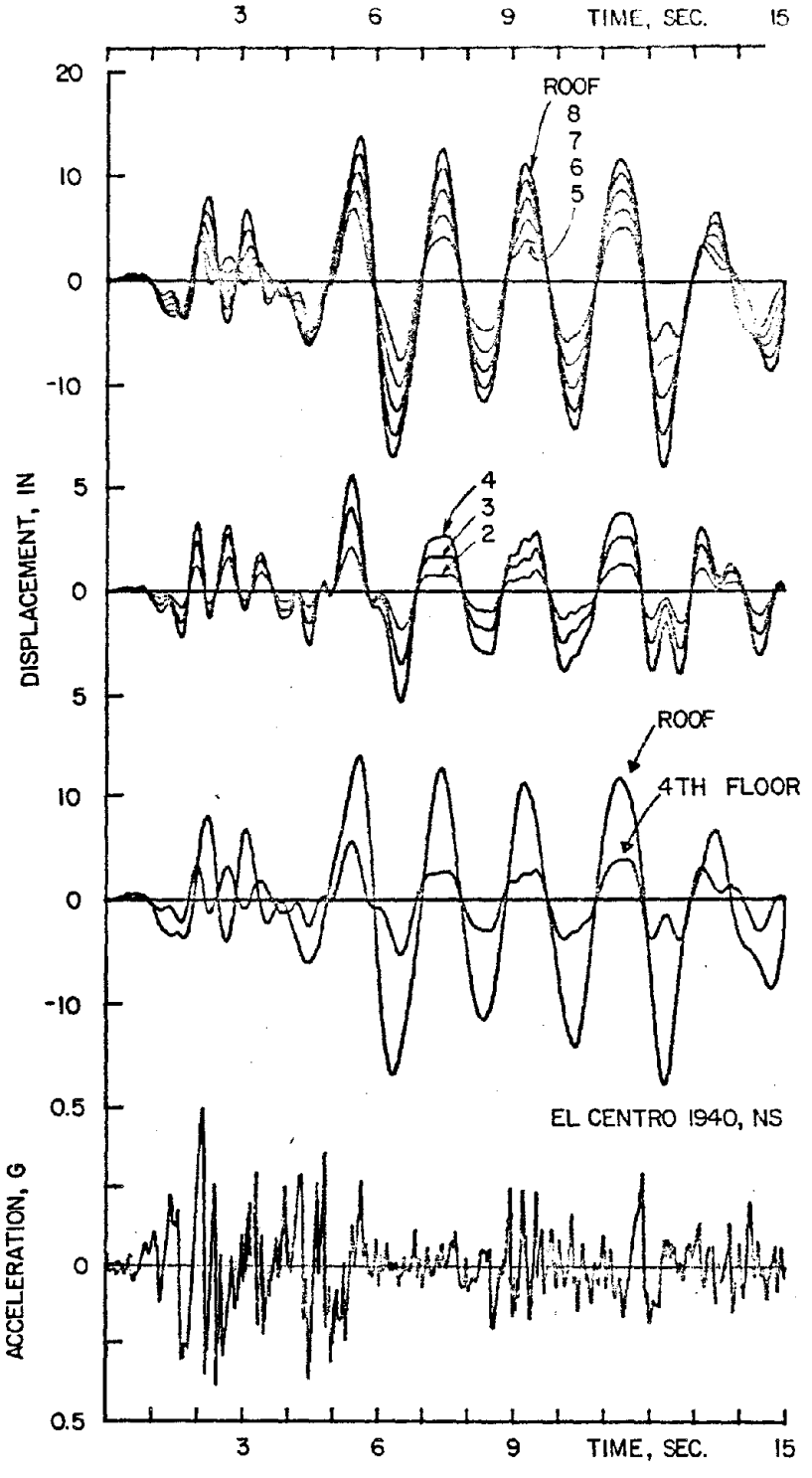

Fig. 6.1 Response of EFS Based on MDOF Analysis

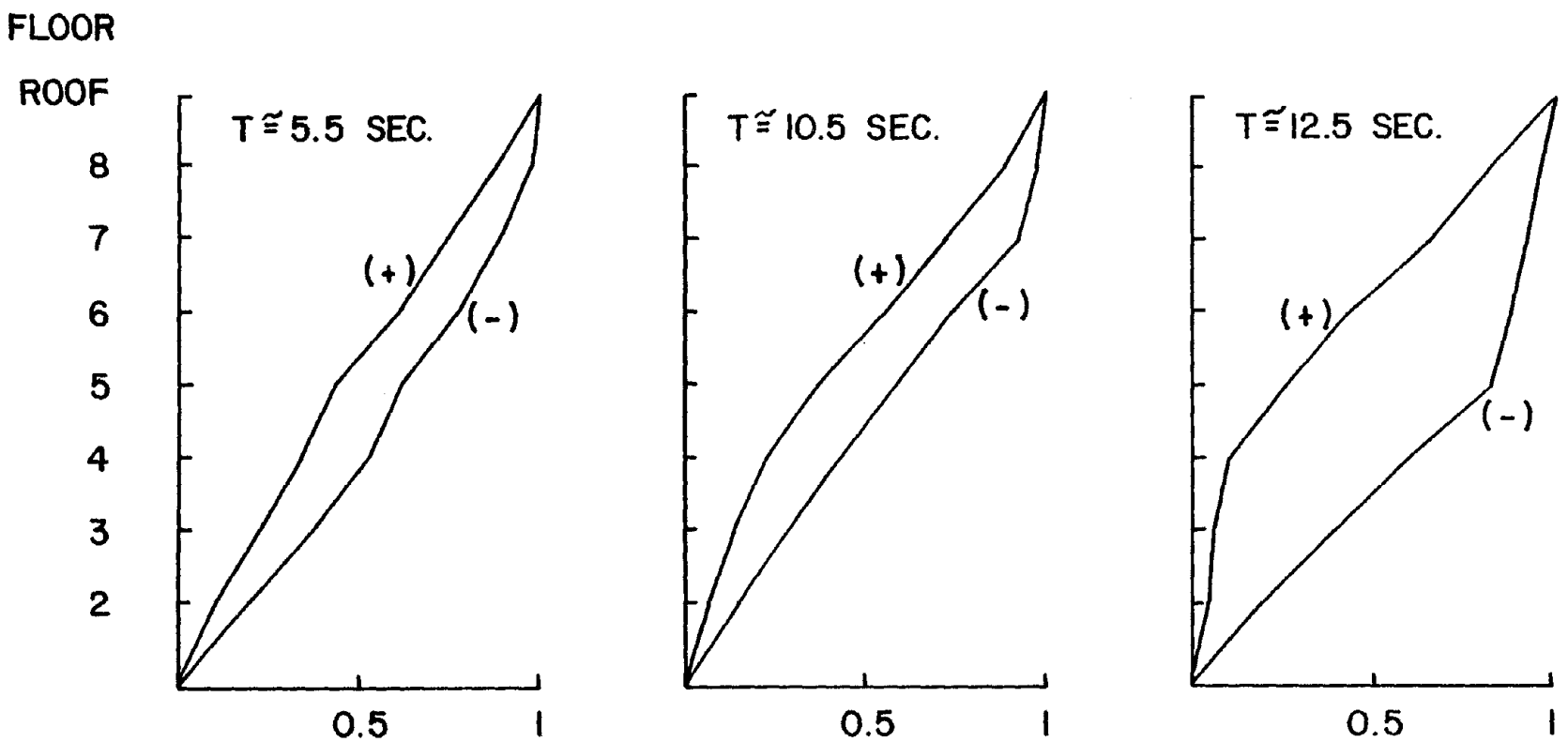

Fig. 6.2 Deflected Shape of EFS Based on MDOF Analysis

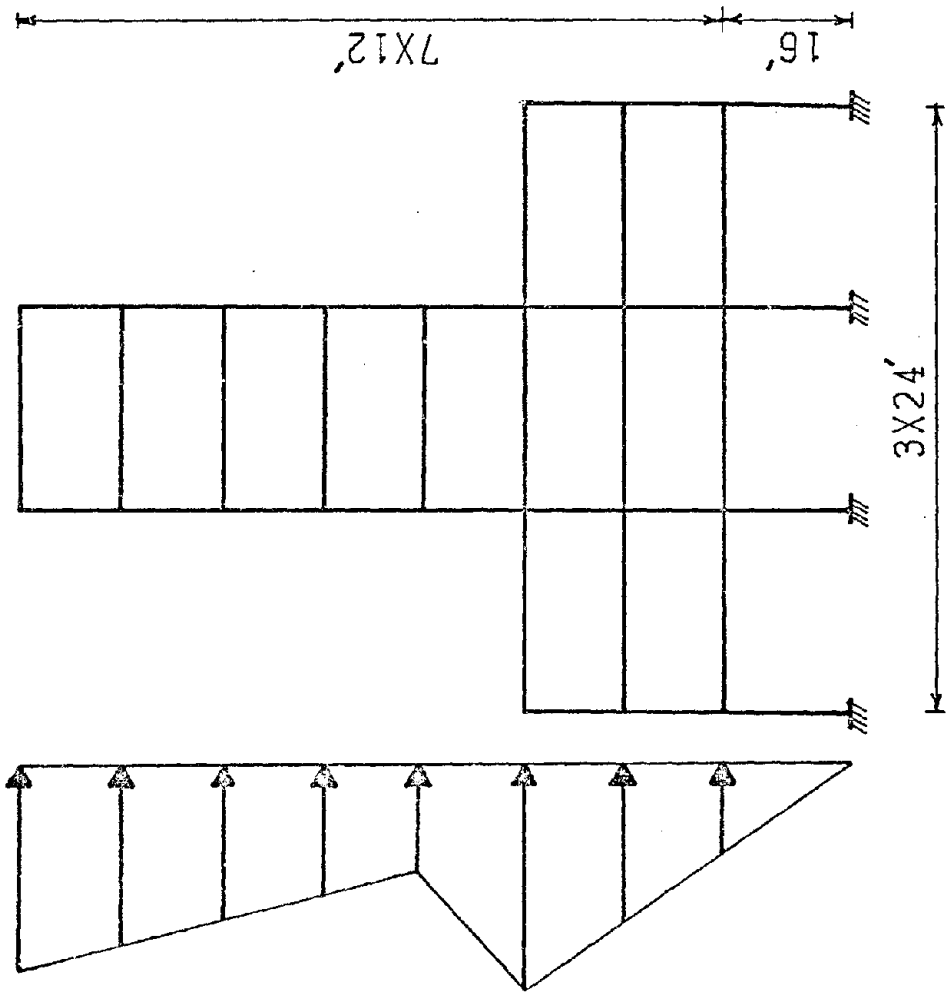

Fig. 6.3 Lateral Load Distribution for EFS

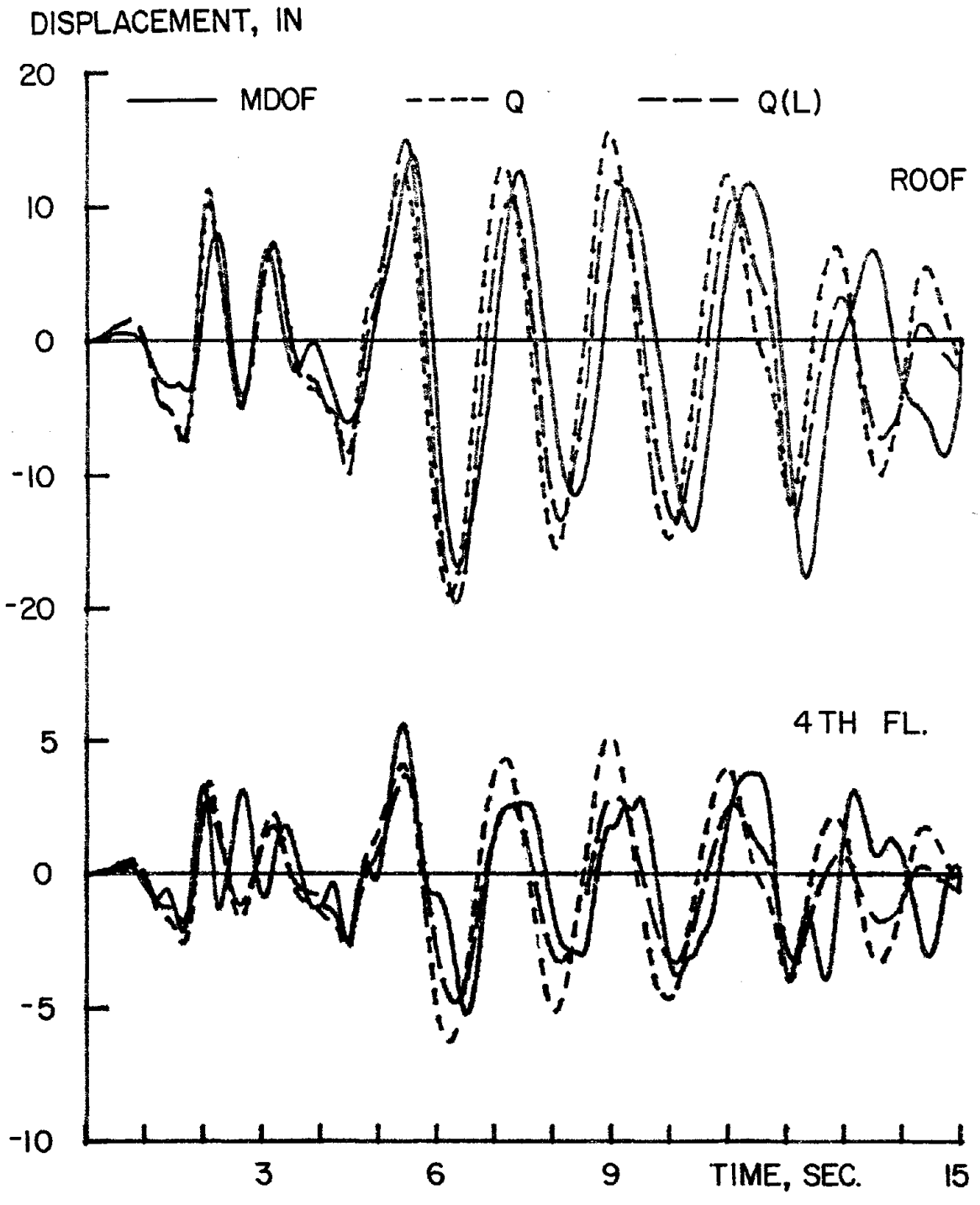

Fig. 6.4 Q-Model Response for EFS

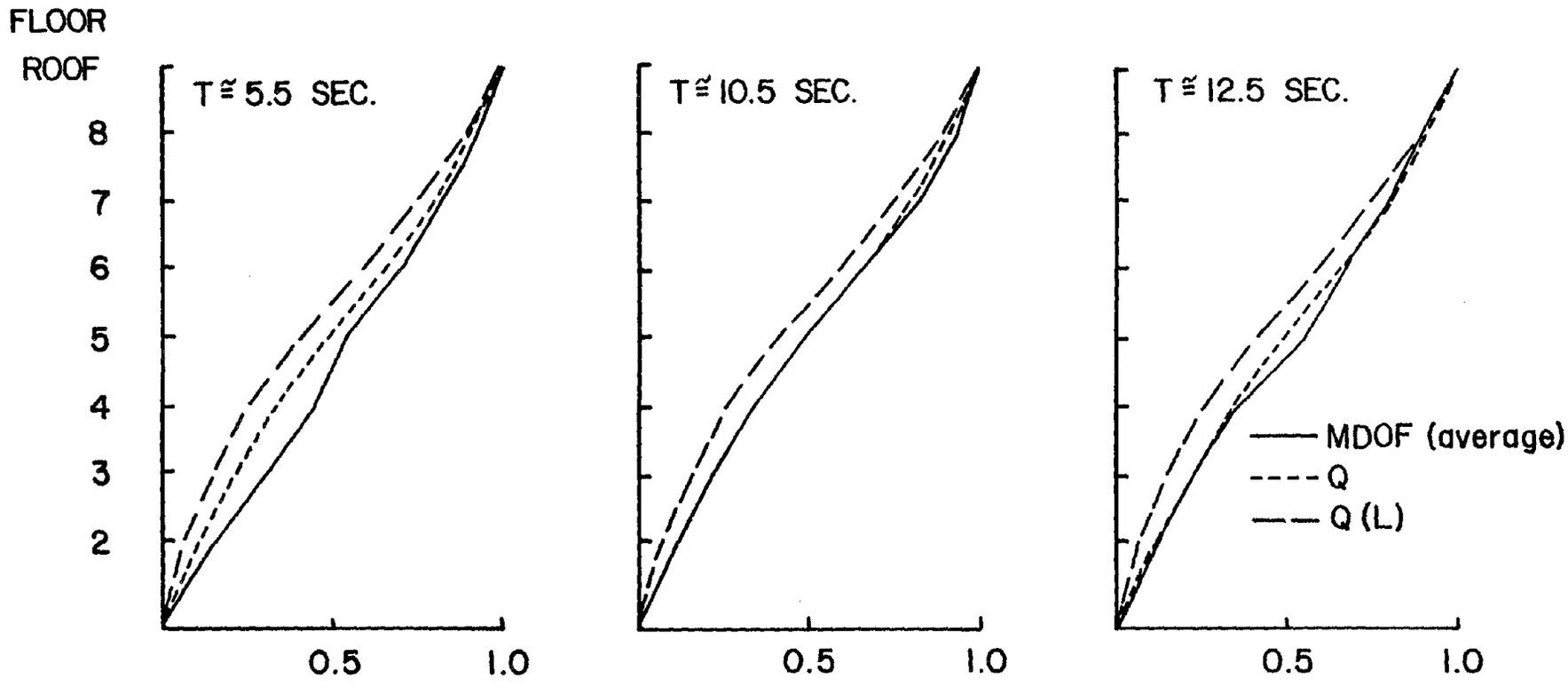

Fig. 6.5 Lateral Deflection Based on Different Models

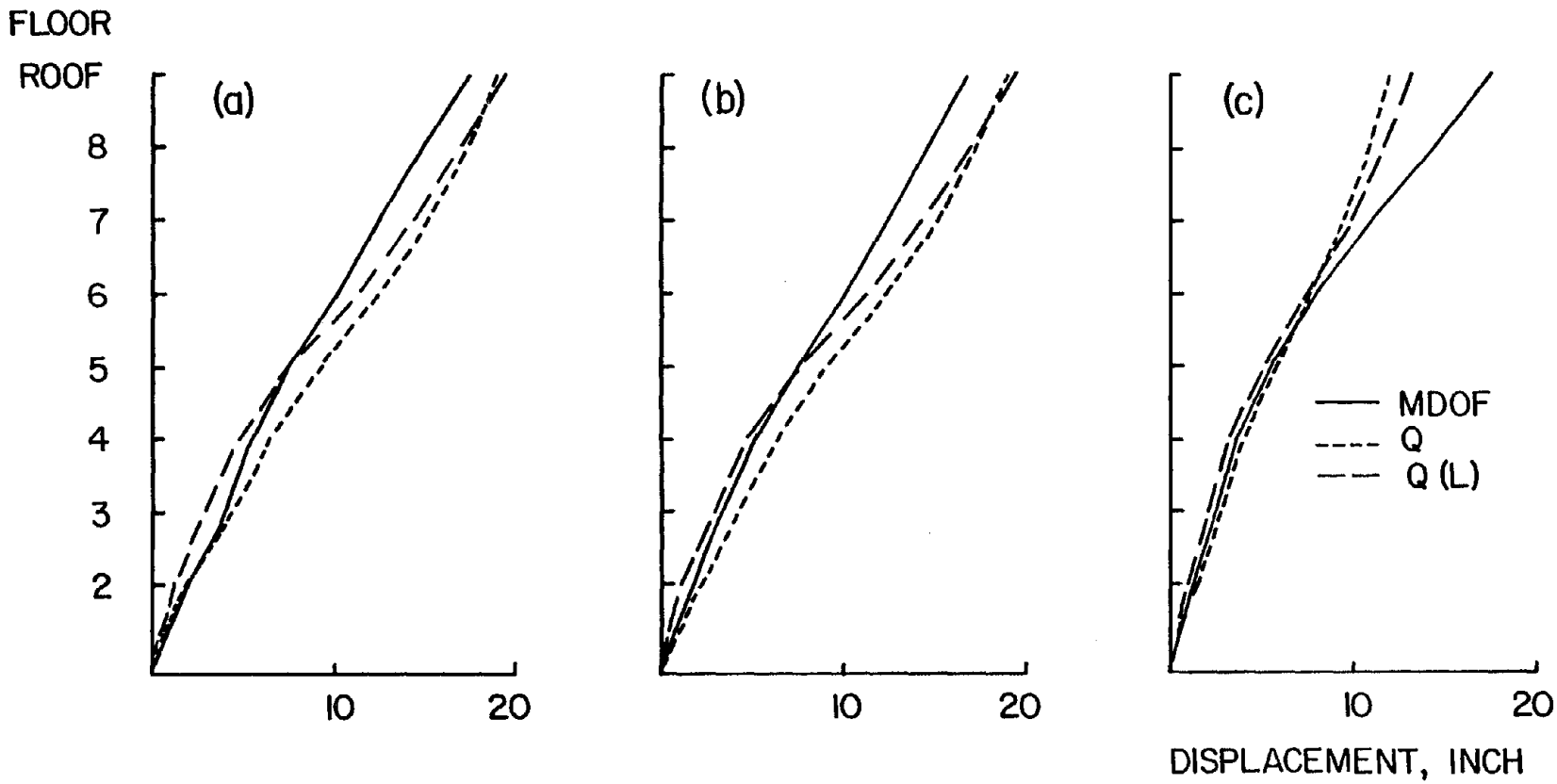

Fig. 6.6 Maximum Displacements for EFS

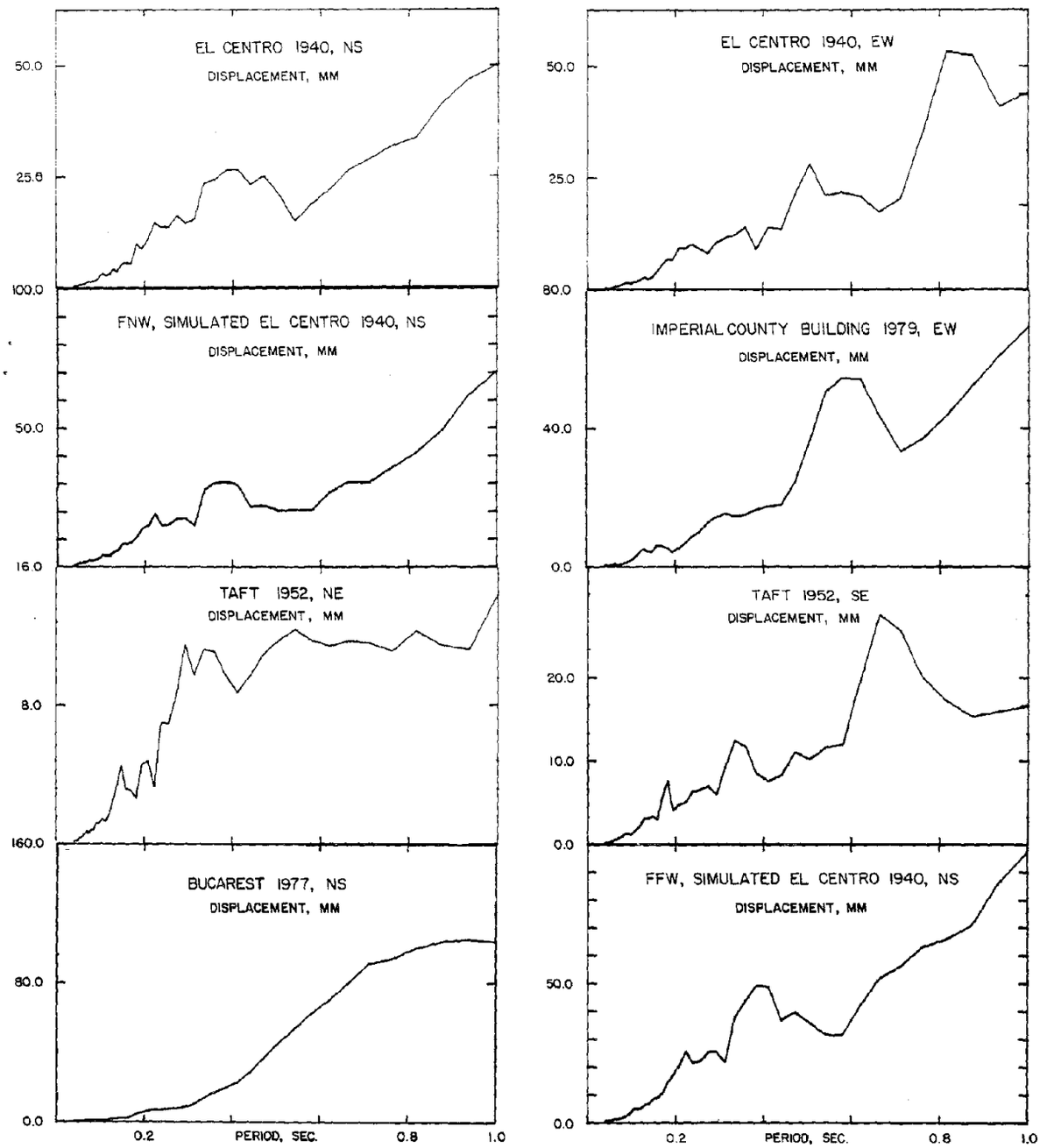

Fig. 7.1 Response Spectra for Different Earthquakes

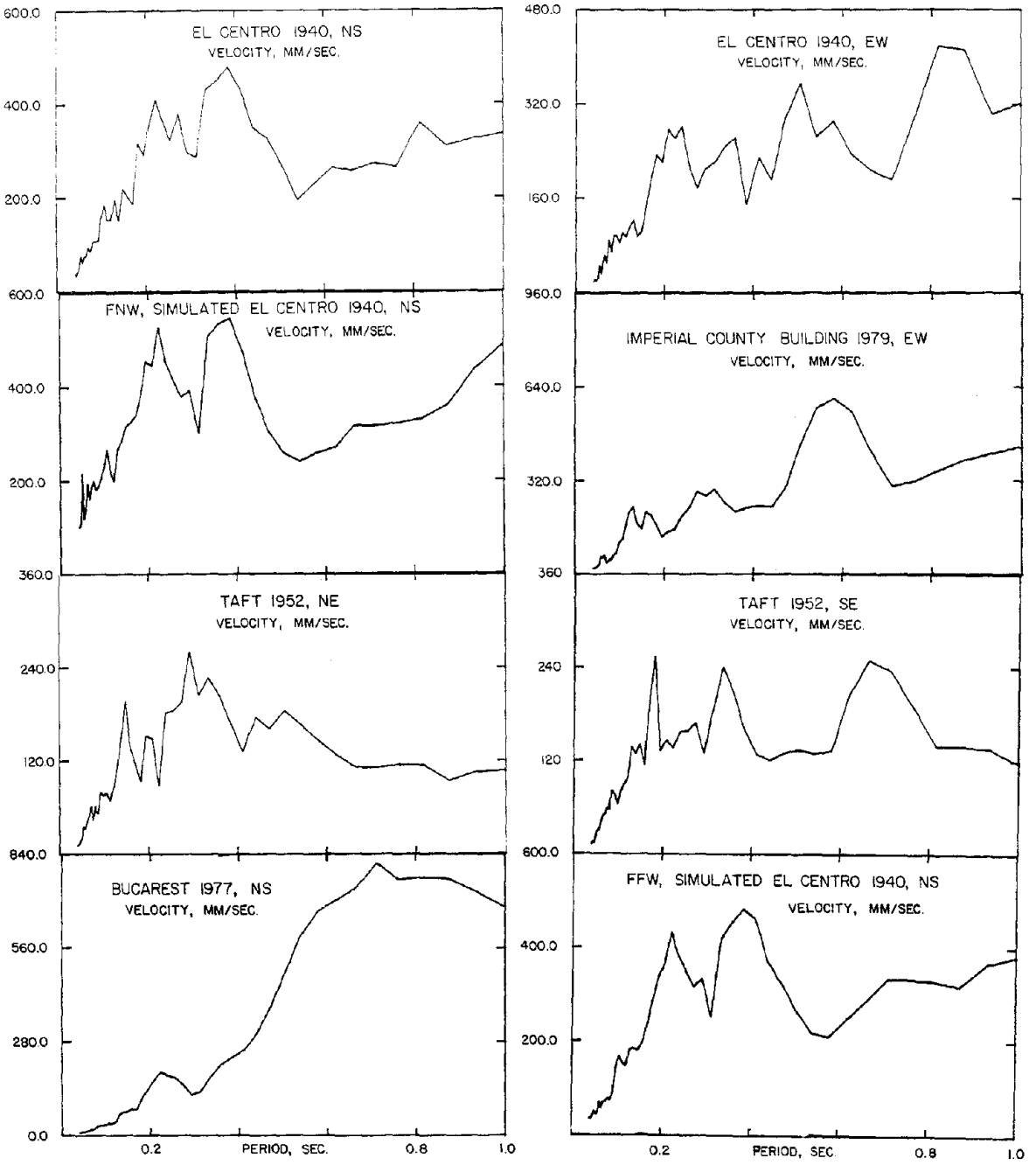

Fig. 7.1 (cont'd) Response Spectra for Different Earthquakes

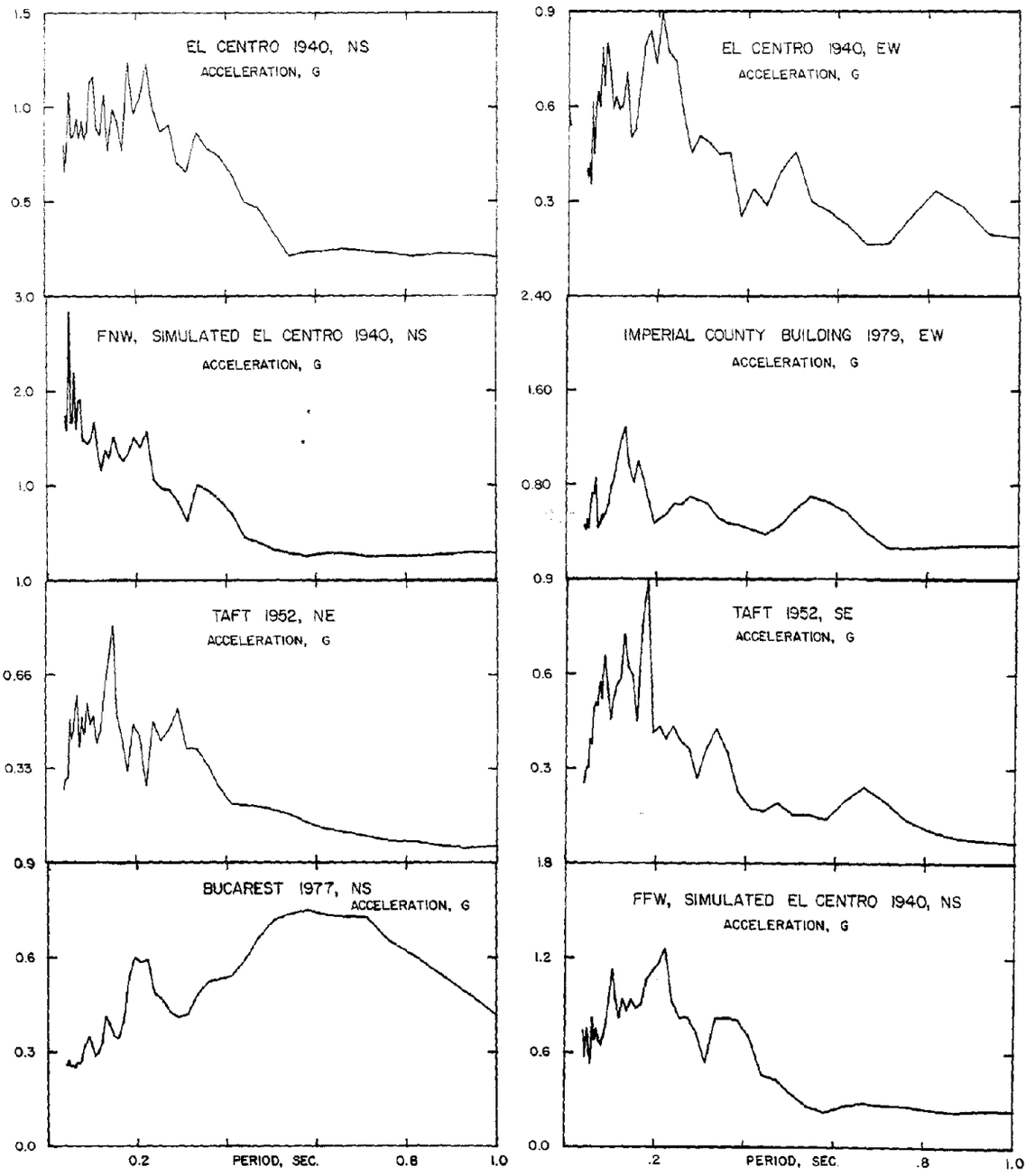

Fig. 7.1 (cont'd) Response Spectra for Different Earthquakes

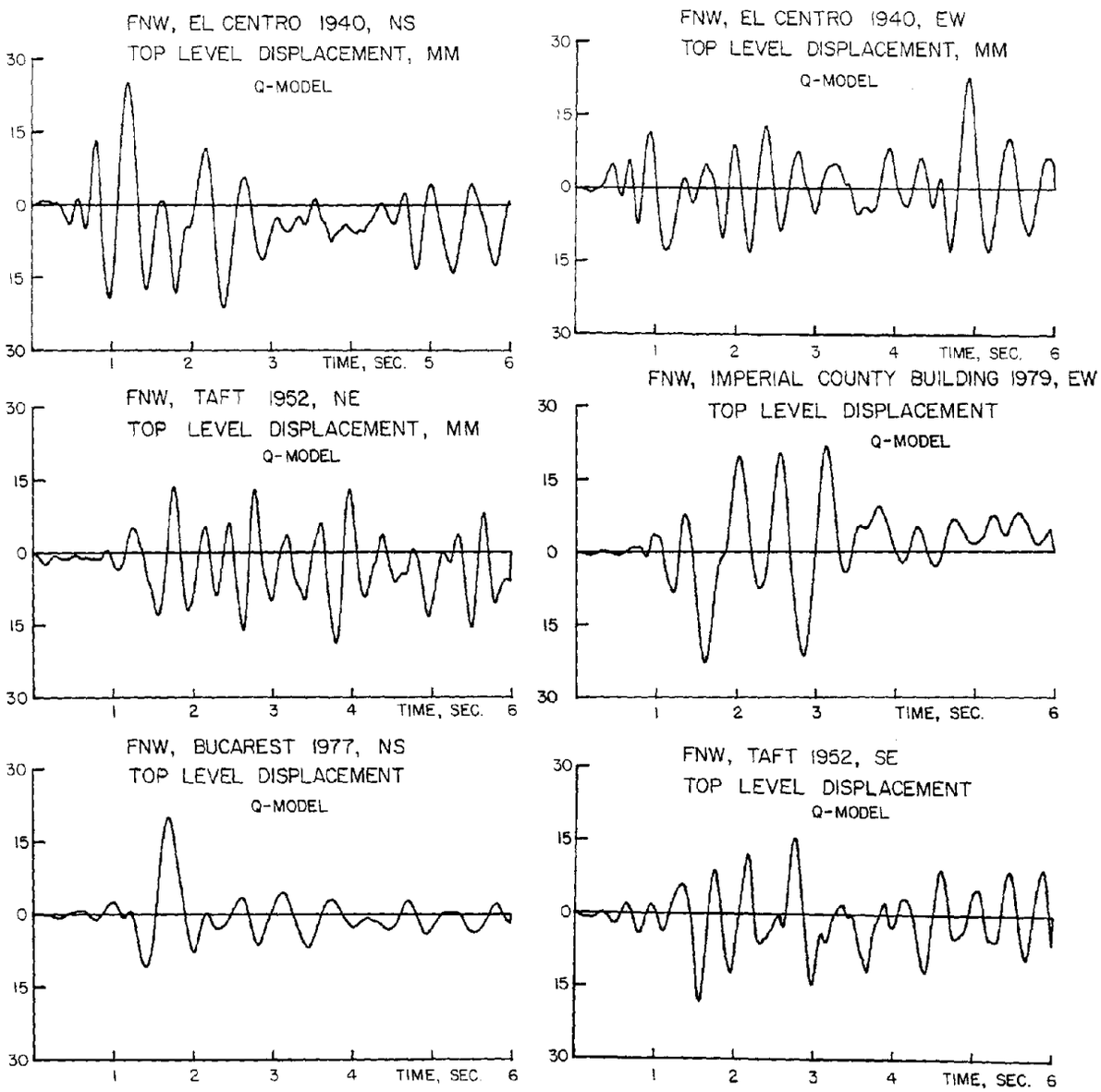

Fig. 7.2 Response Histories for FNW Subjected to Different Earthquakes

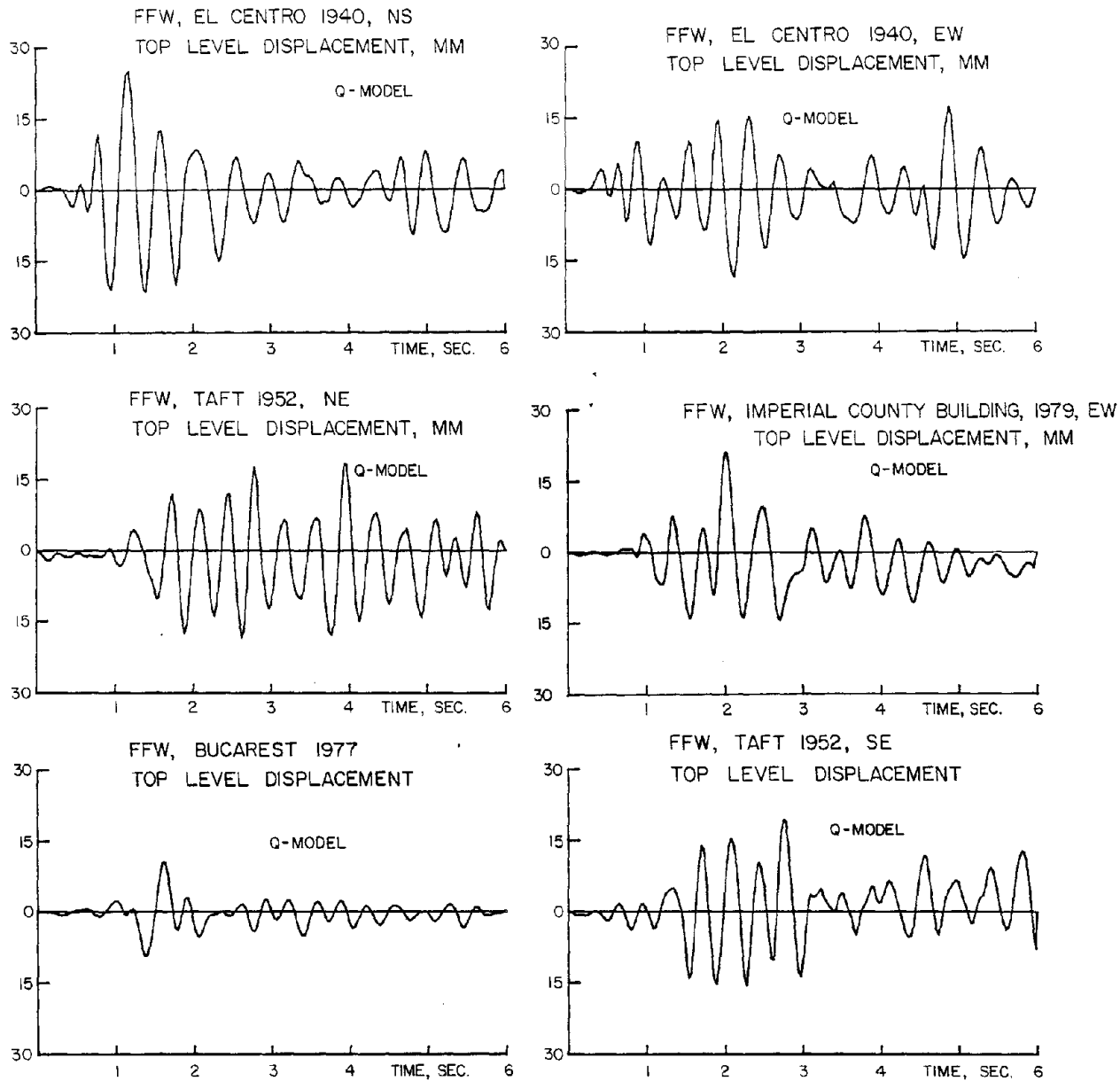

Fig. 7.3 Response Histories for FFW Subjected to Different Earthquakes

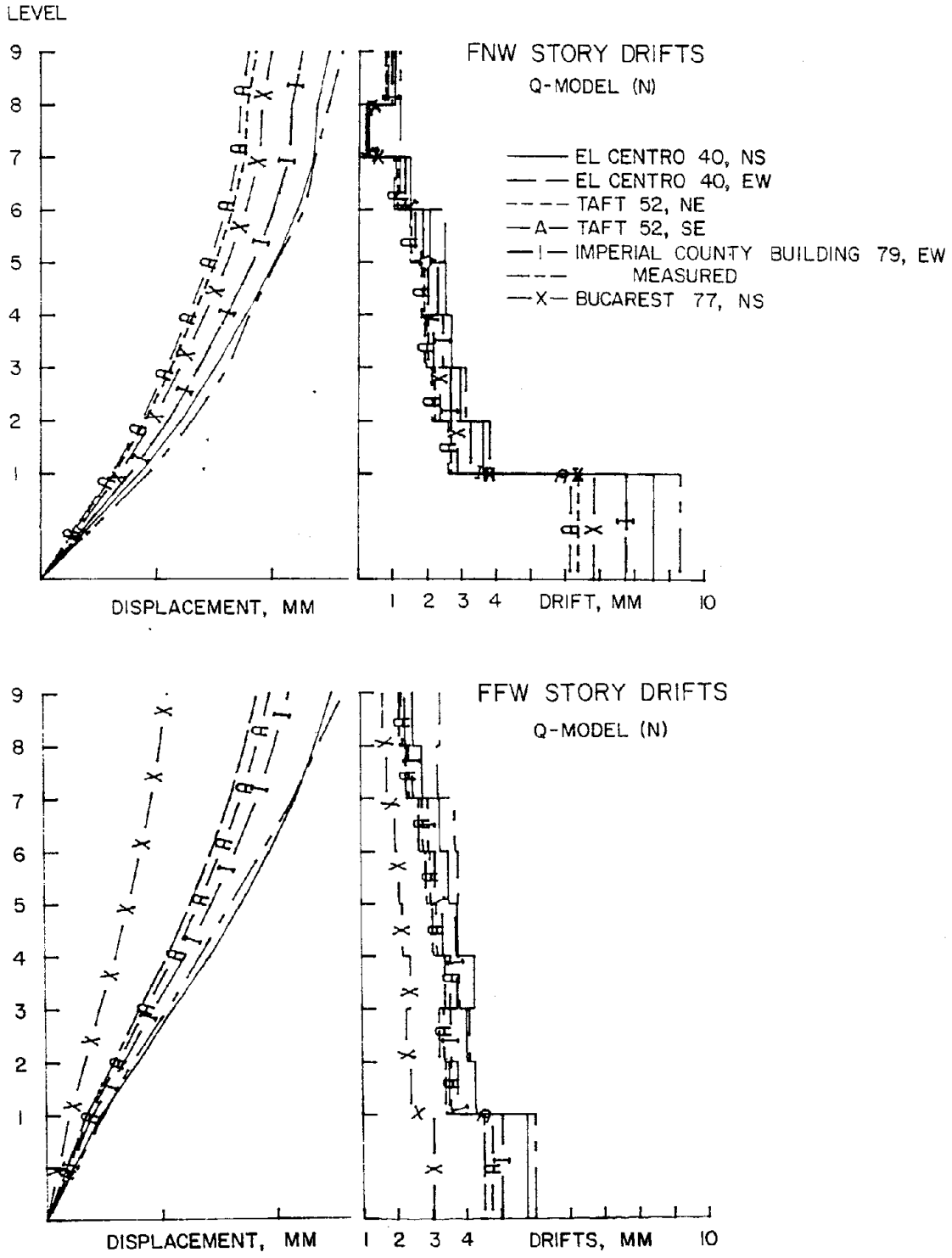

Fig. 7.4 Maximum Displacements Due to Different Earthquakes

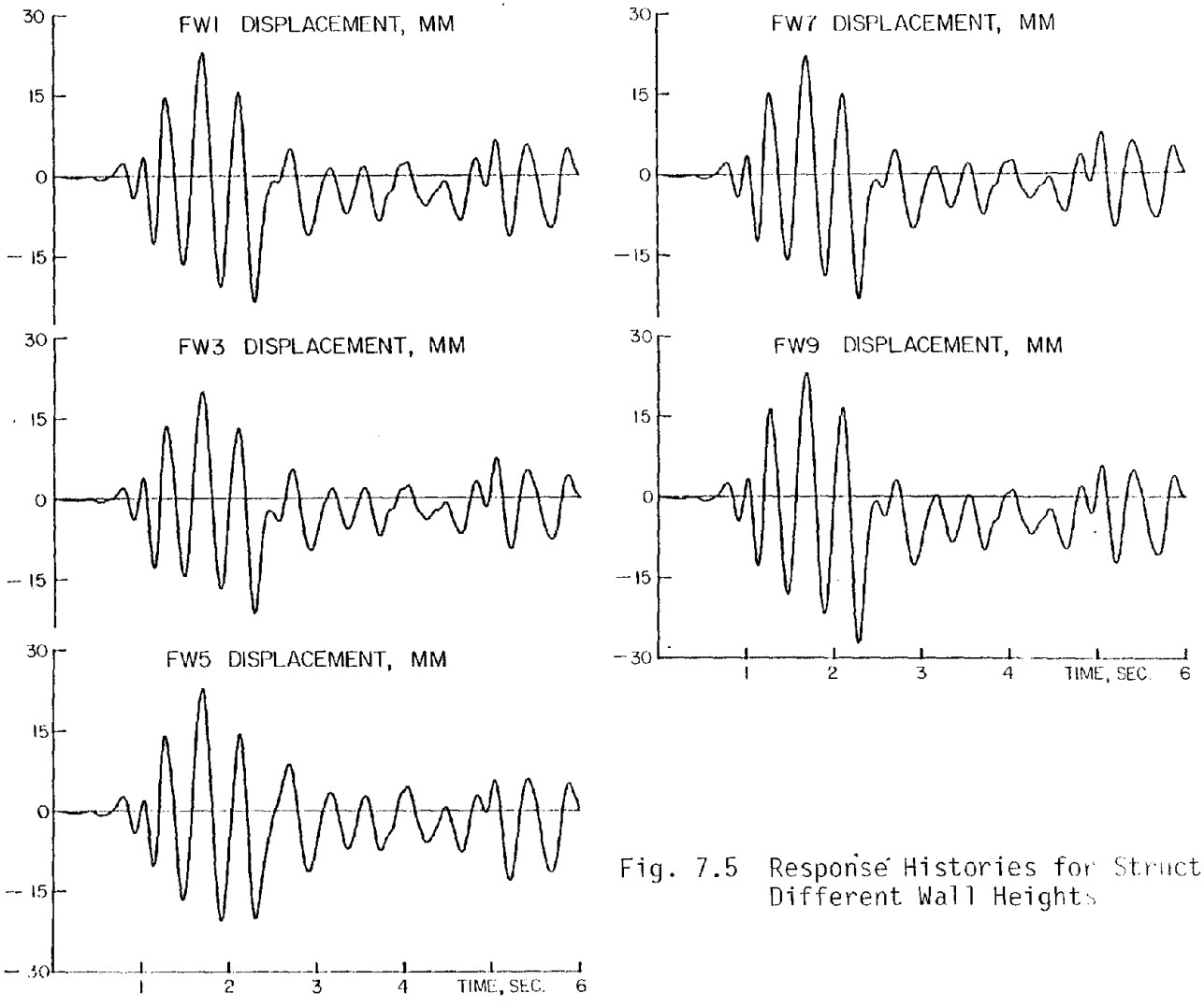

Fig. 7.5 Response Histories for Structures with Different Wall Heights

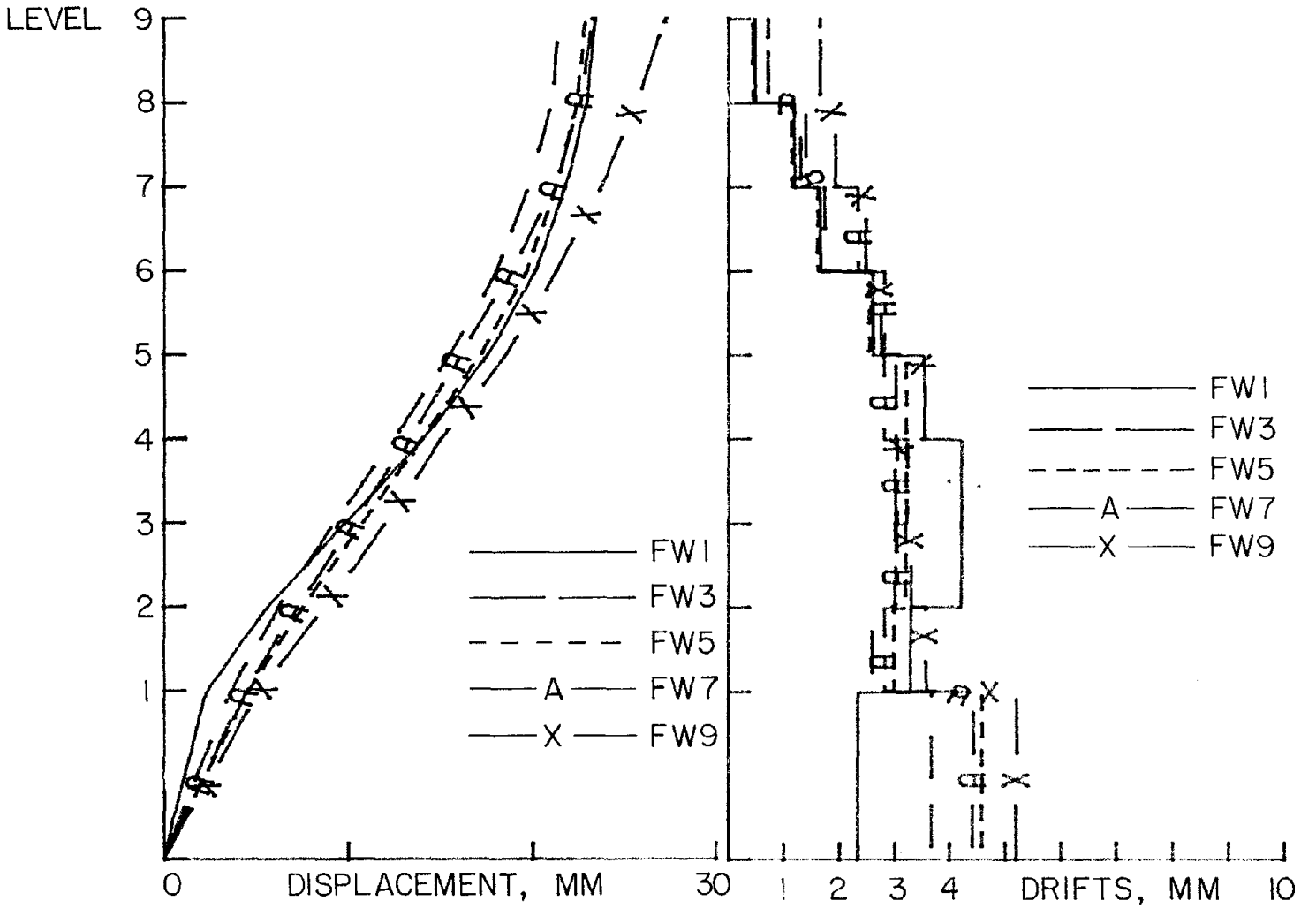

Fig. 7.6 Maximum Displacements for Structures with Different Wall Heights

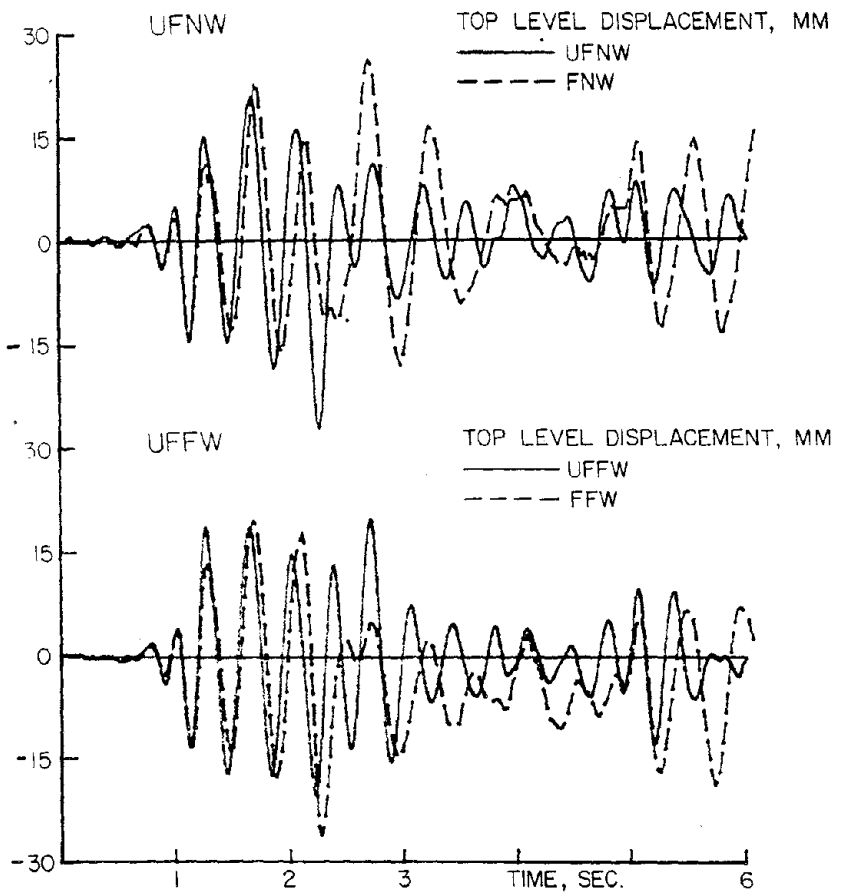

Fig. 8.1 Response of Structures Designed Based on UBC

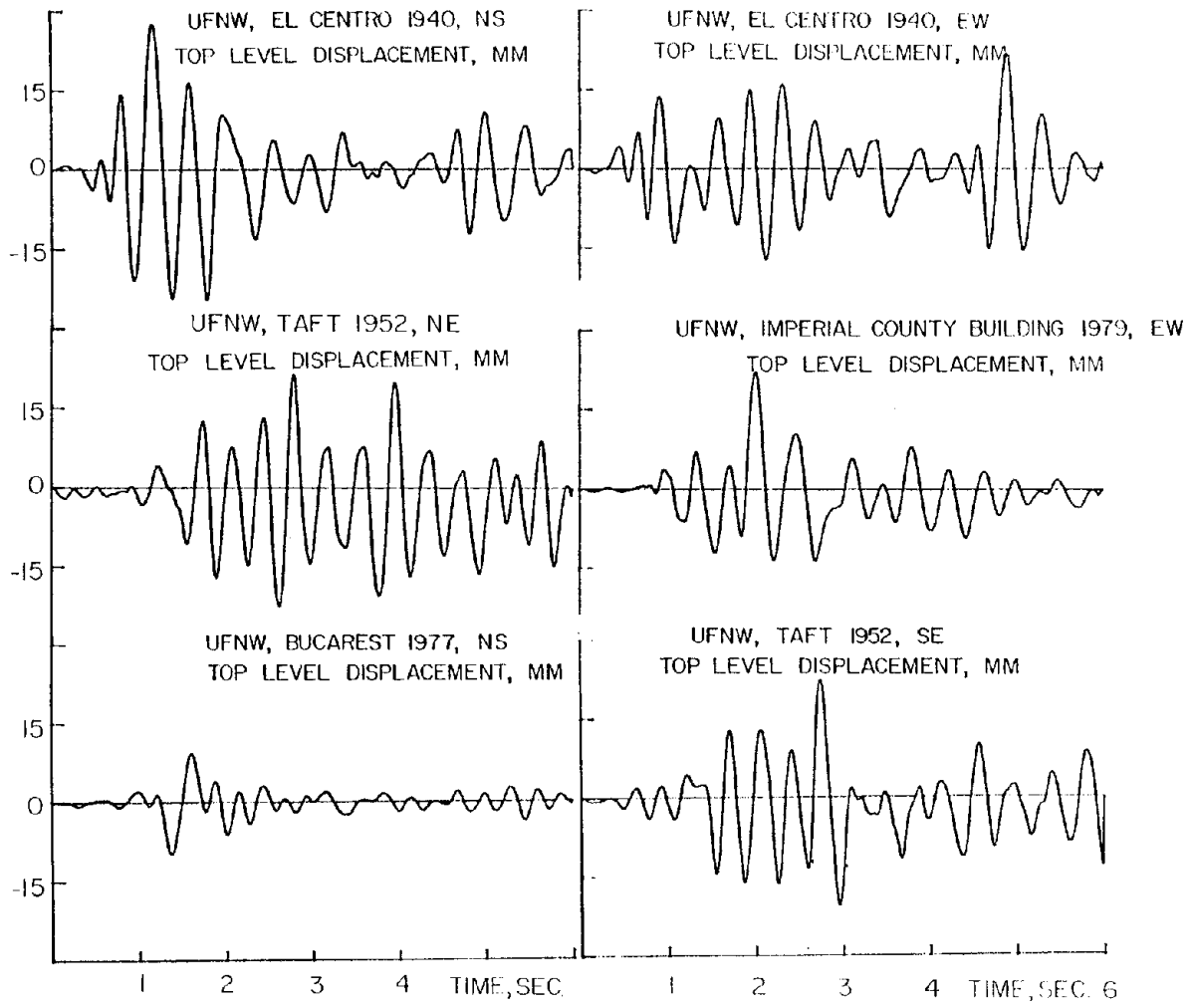

Fig. 8.2 Response of UFNW for Different Earthquakes

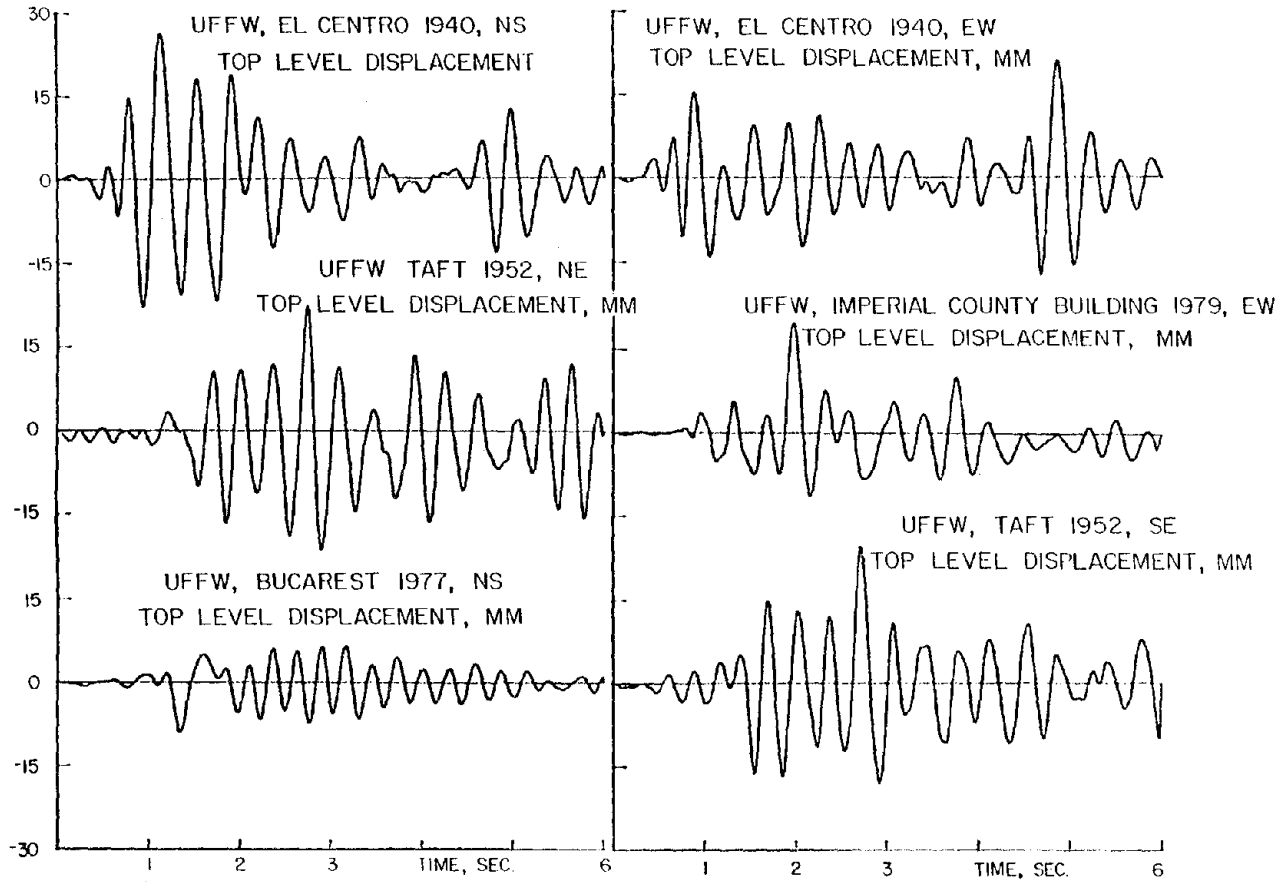

Fig. 8.3 Response of UFFW for Different Earthquakes

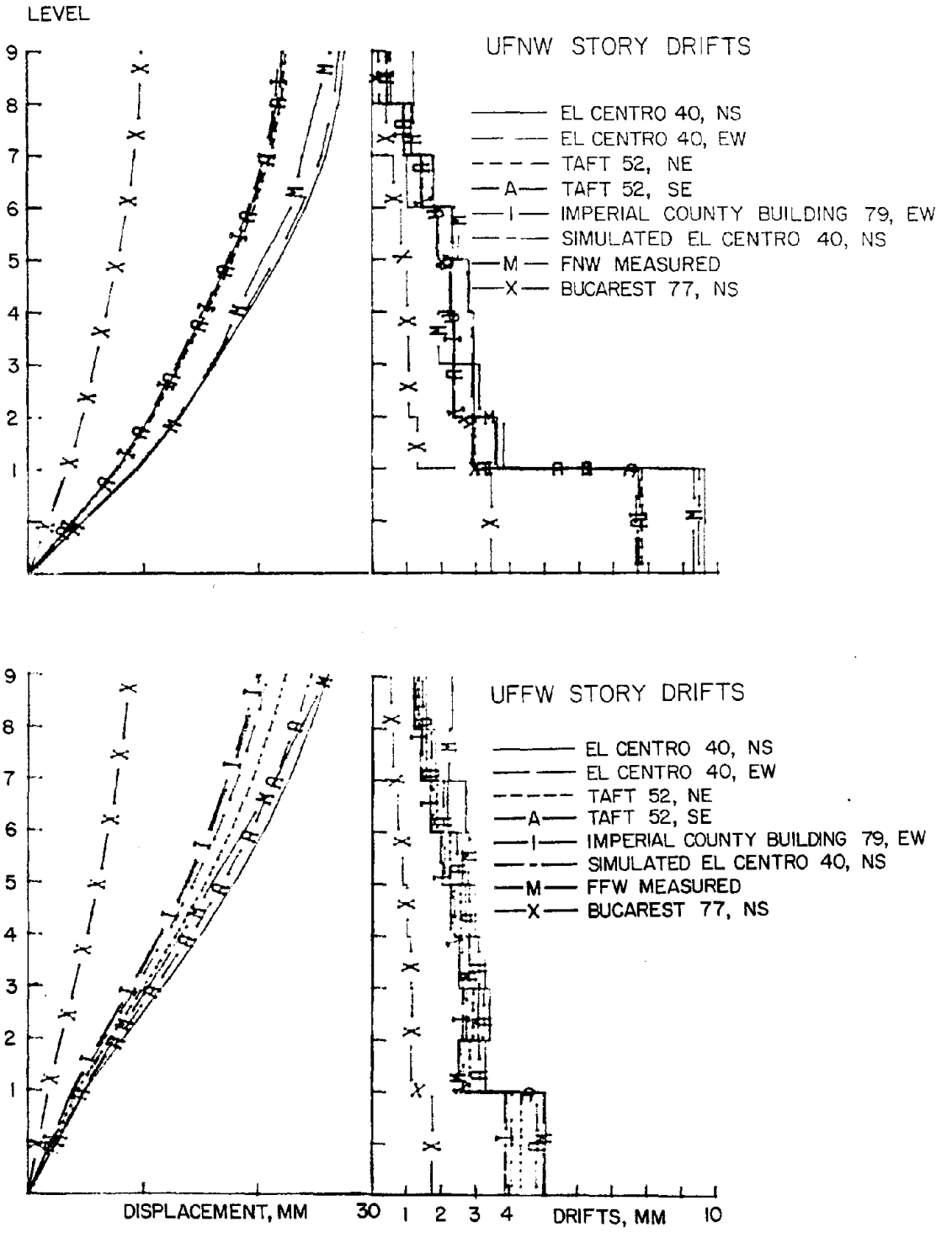

Fig. 8.4 Maximum Displacements for UFNW and UFFW

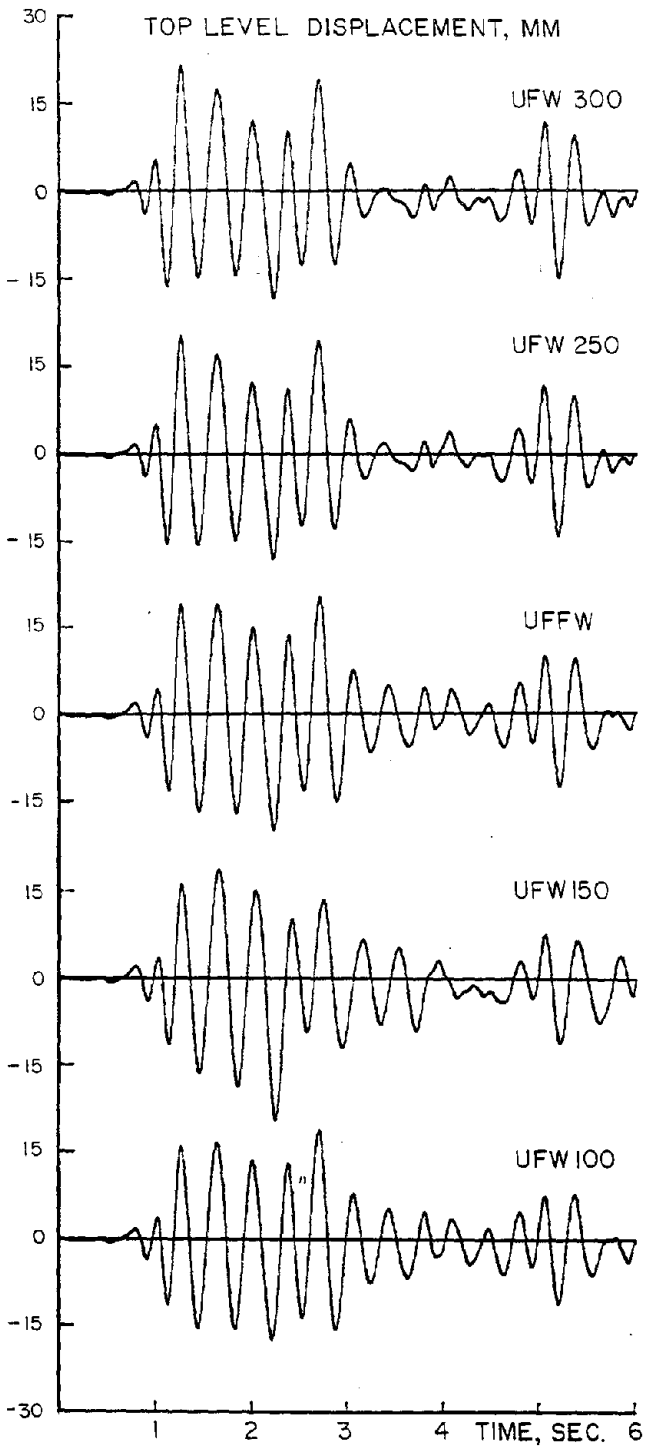

Fig. 8.5 Response of Structures with Different Wall Widths

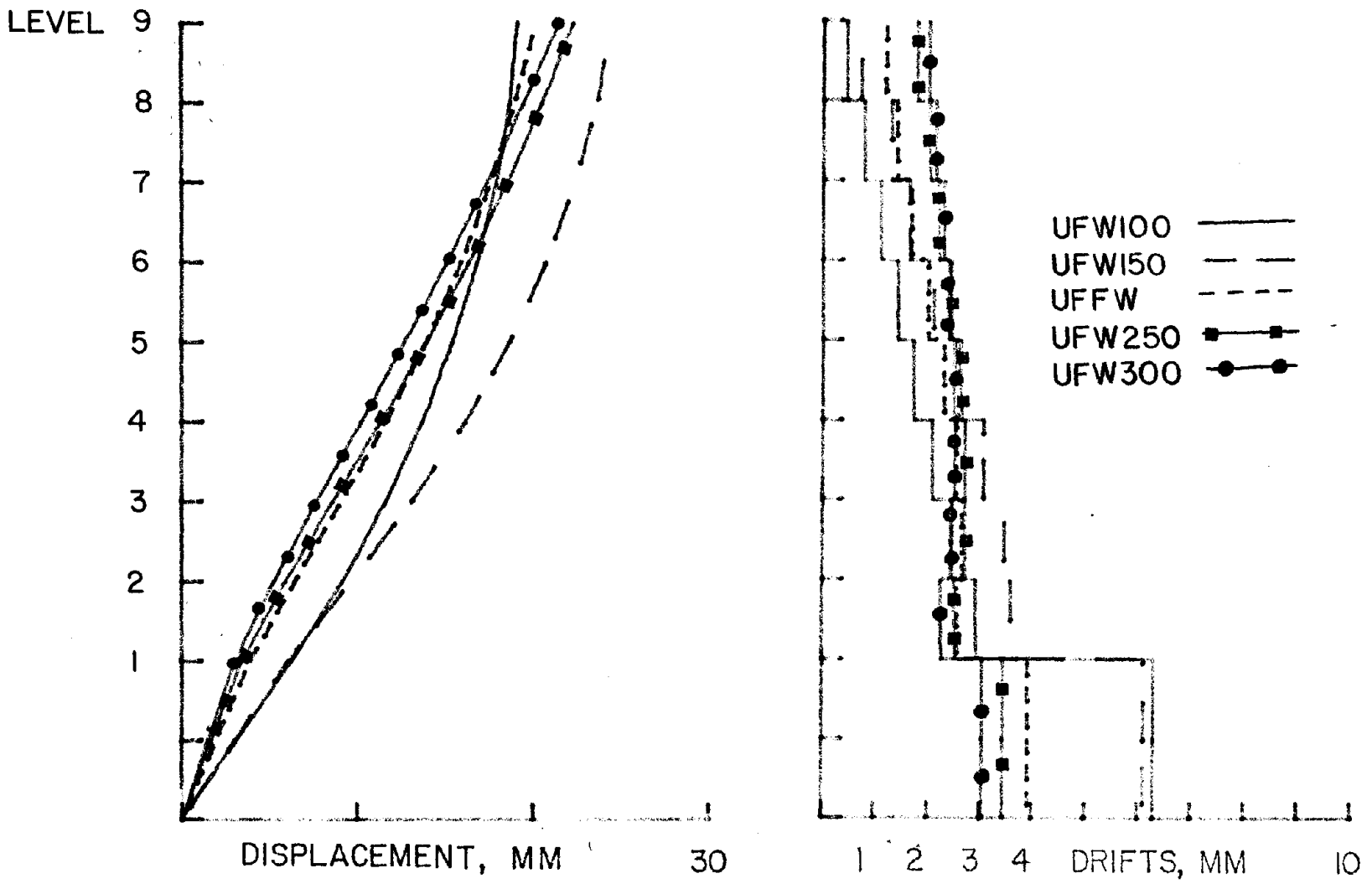

Fig. 8.6 Maximum Displacements for Structures with Different Wall Widths

APPENDIX A

USER'S MANUAL FOR THE UPDATED VERSION OF LARZ2

The following new features have been added:

1. Shear deformations may be included (cards 2.4.3 and 2.4.7.a).
2. "P-Delta" effects may be ignored (card 2.4.4).
3. Bending moments and rotational "ductilities" may be obtained for each loading.
4. Output for certain number of loadings may be skipped (card 2.4.4).
5. Location of inflection point with respect to member end may be specified. This distance is used to calculate nonlinear rotations. The default value is one-half of the clear length of the member. This feature is particularly useful for walls, because inflection point in walls of constant cross section is not usually at the middle point.
6. Elastic flexible diaphragms between any two horizontal degrees-of-freedom may be used. No out-of-plane deformations allowed (cards 2.4.4 and 2.4.8).

The new Section 2.4 in this version will supersede Section 2.4 in the old manual [26].

2.4 Program LARZ2

This program is used to analyze reinforced concrete frame and frame- wall structures subjected to a series of monotonically changing static lateral loads applied at floor levels. Nonlinearity of materials is taken into account at member level. Lateral loads may change sign; in other words, cyclic loads may be applied. Takeda hysteresis model is used to calculate stiffness changes [35].

Load increments have to be sufficiently small to allow gradual change of stiffness. Special precautions must be exercised in the vicinity of the apparent yield point of the structure. If large load increments are applied, the lateral strength of the structure will be overestimated.

2.4.1 Project Title (7A10)

COLUMN NO: 1-70
NOTATION: PRJ(*): project title
LIMIT: 70 Characters
COMMENTS: The title of the structure and/or project is provided on this card. The title may consist of any combination of numerical values and upper-case alphabetic symbols. The data on this card will appear in the front page of the output.

2.4.2 Units (3A10)

COLUMN NO.: 1-30
NOTATION: UNIT (*): units
LIMIT: 30 characters
COMMENTS: This card allows the user to specify the units being used. All the input data have to be in the same units. The output will have the same units as those of the input. The units involved are for length and force. The user may use any part of the specified range (columns 1 through 30) to punch (type) the units.

2.4.3 General Information (E15.6,5F10.5)

COLUMN NO: 1-15
NOTATION: E: modulus of elasticity of concrete
LIMIT: -
COMMENTS: none

COLUMN NO: 16-25
NOTATION: G: gravity acceleration
LIMIT: -
COMMENTS: none

COLUMN NO: 26-45
NOTATION: blank
LIMIT: -
COMMENTS: none

COLUMN NO: 46-55
NOTATION: GG: shear modulus
LIMIT: -
COMMENTS: none

2.4.4 Structural Information (12I5)

COLUMN NO: 1-5
NOTATION: NFRM: number of frames
LIMIT: 5
COMMENTS: The structure may consist of more than one but less than six frames or walls, or both.

COLUMN NO: 6-10
NOTATION: NFMAX: the total number of horizontal degrees-of-freedom in the structure
LIMIT: 20
COMMENTS: none

COLUMN NO: 11-15
NOTATION: NFLX: number of flexural element types
LIMIT: 20
COMMENTS: Usually in a structure, cross sectional dimensions and reinforcement distribution of some elements are identical. If such elements have the same anchorage conditions, unit length flexural properties for all of them are the same; hence, they represent one type of flexural element.

COLUMN NO: 16-20
NOTATION: NG: number of element dimension types
LIMIT: 20
COMMENTS: Members having the same left rigid end length, the same middle portion length, and the same right rigid end length represent one type of element dimension.

COLUMN NO: 21-25
NOTATION: MBMAX: maximum number of bays
LIMIT: 8
COMMENTS: Different constituent frames of a structure may have different number of bays. MBMAX is the number of bays of the frame with the largest number of spans.

COLUMN NO: 26-35
NOTATION: blank
LIMIT: -
COMMENTS: none

COLUMN NO: 36-40
NOTATION: NLD: number of load increments
LIMIT: 50
COMMENTS: none

COLUMN NO: 41-45
NOTATION: IWEI: index to specify if mass or weight will be given in the input
LIMIT: -
COMMENTS: IWEI = 0 mass will be given
= 1 weight will be given

COLUMN: 46-50
NOTATION: NUT: index to specify the contents of the output
LIMIT: -
COMMENTS: NUT = 0 print both input and output
= 1 print input only; do not analyze the structure
= 2 print output only

It is recommended that first NUT = 1 be used and the output, which reflects only the input data, be checked. After the user is certain about the correctness of the input, NUT = 0 or 2 can be used.

COLUMN NO: 51-55
NOTATION: IPDL: index to specify if "P-Delta" effects should be included
LIMIT: -
COMMENTS: IPDL = 0 ignore "P-Delta" effects
= 1 include "P-Delta" effects

COLUMN NO: 56-60
NOTATION: IS: number of loadings to be skipped in the output
LIMIT: -
COMMENTS: This parameter is used only to reduce the size of output, and it will not affect internal computations. Outputs for the first and last loading are printed regardless of the value of IS.

COLUMN NO: 61-65
NOTATION: NDPH: number of flexible diaphragms
LIMIT: 20
COMMENTS: Any flexible floor bounded by two horizontal degrees-of-freedom is considered one diaphragm. There can be more than one flexible diaphragm with the same elevation.

2.4.5 Frame Information (4I5)

One card is needed for each frame. The data on the ith "Frame Information" card will be considered for frame i.

COLUMN NO: 1-5
NOTATION: NM: number of members in the frame
LIMIT: 80 members in structure
COMMENTS: none

COLUMN NO: 6-10
NOTATION: NJ: number of joints (including supports) in the frame
LIMIT: 50 joints (excluding supports) in structure
COMMENTS: none

COLUMN NO: 11-15
NOTATION: NS: number of supports in the frame
LIMIT: 9
COMMENTS: none

COLUMN NO: 16-20
NOTATION: NF: number of horizontal degrees-of-reedom in the frame

LIMIT: 20
COMMENTS: none

2.4.6 Mass or Weight (5E15.5)

COLUMN NO: 1-15, 16-30, ...
NOTATION: AMASS(i): mass or weight at the level where the ith horizontal degree of freedom is defined
LIMIT: -
COMMENTS: AMASS(1) is punched (typed) in the first 15 columns, AMASS(2) is punched (typed) in the second 15 columns and so on.

2.4.7 Flexural Properties and Bond Slip

For each typical flexural element, there are two cards to be prepared: first, card (a) followed by card (b).

a. Flexural Properties (4E10.3, 3F10.6)

COLUMN NO: 1-10
NOTATION: ERTI(i): moment of inertia of typical flexural element i
LIMIT: -
COMMENTS: none

COLUMN NO: 11-20
NOTATION: CRM(i): cracking moment of flexural element type i
LIMIT: -
COMMENTS: none

COLUMN NO: 21-30
NOTATION: YIM(i): yielding moment of flexural element type i
LIMIT: -
COMMENTS: none

COLUMN NO: 31-40
NOTATION: ULM(i): moment at a point beyond the yield point of primary curve
LIMIT: -
COMMENTS: This value is used only to calculate the slope of post-yielding segment of M-O curve; it does not impose any limit on the resistance of the member.

COLUMN NO: 41-50
NOTATION: YIC(i): yield curvature of flexural element type i
LIMIT: -
COMMENTS: none

COLUMN NO: 51-60
NOTATION: ULC(i): curvature at a point beyond the yield point
LIMIT: -
COMMENTS: The curvature must be the value of curvature at the point where moment is equal to ULM(i).

COLUMN NO: 61-70
NOTATION: AR(i): shear area
LIMIT: -
COMMENTS: Leave blanks if shear deformations are ignored.

b. Rotation due to Bond Slip (3E15.6)

COLUMN NO: 1-15
NOTATION: SC(i): Unit length rotation due to bond slip corresponding to the cracking moment
LIMIT: -
COMMENTS: Procedure to calculate rotations due to bond slip is described in Chapter 2 in Reference 25.

COLUMN NO: 16-30
NOTATION: SY(i): unit length rotation due to bond slip corresponding to the yield moment
LIMIT: -
COMMENTS: none

COLUMN NO: 31-45
NOTATION: SU(i): unit length rotation due to bond slip corresponding to ULM(i)
LIMIT: -
COMMENTS: none

2.4.8 Flexible Diaphragm Information (2I5,F10.0)

One card is used for each flexible diaphragm. Skip this part if there are no such diaphragms.

COLUMN NO: 1-5
NOTATION: IDPH(*,1): global DOF number adjacent to diaphragm *
LIMIT: -
COMMENTS: none

COLUMN NO: 6-10
NOTATION: IDPH(*,2): global DOF number adjacent to diaphragm *
LIMIT: -
COMMENTS: IDPH(*,1) and IDPH(*,2) should be sorted in ascending order. If one side of the diaphragm is fixed, columns 6-10 should be left blank.

COLUMN NO: 11-20
NOTATION: SDPH(*): stiffness of the *th diaphragm
LIMIT: -
COMMENTS: Diaphragms are assumed to remain elastic throughout the analysis. The value of stiffness is calculated by the user with appropriate consideration of torsional properties of the adjacent members.

2.4.9 Typical Element Dimensions (3F10.3)

The first card of this group represents the dimensions of member

type one.

COLUMN NO: 1-10
NOTATION: TYPT(i): total length of member
LIMIT: -
COMMENTS: none

COLUMN NO: 11-20
NOTATION: TYPL(i): length of left (top) rigid end portion
LIMIT: -
COMMENTS: none

COLUMN NO: 21-30
NOTATION: TYPR(i): length of right (bottom) rigid end portion
LIMIT: -
COMMENTS: none

2.4.10 Member Characteristics (7I5)

One card is used for each member. First, the data for members of frame one are given. The ith card for each frame contains the data for member i of that frame.

COLUMN NO: 1-5
NOTATION: MCH(i,1): element dimension type for member i
LIMIT: NG
COMMENTS: none

COLUMN NO: 6-10
NOTATION: MCH(i,2): flexural element type for the left (top) end of member i
LIMIT: NFLX
COMMENTS: none

COLUMN NO: 11-15
NOTATION: MCH(i,3): flexural element type for the right (bottom) end of member i
LIMIT: NFLX
COMMENTS: none

COLUMN NO: 16-20
NOTATION: NODE (i,1): left (top) end local incidence of member i
LIMIT: 50
COMMENTS: none

COLUMN NO: 21-25
NOTATION: NODE(i,2): right (bottom) end local incidence of member i
LIMIT: 50
COMMENTS: none

COLUMN NO: 26-30
NOTATION: IDIR(i): index to specify whether the member is a beam or a column
LIMIT: -
COMMENTS: IDIR(i) = 0 member i is a column or a wall
= 1 member i is a beam

COLUMN NO: 31-35
NOTATION: IBSE(i): index to specify if the length from member end to inflection point is other than one-half of the member length
LIMIT: up to 10 members with IBSE(i) = 1 allowed
COMMENTS: IBSE(i): = 0 inflection point at the middle
= 1 inflection point at location other than the middle

2.4.11 Main and Dependent Degrees of Freedom

Each horizontal degree-of-freedom may consist of more than one joint. One of the joints in each degree-of-freedom is considered as the main joint; others are assumed to be dependent joints. There are two cards for each horizontal degree-of-freedom: cards (a) and (b). Data cards for frame one come first, followed by the data for frame two and so on.

a. Main Joints (3I5)

COLUMN NO: 1-5
NOTATION: LIST(*): local joint number of main joint
LIMIT: -
COMMENTS: none

COLUMN NO: 6-10
NOTATION: LIST(*): number of dependent joints in the frame
LIMIT: 8
COMMENTS: If there are no dependent joints, use 1.

COLUMN NO: 11-15
NOTATION: IFRE(*): corresponding global degree of freedom
LIMIT: -
COMMENTS: none

b. Dependent Joints (8I5)

COLUMN NO: 1-5,6-10, ...
NOTATION: LIST(*): dependent local joint
LIMIT: -
COMMENTS: Each dependent joint is punched in five columns of this card. If there are no dependent joints, punch the main joint number in the first five columns.

2.4.12 Height of Levels (10F8.3)

COLUMN NO: 1-8,9-16, ...

NOTATION: HT(i): height of the level at which the ith degree-of-freedom is defined

LIMIT: -

COMMENTS: ith 8-column range is for the ith degree-of-freedom. If there are more than ten degrees of freedom, use two cards.

2.4.13 Height of Inflection Points (10F8.3)

Skip this card if there are no members with IBSE equal to 1.

COLUMN NO: 1-8,9-16, ...

NOTATION: CNTF(i): distance of inflection point from member end (see comments) for the ith member with IBSE(i) = 1

COMMENTS: Distances are given in the same sequence that members with IBSE equal to 1 appear in the input. For example, the quantity given in the third 8 columns represents the distance for the third member with IBSE equal to 1 as appeared in the input.

CNTF is the canilever length used for calculation of nonlinear rotations from curvature values. The length is used for both member ends. If yielding is expected at both member ends, CNTF should be the average of distances from the inflection point and the two ends.

2.4.14 Involved Joints

Adjacent to each level, where one horizontal degree-of-freedom is defined, there are joints above and/or below which are connected to the level by means of columns. Any rotation at these joints will cause moment at the joints in the level of concern. Because the program is developed to solve irregular as well as regular frames, it is necessary that information about the joints adjacent to each level and within the level be provided. The data are used to trace the location of non-zero elements of upper right structural submatrix (Appendix B in Reference 25).

a. Number of Involved Joints (16I5)

COLUMN NO: 1-5,6-10, ...

NOTATION: NEF(i): number of adjacent joints and the joints within ith DOF

LIMIT: 50

COMMENTS: none

b. Involved Joints (16I5)

COLUMN NO: 1-5,6-10, ...

NOTATION: JTK(*): global joint number adjacent to or within the level where a degree-offreedom is defined

LIMIT: -

COMMENTS: There are up to two cards for each degree-of-freedom. The joint numbers are to be sorted in ascending order. If there are less than 17 involved joints in a degree of freedom, only one card is needed. The first card is for the first degree of freedom.

2.4.15 Load Increments (10F8.4)

COLUMN NO: 1-8,9-16, ...
NOTATION: DF(i,j): jth load increment at level where ith degree-of-freedom is defined
LIMIT: -
COMMENTS: The first eight columns contain the increment for the first degree-of-freedom. First card contains the value of the first load increment. If there are more than ten degrees-of-freedom, the first two cards define the first series of load increments. During the first loading the structure is assumed to remain elastic.

APPENDIX B

USER'S MANUAL FOR THE UPDATED VERSION OF LARZ

The following new features have been added:

1. Shear deformations may be included (cards 2.2.3 and 2.2.7.a).
2. Location of inflection point with respect to member end may be specified. This distance is used to calculate nonlinear rotations. The default value is one-half of the clear length of the member. This feature is particularly useful for walls, because inflection point in walls of constant cross section is not usually at the middle point.
3. Elastic flexible diaphragms between any two horizontal degrees-of-freedom may be used. No out-of-plane deformations allowed (cards 2.2.4 and 2.2.8).
4. Clough Hysteresis Model may be used.

The new Section 2.2 in this version will supersede Section 2.2 in the old manual [26].

2.2 Program LARZ

This program is used to analyze planar structures, consisting of one or more frames and walls, subjected to an input base acceleration history. Frames are assumed to comprise vertical and horizontal elements. Inelastic deformations are considered by taking into account element nonlinearity. Several assumptions and idealizations described in Chapter 2 of Reference 25 are applied in the program. In the present chapter, only the procedure to prepare input data is provided.

2.2.1 Project Title (7A10)

COLUMN NO: 1-70
NOTATION: PRJ(*): project title
LIMIT: 70 Characters
COMMENTS: The title of the structure and/or project is provided on this card. The title may consist of any combination of numerical values and upper-case alphabetic symbols. The data on this card will appear in the front page of the output.

2.2.2 Units (3A10)

COLUMN NO.: 1-30
NOTATION: UNIT (*): units
LIMIT: 30 characters
COMMENTS: This card allows the user to specify the units being used. All the input data have to be in the same set of units. The output will have the same units as those of the input. The units involved are for length, time, and force. The user may use any part of the specified range (columns 1 through 30) to punch (type) the units.

2.2.3 General Information (E15.6,5F10.5)

COLUMN NO: 1-15
NOTATION: E: modulus of elasticity of concrete
LIMIT: -
COMMENTS: none

COLUMN NO: 16-25
NOTATION: G: gravity acceleration
LIMIT: -
COMMENTS: none

COLUMN NO: 26-35
NOTATION: ALPHA: coefficient of mass matrix in the expression for damping (Chapter 2, Reference 2)
LIMIT: -
COMMENTS: $\alpha = 2\omega_1\omega_2(\xi_2\omega_1 - \xi_1\omega_2)/(\omega_1^2 - \omega_2^2)$

where ω_1 and ω_2 = the damping factors for the first two modes;
ξ_1 and ξ_2 = the frequencies of the first two modes.

COLUMN NO: 36-45
NOTATION: BETA: coefficient of stiffness matrix in the expression for damping.
LIMIT: -
COMMENTS: $\beta = 2(\xi_1\omega_1 - \xi_2\omega_2)/(\omega_1^2 - \omega_2^2)$

COLUMN NO: 46-55
NOTATION: GG: shear modulus
LIMIT: -
COMMENTS: none

2.2.4 Structural Information (12I5)

COLUMN NO: 1-5
NOTATION: NFRM: number of frames
LIMIT: 5
COMMENTS: The structure may consist of more than one but less than six frames or walls, or both.

COLUMN NO: 6-10
NOTATION: NFMAX: the total number of horizontal degrees-of-freedom in the structure
LIMIT: 20
COMMENTS: none

COLUMN NO: 11-15
NOTATION: NFLX: number of flexural element types
LIMIT: 20
COMMENTS: Usually in a structure, cross sectional dimensions and reinforcement distribution of some elements are identical. If such elements have the same anchorage conditions, unit length flexural properties for all of them are the same; hence, they represent one type of flexural element.

COLUMN NO: 16-20
NOTATION: NG: number of element dimension types
LIMIT: 20
COMMENTS: Members having the same left rigid end length, the same middle portion length, and the same right rigid end length represent one type of element dimension.

COLUMN NO: 21-25
NOTATION: MBMAX: maximum number of bays
LIMIT: 8
COMMENTS: Different constituent frames of a structure may have different number of bays. MBMAX is the number of bays of the frame with the largest number of spans.

COLUMN NO: 26-30
NOTATION: IHYST: index to specify the hysteresis type to be used
LIMIT: -
COMMENTS: Currently there are six types of hysteresis models which can be used in the program. Only one hysteresis model can be used in each analysis. In other words, different models cannot be assigned to different members of a structure. Informations about the hysteresis systems are provided in References 1,2, and 3.

The following are the indeces for each model:

IHYST = 1 Takeda model
= 2 Sina model
= 3 Q-Hyst model
= 4 Otani model
= 5 Simple Bilinear model
= 6 Clough model

COLUMN NO: 31-35
NOTATION: NSV: the frequency of checking response for maxima and saving it for plotting
LIMIT: total number of steps at which data are saved shall not exceed 1900(LARZ), 3800(LARZAK)

COLUMN NO: 36-40
NOTATION: NCYC: the frequency of changing stiffness
LIMIT: -
COMMENTS: The hysteresis models used in the program consist of linear segments the slopes of which represent stiffness. The stiffness characteristic of an element does not change unless a break point is passed. If a small time step is used for the analysis, changes of structural stiffness from one step to the next may be small. Furthermore, reconstruction of structural stiffness matrix at all time steps is costly and inefficient. Therefore, stiffness is changed once at every NCYC time steps.

COLUMN NO: 41-45
NOTATION: IWEI: index to specify if mass or weight will be given in the input
LIMIT: -
COMMENTS: IWEI = 0 mass will be given
= 1 weight will be given

COLUMN: 46-50
NOTATION: NUT: index to specify the contents of the output
LIMIT: -
COMMENTS: NUT = 0 print both input and output
= 1 print input only; do not analyze the structure
= 2 print output only

It is recommended that first NUT = 1 be used and the output, which reflects only the input data, be checked. After the user is certain about the correctness of the input, NUT = 0 or 2 can be used.

COLUMN NO: 51-60
NOTATION: blank
LIMIT: -
COMMENTS: None

COLUMN NO: 61-65
NOTATION: NDPH: number of flexible diaphragms
LIMIT: 20
COMMENTS: Any flexible floor bounded by one or two horizontal degrees-of-freedom is considered one diaphragm. There can be more than one flexible diaphragm at the same elevation.

2.2.5 Frame Information (4I5)

One card is needed for each frame. The data on the ith "Frame Information" card will be considered for frame i.

COLUMN NO: 1-5
NOTATION: NM: number of members in the frame
LIMIT: 80 members in structure
COMMENTS: none

COLUMN NO: 6-10
NOTATION: NJ: number of joints (including supports) in the frame
LIMIT: 50 joints (excluding supports) in structure
COMMENTS: none

COLUMN NO: 11-15
NOTATION: NS: number of supports in the frame
LIMIT: 9
COMMENTS: none

COLUMN NO: 16-20
NOTATION: NF: number of horizontal degrees-of-reedom in the frame
LIMIT: 20
COMMENTS: none

2.2.6 Mass or Weight (5E15.5)

COLUMN NO: 1-15, 16-30, ...
NOTATION: AMASS(i): mass or weight at the level where the ith horizontal degree-of-freedom is defined
LIMIT: -
COMMENTS: AMASS(1) is punched (typed) in the first 15 columns, AMASS(2) is punched (typed) in the second 15 columns and so on.

2.2.7 Flexural Properties and Bond Slip

For each typical flexural element, there are two cards to be prepared: first, card (a) followed by card (b).

a. Flexural Properties (4E10.3, 4F10.6)

COLUMN NO: 1-10
NOTATION: ERTI(i): moment of inertia of typical flexural element i
LIMIT: -
COMMENTS: If the primary curve considered by the hysteresis model is a trilinear curve (Takeda and Sina hysteresis models), ERTI is the moment of inertia for an uncracked section. If a bilinear primary curve is used (Otani, Simple Bilinear, Q-Hyst, and Clough model), ERTI is calculated from

$$ERTI(i) = \frac{YIM(i)}{E.YIC(i)}$$

COLUMN NO: 11-20
NOTATION: CRM(i): cracking moment of flexural element type i
LIMIT: -
COMMENTS: none

COLUMN NO: 21-30
NOTATION: YIM(i): yielding moment of flexural element type i
LIMIT: -
COMMENTS: none

COLUMN NO: 31-40
NOTATION: ULM(i): moment at a point beyond the yield point of the primary curve
LIMIT: -
COMMENTS: This value is used only to calculate the slope of post-yielding segment of moment-rotation curve; it does not impose any limit on the resistance of the member.

COLUMN NO: 41-50
NOTATION: YIC(i): yield curvature of flexural element type i
LIMIT: -
COMMENTS: none

COLUMN NO: 51-60
NOTATION: ULC(i): curvature at a point beyond the yield point
LIMIT: -
COMMENTS: The curvature must be the value of curvature at the point where moment is equal to ULM(i).

COLUMN NO: 61-70
NOTATION: AR(i): shear area of flexural element type i
LIMIT: -
COMMENTS: Leave blanks if shear deformations are ignored.

COLUMN NO: 71-80
NOTATION: FCC(i): crack-closing moment when Sina hysteresis model is used
LIMIT: -
COMMENTS: Program will ignore the data if a hysteresis model other than Sina is used.

b. Rotation due to Bond Slip (3E15.6)

COLUMN NO: 1-15
NOTATION: SC(i): Unit length rotation due to bond slip corresponding to the cracking moment
LIMIT: -
COMMENTS: Procedure to calculate rotations due to bond slip is described in Chapter 2 in Reference 25. Note that the rotation so calculated is the total rotation and has to be divided by member cantilever length (one-half member length if IBSE = 0; see card 2.2.10) to obtain the unit length rotation.

COLUMN NO: 16-30
NOTATION: SY(i): unit length rotation due to bond slip corresponding to the yield moment
LIMIT: -
COMMENTS: See the comments for SC.

COLUMN NO: 31-45
NOTATION: SU(i): unit length rotation due to bond slip corresponding to ULM(i)
LIMIT: -
COMMENTS: See the comments for SC.

2.2.8 Flexible Diaphragm Information (2I5,F10.0)

One card is used for each flexible diaphragm. Skip this part if there are no such diaphragms.

COLUMN NO: 1-5
NOTATION: IDPH(*,1): global DOF number adjacent to diaphragm *
LIMIT: -
COMMENTS: none

COLUMN NO: 6-10
NOTATION: IDPH(*,2): global DOF number adjacent to diaphragm *
LIMIT: -
COMMENTS: IDPH(*,1) and IDPH(*,2) should be sorted in ascending order. If one side of the diaphragm is fixed, columns 6-10 should be left blank.

COLUMN NO: 11-20
NOTATION: SDPH(*): stiffness of the *th diaphragm
LIMIT: -
COMMENTS: Diaphragms are assumed to remain elastic throughout the analysis. The value of stiffness is calculated by the user with appropriate consideration of torsional properties of the adjacent members.

2.2.9 Typical Element Dimensions (3F10.3)

The first card of this group represents the dimensions of member type one.

COLUMN NO: 1-10
NOTATION: TYPT(i): total length of member
LIMIT: -
COMMENTS: none

COLUMN NO: 11-20
NOTATION: TYPL(i): length of left (top) rigid end portion
LIMIT: -
COMMENTS: none

COLUMN NO: 21-30
NOTATION: TYPR(i): length of right (bottom) rigid end portion
LIMIT: -
COMMENTS: none

2.2.10 Member Characteristics (7I5)

One card is used for each member. First, the data for members of

frame one are given. The ith card for each frame contains the data for member i of that frame.

COLUMN NO: 1-5
NOTATION: MCH(i,1): element dimension type for member i
LIMIT: NG
COMMENTS: none

COLUMN NO: 6-10
NOTATION: MCH(i,2): flexural element type for the left (top) end of member i
LIMIT: NFLX
COMMENTS: none

COLUMN NO: 11-15
NOTATION: MCH(i,3): flexural element type for the right (bottom) end of member i
LIMIT: NFLX
COMMENTS: none

COLUMN NO: 16-20
NOTATION: NODE (i,1): left (top) end local incidence of member i
LIMIT: 50
COMMENTS: none

COLUMN NO: 21-25
NOTATION: NODE(i,2): right (bottom) end local incidence of member i
LIMIT: 50
COMMENTS: none

COLUMN NO: 26-30
NOTATION: IDIR(i): index to specify whether the member is a beam or a column
LIMIT: -
COMMENTS: IDIR(i) = 0 member i is a column or a wall
= 1 member i is a beam

COLUMN NO: 31-35
NOTATION: IBSE(i): index to specify if the length from member end to inflection point is other than one-half of the member length
LIMIT: up to 10 members with IBSE(i) = 1 allowed
COMMENTS: IBSE(i): = 0 inflection point at the middle
= 1 inflection point at location other than the middle

2.2.11 Main and Dependent Joints

Each horizontal degree-of-freedom may consist of more than one joint. One of the joints in each degree-of-freedom is considered as the main joint; others are assumed to be dependent joints. There are two cards for each horizontal degree-of-freedom: cards (a) and (b). Data cards for frame one come first, followed by the data for frame two and so on.

a. Main Joints (3I5)

COLUMN NO: 1-5
NOTATION: LIST(*): local joint number of main joint
LIMIT: -
COMMENTS: none

COLUMN NO: 6-10
NOTATION: LIST(*): number of dependent joints in the frame
LIMIT: 8
COMMENTS: If there are no dependent joints, use 1.

COLUMN NO: 11-15
NOTATION: IFRE(*): corresponding global degree of freedom
LIMIT: -
COMMENTS: none

b. Dependent Joints (8I5)

COLUMN NO: 1-5,6-10, ...
NOTATION: LIST(*): dependent local joint
LIMIT: -
COMMENTS: Each dependent joint is punched in five columns of this card. If there are no dependent joints, punch the main joint number in the first five columns.

2.2.12 Height of Levels (10F8.3)

COLUMN NO: 1-8,9-16, ...
NOTATION: HT(i): height of the level at which the ith degree-of-freedom is defined
LIMIT: -
COMMENTS: ith 8-column range is for the ith degree-of-freedom. If there are more than ten degrees of freedom, use two cards.

2.2.13 Height of Inflection Points (10F8.3)

Skip this card if there are no members with IBSE equal to 1.

COLUMN NO: 1-8,9-16, ...
NOTATION: CNTF(i): distance of inflection point from member end (see comments) for the ith member with IBSE = 1
COMMENTS: Distances are given in the same sequence that members with IBSE equal to 1 appear in the input. For example, the quantity given in the third 8 columns represents the distance for the third member with IBSE equal to 1 as appeared in the input.

CNTF is the cantilever length used for calculation of nonlinear rotations from curvature values. The length is used for both member ends. If yielding is expected at both member ends, CNTF should be the average of distances from the inflection point and the two ends.

2.2.14 Involved Joints

Adjacent to each level, where one horizontal degree-of-freedom is defined, there are joints above and/or below which are connected to the level by means of columns. Any rotation at these joints will cause moment at the joints in the level of concern. Because the program is developed to solve irregular as well as regular frames, it is necessary that information about the joints adjacent to each level and within the level be provided. The data are used to trace the location of non-zero elements of upper right structural submatrix (Appendix B in Reference 25).

a. Number of Involved Joints (16I5)

COLUMN NO: 1-5,6-10, ...
NOTATION: NEF(i): number of adjacent joints and the joints within ith global DOF
LIMIT: 50
COMMENTS: none

b. Involved Joints (16I5)

COLUMN NO: 1-5,6-10, ...
NOTATION: JTK(*): global joint number adjacent to or within the level where a degree-of-freedom is defined
LIMIT: -
COMMENTS: There are up to two cards for each degree-of-freedom. The joint numbers are to be sorted in ascending order. If there are less than 17 involved joints in a degree of freedom, only one card is needed. The first card is for the first degree-of-freedom.

2.2.15 Hysteresis Parameters (2F10.4)

COLUMN NO: 1-10
NOTATION: BTO: power of slope of unloading branch from post-yielding portion of the primary curve (in Eq. 3.1, Reference 2)
LIMIT: -
COMMENTS: For Takeda, Sina, and Q-Hyst systems, BTO=0.4 or 0.5 can be used. For Otani system, BTO=0.0 is used if unloading slope is to be the same with the slope of unyielded portion of the primary curve. However, the routine for Otani model (developed by Otani, Reference 19) is capable to work with different values of BTO.

BTO is ignored if simple bilinear hysteresis model is used; the space can be left blank.

COLUMN NO: 11-20
NOTATION: CTO: coefficient for crack-closing rotation (Eq. 3.4 in Reference 25)
LIMIT: 1.0
COMMENTS: This parameter is needed only when Sina model is used. If other models are used, the space can be left blank.

2.2.16 Earthquake Title (7A10)

COLUMN: 1-70
NOTATION: ENAM(*): name or any title describing the base motion
LIMIT: -
COMMENTS: none

2.2.17 Earthquake Information (4I5,5F10.6)

COLUMN NO: 1-5
NOTATION: NCRD: number of base acceleration cards
LIMIT: see comment for the next parameter
COMMENTS: none

COLUMN NO: 6-10
NOTATION: NDT: number of data points per card
LIMIT: 8
COMMENTS: If plots are requested, NDT*NCRD has to be less than 2000. The last card may contain less than NDT data points.

COLUMN NO: 11-15
NOTATION: ICODE: index to specify if base acceleration is given in equal time intervals
LIMIT: -
COMMENTS: ICODE = 0 data are not provided in equal time intervals; input includes time.
= 1 data are provided in equal time intervals; input does not include time.

COLUMN NO: 16-20
NOTATION: IPLOT: index to specify if response history plots are desired
LIMIT: -
COMMENTS: IPLOT = 0 no plots are desired
= 1 plots are desired

COLUMN NO: 21-30
NOTATION: ACCM: factor to normalize the base acceleration
LIMIT: -
COMMENTS: none

COLUMN NO: 31-40
NOTATION: DT: time step for numerical integration
LIMIT: -
COMMENTS: The program may automatically reduce DT for parts of the analysis, if a break point in the input acceleration is to be reached in a time less than DT. For example, in Fig. 2.2, during the period between T_A and T_B a smaller time interval is used.

COLUMN NO: 41-50
NOTATION: DTAC: time interval of data, if base acceleration is given in constant time increments (ICODE = 1)
LIMIT: -
COMMENTS: If the base acceleration is provided in varying time in-

tervals, the space can be left blank.

COLUMN NO: 51-60
NOTATION: TM: factor to scale the time axis of the base acceleration LIMIT: -
COMMENTS: This factor is used whether or not base acceleration data are given in constant time intervals. If no change in the time axis is desired, TM = 1.0 is to be used.

COLUMN NO: 61-70
NOTATION: SUBT: value to be subtracted from ordinates of base acceleration points
LIMIT: -
COMMENTS: SUBT is used in the program before the acceleration is scaled by ACCM.

2.2.18 Format of the Base Acceleration (7A10)

COLUMN NO: 1-70
NOTATION: FRMT(*): format used in the input acceleration
LIMIT: format needs to be enclosed in parenthesis
COMMENTS: none

2.2.19 Base Acceleration (FRMT)

COLUMN NO: as specified by FRMT
NOTATION: if ICODE=0, TT(*) and ETQ(*): time and acceleration, respectively
if ICODE=1, ETQ(*): acceleration
LIMIT: -
COMMENTS: none

APPENDIX C

STEP-BY-STEP PROCEDURE

FOR Q-MODEL(L) ANALYSIS

To use the Q-Model(L), the following steps need to be taken:

Step 1: Determine Yield Moments - Yield moments for different sections are determined based on specified (or measured) material properties, geometry and reinforcement, and the existing axial loads. The routine methods of yield moment calculation may be used.

Step 2: Determine Lateral Load Distribution - Lateral loads to be used in static analysis are applied at floor levels and are proportional to floor weights (or masses) and floor heights from the base. For convenience, lateral loads may be expressed in terms of an unknown total base shear, V.

Step 3: Determine the Minimum Collapse Load - A limit analysis is carried out to determine the collapse load. The multistory structure is anlayzed for loads determined in step 2 and the collapse base shear (V) and moment are found. The element yield moments found in step 1 will be used as plastic moments. For this step, members are assumed to be elasto-plastic.

Step 4: Determine Deflected Shape, Equivalent Mass and Equivalent Height - Lateral floor displacements of the multistory structure are found through a static analysis using the minimum collapse load found in Step 3. Load distribution is the same as the one used in that step. Cracked moment of inertia is used for beams and first-story columns. The lateral displacements are normalized with respect to the top-level displacement. The resulting values constitute the deflected shape of the structure (ϕ). Equivalent mass and height are found using Eq. 2.2

and 2.3.

Step 5: Determine the Primary Curve and Damping - Displacement at the equivalent height is found using a linear interpolation of the displacements (calculated in Step 4) at the floors immediately below and above the equivalent height. The elastic branch of the primary curve is drawn by connecting the origin to a point with displacement equal to that at the equivalent height and moment equal to the collapse base moment. The slope of this line is divided by the equivalent height to obtain the elastic stiffness. This stiffness and the equivalent mass are used to calculate elastic frequency. The damping coefficient is twice the product of a damping factor and the elastic frequency.

Step 6: Determine Response History - A computer software incorporating the hysteresis model for a nonlinear response history analysis is used to integrate Eq. 2.4 numerically. An important point to note is the fact that on the right-hand side of the equation the total mass is used.

The time interval used for numerical integration should be sufficiently small so that break points in the hysteresis model will be closely followed. A time interval of approximately one-twentieth of elastic period appears to be reasonable.

For each time interval, displacement at the equivalent height and base moment are found, normalized to find response at a particular floor, and plotted. Displacements at different floors may be determined from Eq. 2.5.

APPENDIX D

UNIT CONVERSION FACTORS

To convert from ...	to ...	multiply by
inch	millimeter	25.4
foot	meter	0.3048
kip-force	newton	4448
inch-kip-force	Kilonewton-meter	0.1130
kip/sq.inch	megaposcal (MPa)	6.895
pound-mass	kilogram	0.4536